International PhD Program in Biomolecular Sciences

Department of Cellular, Computational and Integrative Biology – CIBIO

34th Cycle

"Autoreactive B Cells in ANCA-Associated Vasculitis"

Tutor

Guido Grandi – *University of Trento (Italy)*

Advisors

Ulrich Specks – *Mayo Clinic, Rochester (MN, USA)*

Divi Cornec – *University of Brest (France)*

Ph.D. Thesis of

Alvise Berti

University of Trento (Italy)

Academic Year 2021-2022

Declaration of authorship

I, Alvise Berti, confirm that this is my own work or work I have done together with other members of our group and collaborators, and the use of all material from other sources has been properly and fully acknowledged.

September 3rd, 2021 Alvise Berti

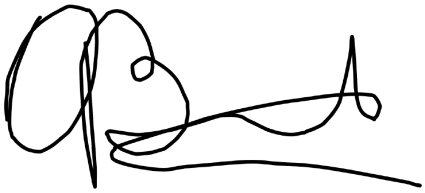

Contents

Abbreviations 6
List of Figures 7
List of Tables 9
List of Supplemental Figures 10
List of Supplemental Tables 11
Abstract 12
Introduction 14
- **B Cell Biology and Development** 14
  - **B cell receptor, B cell lineage and functions** 14
  - **Developmental stages of B cells** 16
  - **B cell tolerance checkpoints** 20
  - **Circulating B cell subsets** 23
- **Autoreactive B Cells** 25
  - **B cell functions in autoimmune conditions** 25
  - **Autoreactive B cells in autoimmune diseases** 28
  - **Autoreactive B Cells in ANCA-Associated Vasculitis** 31
- **Autoreactive B Cells in ANCA-Associated Vasculitis: A Human Model Of Autoimmune Vasculitis** 33
  - **B cells, ANCA and neutrophils interaction in AAV** 33
  - **The clinical spectrum of ANCA-associated vasculitis** 36
  - **Treatments and outcomes of the disease** 39

Aims of the thesis 42
Aim #1: Phenotypic and functional characterization of autoreactive PR3$^+$ B cells 44
- **Summary Aim #1** 44
- **Results Aim #1** 46
  - **Perturbations of circulating B cell subsets are similar in patients with PR3-AAV and MPO-AAV** 46
  - **Circulating PR3$^+$ B cells are higher in patients with PR3-AAV than in controls** 48
  - **PBMC from patients with PR3-AAV contain PR3$^+$ B cells capable of secreting PR3-ANCA IgG in vitro** 48
  - **Functional validation of autoreactive PR3$^+$ B cells by flow cytometry** 50

Autoreactive PR3⁺ memory B cells accumulate through the maturation process only in patients with PR3-AAV. 51
Selection of mature PR3⁺ B cells and determinants of the maturation of autoreactive B cells 56
Maturation of PR3⁺ B cells and clinical manifestations in PR3-AAV subjects 59
Discussion Aim #1 62
Aim #2: The ontogeny of PR3⁺ B cells 68
Summary Aim #2 68
Results Aim #2 70
Study cohorts 70
PR3⁺ B cells are increased in BMMC in non-vasculitis subjects and in PBMC of PR3-AAV patients 70
Immature/Transitional B cells in bone marrow and peripheral blood 73
Maturation of PR3⁺ B cells from BM to periphery in non-vasculitis subjects and AAV patients 75
Discussion Aim #2 78
Aim #3: Longitudinal dynamics of PR3⁺ B cells after B cell depletion 83
Summary Aim #3 83
Results Aim #3 85
Remission, relapse and B cell recurrence in PR3-AAV 85
Recurrence and subset redistribution of circulating autoreactive B cells following RTX-induced remission in PR3-AAV 88
Dynamics of total B cells and autoreactive B cells and relapse during long-term follow-up 90
Relationship of enrichment of plasmablasts within circulating autoreactive B cells with relapse 92
Discussion Aim #3 94
Conclusion and Future Perspectives 98
Materials and Methods 102
Study Populations and definitions 102
Recombinant proteinase 3 production and labelling 104
PR3⁺ B cell detection and flow cytometry analysis 105
In vitro PR3-ANCA production by PBMC and detection of PR3⁺ B cells with ELISPOT 107
ANCA testing 109
Data availability 110

Statistics 110
Study approvals 111
Supplemental Material 113
Supplemental Figures 113
Supplemental Tables 125
References 132
Publications During the PhD Course 164
Experimental work related to the PhD project 164
Publications on AAV 165
Other publications 168
Acknowledgments 170

Abbreviations

ANCA	Anti-neutrophil cytoplasmic antibodies
AAV	ANCA-Associated Vasculitis
BCR	B cell receptor
BM	Bone Marrow
BMMC	Bone marrow mononuclear cells
CpG	CpG oligodeoxynucleotides (Toll like receptor 9 agonists)
DN	Double Negative (B cells)
GC	Germinal Center
HC	healthy controls
Ig	Immunoglobulin
IL	Interleukin
MPO	Myeloperoxidase
PB	Plasmablasts
PBMC	Peripheral blood mononuclear cells
PC	Plasma cells
Pe	Pemphigus
PR3	Proteinase-3
$PR3^+$ B cells	PR3-positive (autoreactive) B cells
RA	Rheumatoid Arthritis
RTX	Rituximab
RAVE	Rituximab in ANCA-Associated Vasculitis trial
SLE	Systemic Lupus Erythematosus
SW	Switched (memory B cells)
Tfh	T follicular helper (cells)
Transi	Transitional (B cells)
UnSW	Unswitched (memory B cells)

List of Figures

Figure 1. Multifunctional attributes of B cells. *Pag.16*

Figure 2. Developmental stages of B cells in bone marrow and peripheral blood. *Pag.17*

Figure 3. Schematic representation of B cell subsets in the blood. *Pag.25*

Figure 4. The functions of B cells in autoimmune disease. *Pag.27*

Figure 5. Customized flow cytometry-based assay labeling autoreactive B cells with recombinant PR3 and validation by staining of hybridoma cell lines. *Pag.32*

Figure 6. Clinical features of AAV: organ involvement in granulomatosis with polyangiitis (GPA), microscopic polyangiitis (MPA) and eosinophilic GPA (EGPA). Pag.37

Figure 7. Aim #1 graphical summary. *Pag.45*

Figure 8. Circulating B cells in patients with PR3-AAV, MPO-AAV and HC subjects. *Pag.47*

Figure 9. Circulating $PR3^+$ B cells and PR3-ANCA production in patients with PR3-AAV, MPO-AAV and HC subjects. *Pag.49*

Figure 10. Functional validation of autoreactive $PR3^+$ B cells by sorting $PR3^+$ and $PR3^-$ B cells. *Pag.50*

Figure 11. Frequency of $PR3^+$ B cells within each B cell subset. *Pag.52*

Figure 12. Selected PR3-reactive B cell clusters significantly more represented or activated in PR3-AAV patients. *Pag.54*

Figure 13. Maturation of $PR3^+$ B cells among different participant groups. *Pag.57*

Figure 14. SW memory/naïve $PR3^+$ B cell ratio and clinical manifestations in PR3-AAV patients. *Pag.60*

Figure 15. Aim #2 graphical summary. *Pag.69*

Figure 16. $PR3^+$ B cells in BMMC and PBMC non-vasculitis subjects and vasculitis patients. *Pag.72*

Figure 17. Immature/Transitional B cells in bone marrow and peripheral blood. *Pag.74*

Figure 18. Characterization of the Transitional Subset in BMMC and PBMC. *Pag.75*

Figure 19. Comparison of the proportions of $PR3^+$B cells among the different bone marrow B-cell subsets to peripheral B cells subsets in non-vasculitis patients. *Pag.77*

Figure 20. Aim #3 graphical summary. *Pag.84*

Figure 21. Swimmer plot showing response to RTX, relapse and B cell dynamics in PR3-AAV trial participants during follow-up. *Pag.85*

Figure 22. B cells comparisons of absolute count and frequency of B cells and B cell subsets at baseline and at B cell recurrence. *Pag.87*

Figure 23. B cells comparisons of frequency of autoreactive $PR3^+$B cells and subsets at baseline and at B cell recurrence. *Pag.89*

Figure 24. B cells and autoreactive $PR3^+$ B cells during follow up. *Pag.91*

Figure 25. Relapse, severe relapse and autoreactive $PR3^+$ plasmablasts. *Pag.92*

List of Tables

Table 1. The subsets of B cells. *Pag.20*

Table 2. The main human antigen-specific B cells identified in systemic autoimmune diseases detected by flow cytometry methods. *Pag.29*

Table 3. Phenotypic characterization of selected PR3+ B cell clusters. *Pag.55*

Table 4. Baseline $PR3^{+}$ B cell subsets by switched memory/naïve B cell ratio in 105 subjects with PR3-AAV. *Pag.58*

Table 5. Lymphocytes and B cell subsets of BMMC and PBMC of non-vasculitis controls (n=8), and PBMC of AAV patients (n=9). *Pag.71*

List of Supplemental Figures

Supplemental Figure 1. B cells and distribution of B cells among different subsets in HC, MPO-AAV and PR3-AAV. *Pag.113*

Supplemental Figure 2. Circulating PR3$^+$ B cells and PR3-ANCA production. *Pag.114*

Supplemental Figure 3. Representative B cell subset plots of a HC subject, a MPO-AAV patient and a PR3-AAV patient. *Pag.115*

Supplemental Figure 4. Unsupervised clustering of circulating PR3+ B cells. *Pag.116*

Supplemental Figure 5. Determinants of PR3$^+$ B cell maturation. *Pag.117*

Supplemental Figure 6. SW memory/naïve PR3$^+$ B cell ratio and clinical manifestations in PR3-AAV patients. *Pag.118*

Supplemental Figure 7. Frequency of PR3$^+$ B cells and clinical manifestations in PR3-AAV participants. *Pag.119*

Supplemental Figure 8. The gating strategy for the aim #2 set of experiments. *Pag.120*

Supplemental Figure 9. PR3$^+$ B cells among transitional B cells. *Pag.121*

Supplemental Figure 10. Proportions of B cell subsets from bone marrow to peripheral B cells subsets in non-vasculitis patients. *Pag.122*

Supplemental Figure 11. Frequency of B cells, PR3$^+$ B cell subsets and PR3-ANCA IgG at baseline and at recurrence of B cells. *Pag.123*

Supplemental Figure 12. Receiver operating characteristic curve showing the ability of PB within PR3$^+$ pool to distinguish relapsing from non-relapsing patients. *Pag.124*

List of Supplemental Tables

Supplemental Table 1. Baseline features of patients with AAV and HC included in the aim #1 of the study. *Pag.125*

Supplemental Table 2. Glucocorticoid treatment at screening (before sample collection) in subjects studied in the aim #1 of the study. *Pag.127*

Supplemental Table 3. Baseline features of subjects included in the aim #2 of the study. *Pag.128*

Supplemental Table 4. Baseline features of AAV subjects included in the aim #2 of the study. *Pag.129*

Supplemental Table 5. Baseline features of subjects with AAV included in the aim #3 of the study, by future relapse. *Pag.130*

Supplemental Table 6. Relationship between PR3-ANCA IgG titer increase and frequency of plasmablasts within PR3-reactive B cell increase. *Pag.131*

Abstract

Anti-neutrophil cytoplasmic antibody (ANCA)-associated vasculitis (AAV) is a group of B-cell driven, autoimmune systemic vasculitides characterized by a relapsing course and the presence of ANCA autoantibodies which are instrumental in their pathogenesis. We aimed to investigate autoreactive proteinase 3 ($PR3^+$) B cells involved in the development of human AAV.

We previously developed a customized flow-cytometry method to identify autoreactive B cells among cryopreserved peripheral blood mononuclear cells (PBMC), using labeled PR3, one of the main AAV autoantigens, as a ligand. We therefore used multicolor flow cytometry in combination with bioinformatics and functional in *vitro* studies on 1) baseline samples of PBMC from 154 well-characterized participants of the RAVE trial (NCT00104299) with severely active PR3-$ANCA^+$ AAV (PR3-AAV) and myeloperoxidase (MPO)-AAV, and 27 healthy controls (HC); 2) samples of matched bone marrow (BM) and peripheral blood from 8 non-vasculitis patients; and 3) 148 longitudinal samples from 23 PR3-AAV patients of the RAVE trial. Clinical data and outcomes from the trial and medical records were correlated with $PR3^+$ B cells (total and subsets).

In brief, we identified and phenotypically characterized autoreactive B cells in AAV and healthy controls, reporting their perturbations among the different B cell subsets, and their functional ability to produce PR3-ANCA autoantibodies in *vivo* and in *vitro*. We reported their maturation through central and peripheral tolerance checkpoints from BM to peripheral blood, leading to an accumulation of atypical autoreactive $PR3^+$ memory B cells in PR3-AAV patients but not in MPO-AAV and HC. We also described the longitudinal association between autoreactive plasmablast redetection after anti-B cell

targeted therapy with the main disease outcome, relapse. Overall, our findings suggest the presence of defective central antigen-independent and peripheral antigen-dependent checkpoints in patients in PR3-AAV, elucidating the selection process of autoreactive B cells, and their association with disease relapse.

Introduction

B Cell Biology and Development

B cell receptor, B cell lineage and functions

B cells constitute one arm of the adaptive immune response, which has been historically classified as cellular, T-cell mediated, and humoral, characterized by the production of antibodies by the B lymphocytes *(1–4)*. In fact, B cells have been traditionally associated to antibody production, but this is not the only function they exert *(1)*.

The defining feature of B cells is the antigen(s)-specific B cell receptor (BCR) they bear on their surface. BCR is the transmembrane form of soluble antibodies or immunoglobulins (Ig), glycosylated proteins secreted into the extracellular space, where they can bind and neutralize their target extracellular antigens, protecting against infection and contributing to tissue injury in autoimmunity and transplantation *(2)*.

The structure of the Ig consists of four protein chains: two heavy chains and two light chains, linked to each other by disulfide bonds to form a Y. Both variable fractions of the heavy (H) and light (L) chains contribute to the site of antigen binding - the antigen-binding fragment (Fab), containing the hypervariable regions i.e. complementarity-determining regions (CDRs), whereas the remaining fraction of the heavy chains constitute the fragment crystallizable region (Fc region)*(5)*. The diversity of the Fab, able to recognize a wide variety of antigens, is generated by a site-specific recombination reaction through the rearrangement of H and L Ig chain gene segments (V variable, D diversity, J joining), known as VDJ recombination. This occurs in the BM and culminates in the expression of a mature IgM BCR able to bind antigens on the cell surface of B cells *(2, 5)*.

Signaling through the BCR is required for peripheral B cell maturation, maintenance, activation, and silencing *(1, 6)*. When the BCR is engaged with its specific antigen in the secondary lymphoid tissue, the B cell can undergo proliferation and differentiation mediated by dynamic changes in gene expression that give rise to the germinal center (GC) reaction, following T cell help by T follicular helpers (Tfh) promoting B cell activation *(2, 7, 8)*. BCR can therefore maturate their affinity towards the specific antigen (a process called somatic hypermutation) leading to the survival of those B cells that bind to the specific antigen with high affinity (clonal selection), and meanwhile switch Ig class from IgM to IgG, IgA, IgE (class switch recombination) *(2, 5)*. Similarly, to eliminate or restrict autoreactive clones and prevent autoimmune disease, BCR engagement in the BM and periphery by the specific antigen is critical to eliminate or maintain functionally silenced (anergic) B cells *(2, 3)(6)*.

Besides Ig production, B cells mediate several other essential functions for immune homeostasis (**Figure 1**) *(1)*. B cells can release pro-inflammatory or inhibitory cytokines that can influence a variety of T-cells, dendritic cells, and antigen-presenting cell functions; orchestrate lymphoid organ remodeling and neogenesis; regulate wound healing and transplanted tissue rejection; and influence tumor development and immune-host interaction *(9)*. Importantly, B cells can present antigens to and co-stimulate T-cells, leading to their activation and differentiation through polarized cytokine production *(10)*. In addition, a distinct subset of regulatory B cells has been described *(11)*, B10 cells, which have been shown to suppress T cell–mediated responses through the production of IL-10 (**Figure 1**) *(12)*. Taken altogether, B cells can contribute in numerous and diverse ways to the immune response.

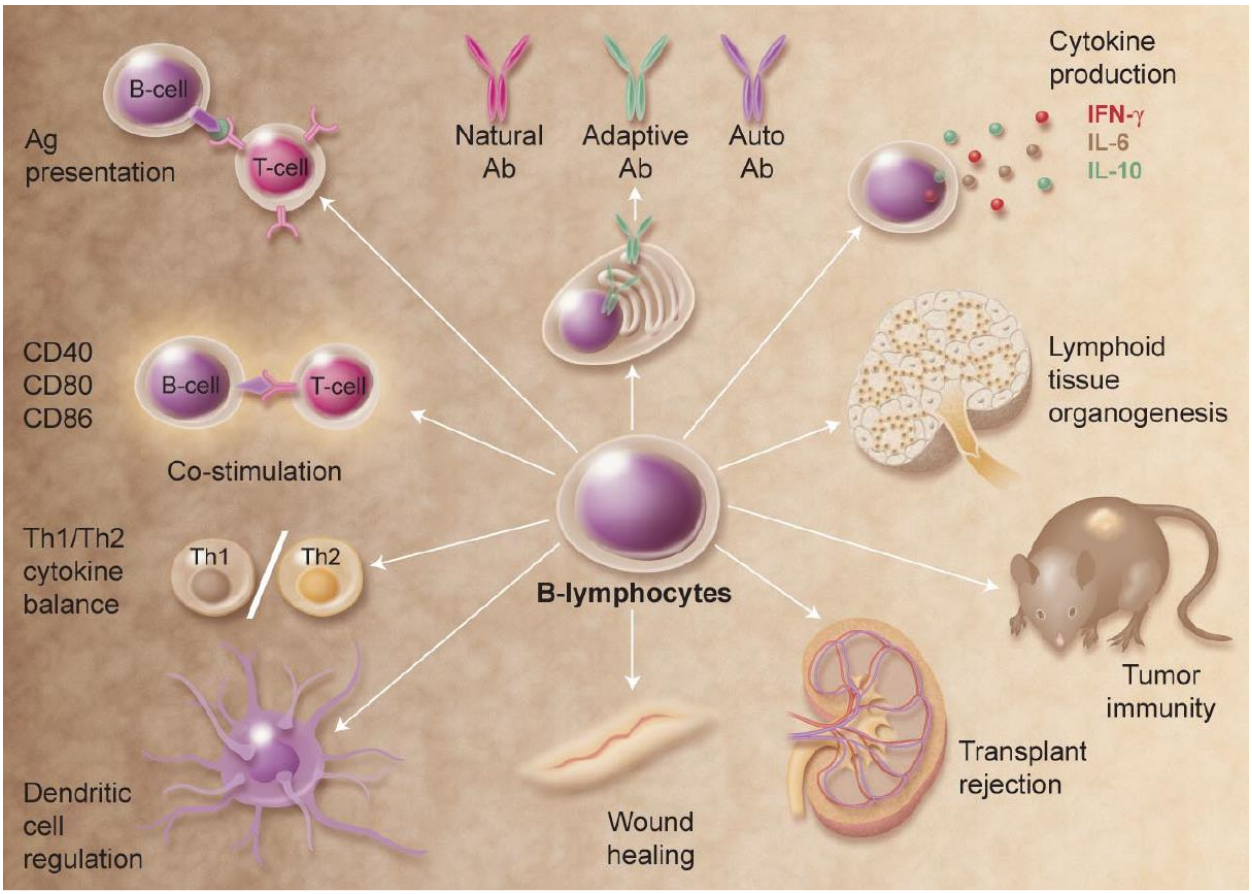

Figure 1. Multifunctional attributes of B cells. Examples of how B cells regulate immune homeostasis are shown; many of these functions are independent of Ig production (from LeBien TW et al. 2008 *(1)*).

Developmental stages of B cells

In adult humans, B cells are generated in the BM, where they start their developmental process before the transition to the periphery (**Figure 2**) *(2)*. Here, B cell development is accompanied by Ig gene rearrangements leading to the generation of a diverse immature B cell pool. Those reactive with self- or auto-antigen are deleted or functionally silenced, while the remaining immature B cells can migrate into the peripheral compartment *(6, 13)*.

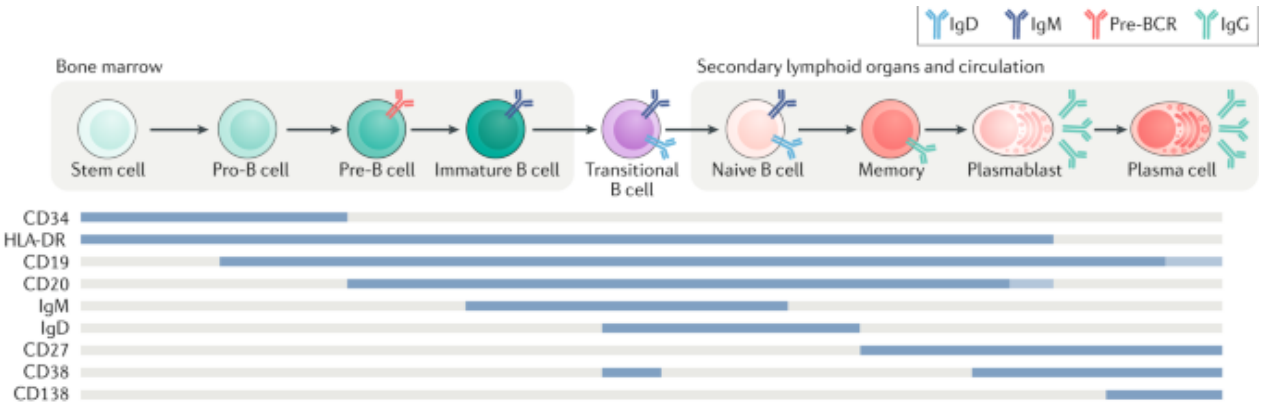

Figure 2. Developmental stages of B cells in bone marrow and peripheral blood (from Sabatino jr. J.J. 2018 *(14)*).

In the BM, pro-B cells which derive from lymphoid progenitor cells, initiate H-chain gene rearrangement through expression of recombination-activating genes (RAG1 and RAG2) and epigenetic modifications of the H-chain loci that promote accessibility *(13)*. When H-chain genes are assembled, it is associated with a temporary surrogate of the light-chain (SLC), leading to the membrane expression of the pre-B cell receptors (pre-BCR, that do not bind antigens) in large pre-B cells and permitting B cell proliferation and RAG1-2 downregulation. At pre-B cell stage, SLC components are downregulated, H chain internalized, RAG is re-expressed and its activity redirected to the L-chain genes *(13)(15)*.

Once L chain genes are assembled, L chains pair with H chains, triggering tonic BCR signaling which promotes positive selection when the BCR is non-autoreactive. When non-autoreactive, B cells express the membrane isoform of IgM, a dimer of IgM H chain (μ-chain) associated with L chain, that can engage with marrow microenvironment antigens, almost always self-antigens, which makes regulation at this stage crucial. It is by ligation of the BCR that self-antigens promote signaling that triggers regulatory processes to reduce self-reactivity *(13)(15)(16)*. These processes are collectively known

as central tolerance. When the BCR is autoreactive or if tonic signaling is impaired, B cells undergo receptor editing, i.e. a process whereby ongoing Ig gene recombination promotes a change in expression or specificity of the antigen receptor of B cells *(13, 17)*. Receptor editing can lead to either exchange of one functional L chain for another, making the BCR innocuous and allowing the B cell to continue the developmental progression, or secondary rearrangements that prevent L-chain expression. If so, the B cell returns to the pre-B cell compartment, where it undergoes new L-chain formation or clonal deletion (death by neglect) *(13)(15)*.

Cells that go through positive selection enter into the immature and then transitional B cell developmental stages, the latter representing the subset of B cells migrating from BM compartment to peripheral blood *(13)*. At these stages, B cells start to express a second Ig, IgD. After transitional B cells move to the peripheral blood, they maturate into naïve B cells. Naïve B cells are those cells that have not yet encountered the specific antigen for their BCR *(2, 18)*. When the BCR recognizes its cognate antigen, the naïve B cell can receive the T cell help in the lymphoid follicles for the functional differentiation toward plasma cells, GC B cells and memory B cells *(1)*. Here, the antigen-specific naïve B cells in B cell follicles and Tfh cells in the T cell zone are active and migrate toward the follicle T-B cell border, where they proliferate and form cognate interactions *(19–21)*. Some of these antigen-experienced B cells proliferate extensively and differentiate into short-lived plasmablasts (PB) rapidly secreting low-affinity antibodies *(22)*. In addition, activated B cells can differentiate into memory B cells or plasma cells (PC), responsible for producing protective high-affinity, isotype-switched antibodies. PCs are rarely detected in the periphery, since they home to the BM niches where they reside and maintain serologic

memory independent of further antigen exposure *(23)*. In contrast, memory B cells recirculate and form extrafollicular or follicular aggregates in lymphoid tissues, rapidly differentiating into PB or re-entering into GC upon antigen rechallenge, leading to a diversified secondary antibody response *(24)*. Overall, high affinity IgG arise not only from a GC response, but also in extrafollicular locations since activated B cells that encountered their specific antigen can form extrafollicular foci where class switching and somatic hypermutation can occur, leading to PB and PC terminal differentiation *(9)*.

Every step of B cell maturation is characterized by the expression of a specific combination of surface molecules. CD19 is expressed by essentially all B-lineage cells and regulates intracellular signal transduction by amplifying Src-family kinase activity *(25)*. CD20 is a mature B cell marker, that functions as a transmembrane Ca^{2+} channel and, importantly, it is a target for the chimeric anti-CD20 monoclonal antibody rituximab (RTX) *(26)*. The following table (**Table 1**) shows the surface CD molecules that are preferentially expressed by each one of the main subsets of B cells, facilitating identification and phenotyping *(15, 18, 27–29)*

Table 1. The subsets of B cells (adapted from *(15, 18, 27–29)*).

Subset of B cells	Abbreviation	Common surface markers
Stem cell	SC	$CD34^{++}$, $CD38^{-}$, $CD49f^{+}$, $CD90^{+}$, $CD45RA^{-}$, $Flt3^{+}$
Common lymphoid progenitor	CLP	$CD34^{+}$, $CD38^{+}$, $CD19^{-}$, $CD20^{-}$, $CD10^{+}$, IgM^{-}, IgD^{-}
Pro-B cells	Pro-B	$CD19^{+}$, $CD20^{-}$, $CD21^{+}$, $CD10^{+}$, IgM^{-}, IgD^{-}
Pre-B cells	Pre-B	$CD19^{+}$, $CD20^{+}$, $CD21^{+}$, $CD10^{+}$, IgM^{-}, IgD^{-}, pre-BCR^{+}
Immature T1-like / T2-like / T3-like	Immature	$CD19^{+}$, $CD20^{+}$, $CD5^{+}$, $CD27^{-}$, $CD24^{+}$, $CD38^{+}$, $CD21^{+}$, $CD10^{+}$ $IgM^{+}IgD^{-}$ / $IgM^{+}IgD^{+}$ / $IgM^{-}IgD^{-}$
Transitional T1/ T2 / T3	Transi	$CD19^{+}$, $CD20^{+}$, $CD5^{+}$, $CD27^{-}$, $CD24^{++}$, $CD38^{++}$, $CD21^{+/-}$, $CD10^{+/-}$ $IgM^{+}IgD^{-}$ / $IgM^{+}IgD^{+}$ / $IgM^{-}IgD^{-}$
Naïve*	Naïve	$CD19^{+}$, $CD20^{+}$, $CD38^{low}$, $CD27^{-}$, IgM^{+}, IgD^{+}
Unswitched memory*	UnSW	$CD19^{+}$, $CD20^{+}$, $CD38^{low}$, $CD27^{+}$, IgD^{+}
Switched memory*	SW	$CD19^{+}$, $CD20^{+}$, $CD38^{low}$, $CD27^{+}$, IgD^{-}
Double negative*	DN	$CD19^{+}$, $CD20^{+}$, $CD38^{low}$, $CD27^{-}$, IgD^{-}
Plasmablast	PB	$CD19^{+}$, $CD20^{low}$, $CD24^{-}$, $CD38^{high}$, $CD27^{high}$
Plasma cell	PC	$CD19^{+}$, $CD20^{-}$, $CD24^{-}$, $CD38^{high}$, $CD138^{high}$, sIg^{low}

*Collectively called “mature” B cells by some authors ($CD19^{+}$, $CD20^{+}$, $CD38^{low/dim}$)

B cell tolerance checkpoints

The diversity generated by the V(D)J recombinations and the somatic hypermutations not only lead to protective humoral immunity, but also to potentially autoantibody-secreting self-reactive clones *(6, 9)*. During differentiation of B cells, different mechanisms regulate the censoring of autoreactive B cells, and defects in central (within the BM) and peripheral (within the peripheral compartment) B cell tolerance checkpoints are associated with the development of autoimmunity *(30)*.

In BM, regulation of self-tolerance in human B cells occurs by three different mechanisms, clonal deletion, receptor editing and anergy *(13)*. When the BCR signal is strong, the B cells are censored by apoptosis. When the signal is intermediate, recombination of the light chain locus occurs, leading to receptor editing and thus reducing the self-reactivity of the BCR *(2, 6)*. Alternatively, B cells can become anergic downregulating their BCR, a process that permits them to survive and to leave the BM. Altogether, in both mice and

humans, receptor editing occurs in 20-50% of the future peripheral naïve cells, while clonal deletion and anergy provide a smaller contribution to the silencing of autoreactive B cells *(2)*.

Despite the efficient removal of a large numbers of autoreactive B cells in the BM, some autoreactive clones bypass the central tolerance machinery and are able to migrate into the periphery *(14)*. A second tolerance checkpoint occurs there, at the maturation stage from transitional to mature naïve B cells, before B cells encounter the specific antigen. It has been proven that elevated B-cell activating factor (BAFF) levels inhibit the counterselection of autoreactive transitional B cells, highlighting the role of this cytokine for the survival of autoreactive B cells *(31)*. Stimulation through the toll-like receptor 9 (TLR9) with CpG (which does not require BCR-triggering) induces an initial proliferative burst that is followed by apoptotic death, unless survival (BAFF) or costimulatory signals (CD40 co-stimulation with Interleukin (IL)-21) rescue B cells from this fate, promoting an autoimmune-associated B phenotype *(32, 33)*. Besides other protective immune responses, these distinct subset of memory B cells is prone autoantibody production, a function facilitated by the expression of the transcription factor T-bet (T-box expressed in T cells) *(32, 33)*.

In healthy individuals, these autoreactive clones circulating in the peripheral compartments are prohibited to undergo further differentiation by being blocked from entry into GC. Under normal circumstances, these cells that escape central checkpoints are silenced in the peripheral checkpoints *(34)*. Various tolerance checkpoints leading to a removal of autoreactive B cells have been identified in health and autoimmunity by flow cytometry analysis *(1, 34–36)*. Those B cells that acquire autoreactivity in the GC need

to be silenced or prevented from differentiating into antibody-producing cells. At the GC level, in fact, apoptosis and receptor editing have been described, even if the former has been shown not to contribute substantially, maybe because several potentially autoreactive B cells can be cross-reactive with an eliciting antigen during the early phase of infection *(37)*, thus rendering their elimination counterproductive. The positive selection of activated B cells into memory or PBs/PCs cannot occur without T-cell help from Tfh, constituting another mechanism of regulation *(7, 19)*. Therefore, the CD40/CD40L interactions and antigen presentation through HLA II/T cell receptor are essential for the establishment of peripheral naïve B cell tolerance.

Finally, as memory B cells in healthy individuals have higher frequency of autoreactivity than PCs *(38)*, it is likely that an additional tolerance checkpoint exists at this level, preventing the differentiation of autoreactive memory B cells into autoreactive PCs. Nevertheless, in autoimmune diseases such as systemic lupus erythematosus, mechanisms different from a defect of antigen-specific B-cell tolerance exist, as aberrant B cell differentiation has also been demonstrated in mice and humans *(39)*.

Despite this well-structured system of central and peripheral tolerance checkpoints designed to avoid autoimmunity, extensive studies performed during the last decades have clearly shown that a small proportion of mature B cells in healthy individuals are autoreactive and able to secrete autoantibodies, a phenomenon called natural autoimmunity or natural autoantibodies *(40, 41)*. These natural autoantibodies exert physiological functions including the removal of apoptotic debris, the masking of neo-autoantigens, the binding to idiotypic determinants of self-reactive IgG, and the regulation of effector cell functions *(42)*. Therefore, the autoreactive clones producing

autoantibodies are not *per se* associated with autoimmunity. Of note, these autoantibodies in healthy individuals usually have low-affinity, are polyreactive and of the IgM isotype, secreted spontaneously and important for apoptotic cell clearance *(42, 43)*.

To summarize, several B cell tolerance checkpoints exist in central and peripheral compartments to prevent the generation of autoreactive B cell clones. Nevertheless, a small amount of autoreactivity called “natural autoimmunity” occurs even in heathy subjects and is instrumental for the physiological functioning of the immune system. The shift from this “natural autoimmunity” to an “abnormal or pathogenic autoimmunity” arises when one or more of these checkpoints are breached, leading to autoreactive B cells producing high affinity autoantibodies, with pathogenic potential.

Circulating B cell subsets

The differentiation of B cell precursors into transitional B cells in the BM, and the antigen-triggered maturation of GC B cells into memory B cells and PBs/PCs in lymphoid tissues generate a relatively large number of circulating subsets of B cells (**Figure 3**) *(27, 29)*. These B cell subsets produced in the BM and lymphoid tissues recirculate through the peripheral blood into different tissues including spleen and lymph nodes, mucosa-associated lymphoid tissue, chronically inflamed tissues and the BM, where the long-living PCs reside and produce antibodies *(37)*.

Consequently, the circulating B cells represent a mixture of the different B cell subsets that do not reflect their real abundance in the whole body, but rather their relative representation in the peripheral blood. In healthy human adults, naïve B cells represent

about 60-70% of total circulating B cells, while memory (Sw and UnSW) B cells represent 20% to 30%, PBs/PCs around 1% to 3%, and transitional B cells represent 5% to 10%, while variable low frequencies of DN have been reported in different studies *(18, 27, 28)*.

Another classification of B lymphocytes in mice is based on ontogeny and anatomical localizations, categorizing B cells in B1, further divided in B-1a and B-1b, and B2 B lymphocytes, consisting of the marginal zone (MZ) and the follicular (FO) B cells *(2)*. B1 lymphocytes arise from fetal liver and they can self-renew after the neonatal period, they reside in peritoneal and pleural cavities in mice and produce polyreactive IgM directed against self-antigen or microbial antigens by T-independent mechanisms (i.e. without the T help) *(44)*. Canonical B cells are B2, deriving from transitional B cells, with subsequent retention within the marginal sinus of the spleen in the case of MZ B cells, or residing in the lymphoid follicles of the spleen and lymph nodes in the case of FO B cells *(45)*. MZ can produce IgM antibodies with or without antigen recognition via BCR, while FO are primarily responsible of the long-lasting high affinity IgG, after differentiation into memory B cells and PBs/PCs *(45, 46)*. GC B cells reside in the GC, while B regulatory cells can be found in different tissues *(2)*.

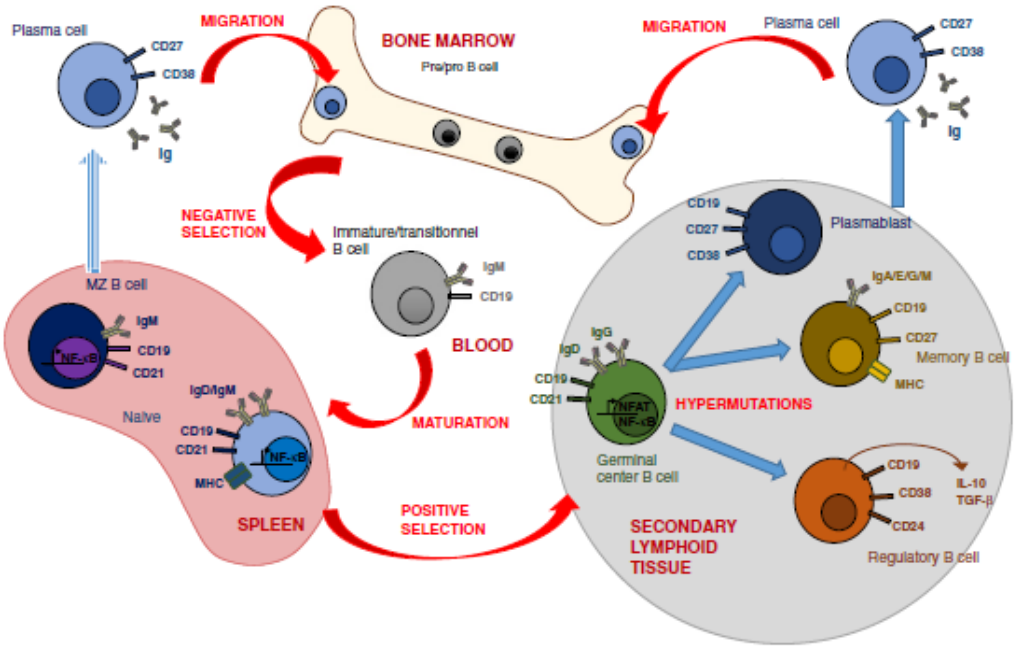

Figure 3. **Schematic representation of B cell subsets in the blood** (from Dumoitier N. 2015 *(29)*)

Autoreactive B Cells

B cell functions in autoimmune conditions

B cells have pivotal pathogenic functions in autoimmune diseases, besides the production of autoantibodies. To date, more than 80 distinct B cell-mediated autoimmune diseases (with specific autoantibodies) have been identified, below a few examples *(5, 34, 47)*:

- Systemic Lupus erythematosus (SLE): anti-nuclear antibodies (ANA), anti-smith antibody (anti-SM), anti-double stranded DNA (anti-dsDNA);
- Rheumatoid arthritis (RA): rheumatoid factor (RF), anti-citrullinated protein antibodies (ACPA) or anti-cyclic citrullinated peptide (anti-CCP) antibodies;
- ANCA-associated vasculitis (AAV): anti-neutrophil cytoplasmic antibodies (ANCA);

- Systemic Sclerosis (SSc): anti-topoisomerase antibodies (ATA), anti-centromere antibodies (ACA), anti-RNA polymerase antibodies (ARA);
- Primary Sjögren's Syndrome (pSS): ANA, anti–Sjögren's-syndrome-related antigen A/Ro (SSA/Ro), anti–Sjögren's-syndrome-related antigen B/La (SSB/La);
- Multiple Sclerosis and Neuromyelitis optica: anti-myelin antibodies, anti-neuronal antibodies, antiganglioside, anti-aquaporin 4, etc;
- Pemphigus (Pe): anti-desmoglein 1 and anti-desmoglein 3 (anti-DSG1/3).

In these diseases, autoreactive B cells and plasma cells are directly involved in the disease pathogenesis. These B lymphocytes show large variability between different conditions, including the secreted autoantibody repertoire, the dynamics and features of the underlying B cell response, and the mechanisms to explain the emergence of autoreactive clones. Of note, most mechanistic insights have been obtained from murine studies using transgenic mouse models, for those autoimmune conditions where reliable animal models exist *(48–50)*.

Overall, autoreactive B cells in different autoimmune diseases have several common functions (**Figure 4**). First, autoantibody production is widely implicated in different ways in the pathogenesis (from immune-complexes formation to complement-dependent toxicities, antibody-dependent cell-mediated toxicities, and neutrophil activation). Autoreactive B cells also contribute in antigen presentation as professional antigen presenting cells (APCs), T cell co-stimulation, and cytokine production *(6, 34)*.

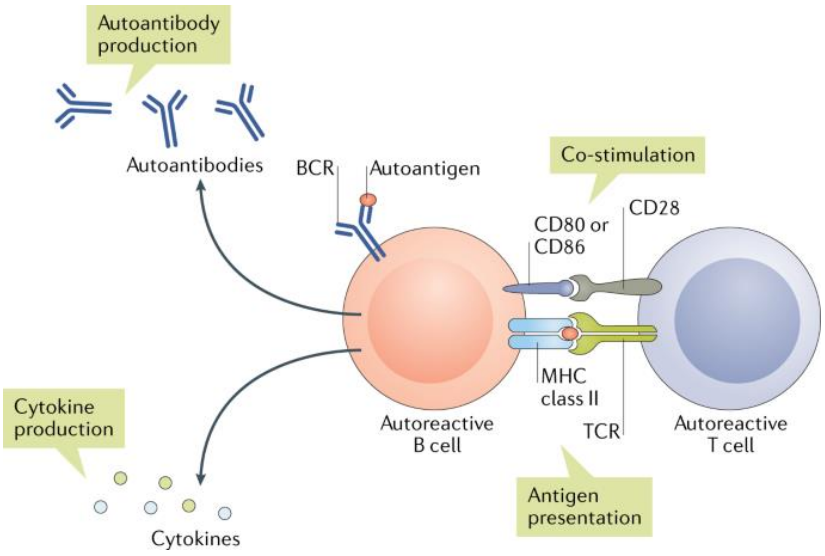

Figure 4. The functions of B cells in autoimmune disease. Central B cell functions, including antibody production, antigen presentation and T cell co- stimulation, and/or cytokine secretion, can all contribute to the pathogenesis of autoimmune diseases (from Rubin SJS. 2019 *(34)*).

This can happen as the result of the interplay between different activating and inhibitory receptors, serving as immune checkpoints that regulate activation and function of autoreactive B cells. Activating receptors include -among others- the antigen-specific BCR, TLRs (and in particular the TLR 9), several cytokine receptors (in particular IL6-R, IL21-R, BAFF-R), CD19, and CD40 *(34, 36, 51–54)*. Inhibitory receptors include the low-affinity immunoglobulin-γ Fc-region receptor IIb (FcγRIIb), CD22, programmed cell death 1 (PD1) and other receptors, which transmit inhibitory signals to B cells *(55, 56)*. Targeting these checkpoints that control B cell activation has therapeutic potential and represents the focus of current and future B cell research.

Autoreactive B cells in autoimmune diseases

Autoantibodies have been identified and studied for decades, but our understanding of the cellular processes underlying autoantibody production has been fairly limited until recently. Autoreactive B cells are responsible for autoantibody production in autoimmune diseases, such as anti-nuclear antibodies in lupus and anti-cyclic citrullinated protein antibodies in rheumatoid arthritis *(36, 57–60)*. The existence of circulating B cells bearing a BCR specific for an autoantigen has been postulated for years, but their reliable detection has been elusive until recently. In the past, several techniques have been used, such as Epstein–Barr virus transformation *(61)*, tracking the usage of V genes that are biased to be autoreactive *(62)*, flow cytometry or cloning approaches *(36, 63)*. The latter, a labor-intensive method which consists of the analysis for antigenic reactivity of cloned recombinant antibodies reconstituted from single B cells, allows the observation of significant differences between healthy individuals and autoimmune patients in a remarkable number of contexts *(64)*. Given the modern technological advances, quicker and accurate identification and isolation of human autoreactive B cells *in vivo* by flow cytometry and single cell sorting have now been made possible. By means of flow cytometry, human autoreactive B cells have been identified in SLE, RA, Pe and AAV (**Table 2**) *(36, 39, 71–75, 58, 60, 65–70)*.

Cell identification based on antigenically-defined specificity led to the evaluation of functionally relevant, and presumably pathologic cell populations, leading to the characterization of their phenotype, function, and active molecular pathways.

Table 2. The main human antigen-specific B cells identified in systemic autoimmune diseases detected by flow cytometry methods.

Autoimmune	Autoreactive B cells	Antigen(s)	Methods	Validation	Phenotype	Function	Molecular pathway(s)
SLE *(36, 37, 39, 57, 65, 66)*	ANA$^+$ B cells	Extractable nuclear antigen	Biotinylated nuclear antigens from HeLA cells	Single-cell cloning of Ig genes from ANA+ B cells, then testing reactivity with ELISA	yes	yes	yes
	ENA$^+$ B cells	Extractable nuclear antigen	Immunobeads-bound peptides	Ex vivo secretion in culture			
RA *(57, 58, 60, 67–69)*	CCP$^+$ B cells	Citrullinated antigens	FITC-labelled citrullinated vimentin (VIM), citrullinated type II collagen (cCOII), citrullinated fibrinogen (cFib), citrullinated tenascin-C (cTNC-5), cyclic citrulline peptide (CCP-1). Biotinylated cyclic citrulline peptide (CCP-2) by multicolor antigenic tetramer	Hybridoma assays; Ex vivo secretion in culture	yes	yes	yes
			Immunobeads bound peptides	Ex vivo secretion in culture			
Pe *(70–74)*	Dsg1$^+$/Dsg3$^+$ B cells	Desmoglein1-3	Histidine-tagged desmoglein 1 or desmoglein 3	Ex vivo stimulation of PBMC and enzyme-linked immunospot assay	yes	yes	yes
AAV *(75)*	PR3$^+$ B cells	Proteinase-3	FITC-labelled PR3, biotin-streptavidin PR3	Hybridoma assays	yes	-	-

Abbreviations: Systemic Lupus erythematosus (SLE); Rheumatoid arthritis (RA); Pemphigus (Pe); ANCA-associated vasculitis (AAV); Anti-nuclear antibodies (ANA).

In lupus, Betty Diamond's group significantly contributed by the identification of ANA$^+$ B cells in humans, and ANA$^+$ and dsDNA$^+$ B cells in lupus prone mouse models. Using their novel flow cytometry-based methodology, they were able to identify autoreactive B cells, to observe their progressive removal in SLE patients and healthy controls in the circulation, the restoration of anergy and the reduction of autoreactive naïve B cells in SLE patients treated with belimumab *(36, 65)*. They showed the aberrancy of B cell differentiation into plasma cells in lupus mice models and in SLE patients *(39)*,

demonstrating the presence of distinct profiles of ANA$^+$ antigen-experienced B cells in SLE *(66)*, which contributed to clarify pathways of autoreactive PBs/PCs differentiation *(37)*.

In RA, autoreactive class-switched memory B cells and PBs were shown not to be broadly cross-reactive to a range of citrullinated epitopes but, in contrast, to be characterized by a more restricted ACPA fine-specificity pattern, recognizing citrulline within a specific amino acid context beyond the citrulline residue itself *(58)*. These cells correlated with ACPA serum titres and spontaneous ACPA production in culture *(60, 67)*; they had a distinct molecular phenotype showing differential molecule expression or activation compared to non-autoreactive B cells of CD40, IL-7R, C5aR1 *(58)*, IL15Ra *(68)*, and CD80, CD86, Ki67, CD19 *(69)*, and were capable of producing epidermal growth factor ligand amphiregulin (AREG), TNF-alpha, IL-8, IL-6 *(68, 69)*.

Circulating antigen-specific B cells have also been detected in patients with Pe *(70, 71)*. The functional ability of anti-Dsm1 and anti-Dsm3 autoreactive clones to produce specific autoantibodies in *vitro* has been shown *(72)*, as well as the re-emergence of autoreactive clones related to the activation of BAFF pathways *(73)*, and the modification of the circulating fraction and of transcriptomic profile (precisely of IL-1beta, CD27 and IL-23p19 mRNA) after RTX treatment or standard glucocorticoid regimen *(74)*.

Circulating autoreactive B cells and their precursors in AAV will be discussed in the next paragraph. Besides these autoimmune systemic conditions, a few preliminary reports on the identification of autoreactive B cells in other autoimmune disease have been published *(76, 77)*.

Autoreactive B Cells in ANCA-Associated Vasculitis

The presence of circulating autoreactive B cells and their precursors has been postulated in AAV, with detection likely limited by their low frequency in peripheral blood. PR3 or MPO are the two main autoantigens identified in AAV. Our group first identified PR3-reactive B-cells ($PR3^+$ B cells) in a small number of AAV patients *(75)*.

We developed a customized flow-cytometry method to enumerate $PR3^+$ B cells, and observed a higher frequency of circulating $PR3^+$ B cells that were enriched within memory B cells and PBs in a small cohort of patients with PR3-AAV as compared to healthy controls (HC) *(75)*. Conversely, in HC the proportion of $PR3^+$ B cells was highest among the transitional B-cell subset and decreased with the maturation of B cells. We also observed a trend towards a higher proportion of $PR3^+$ B cells among patients with active disease compared to patients in remission: 2.91% (1.18-6.52) vs 0.99% (0.72-1.58).

The methodology by which we labelled autoreactive B cells first consisted of FITC-labelled recombinant PR3 (rPR3), and subsequently biotin-streptavidin conjugated rPR3, that binds to PR3-specific BCR, leading to the identification of the antigen-specific B cells (**Figure 5**) *(75)*. rPR3 was produced in Ulrich Specks' lab, by means of amino acid modifications rendering the rPR3 molecule enzymatically inactive while at the same time ensuring the original folding of the protein and preservation of conformational epitopes recognized by the autoantibodies (PR3-ANCA) *(78)*. The flow cytometry methodology we relied on was validated by staining hybridoma cell lines, which released and expressed on the cell surface antibodies recognizing human PR3 (MCPR3-2) *(79)*, antibodies directed against mouse PR3 (MCPR3-13)*(80)*, with no cross reactivity between the two species [21,25], and anti-human neutrophil elastase (HNE) antibodies *(81)*. No significant

staining was shown for MPCR3-13 and HNE hybridomas, while dose-dependent staining of MCPR3-2 hybridomas was observed, which was further validated by competition experiments with pre-incubation of PBMC with human and mouse rPR3 at different concentrations *(75)*.

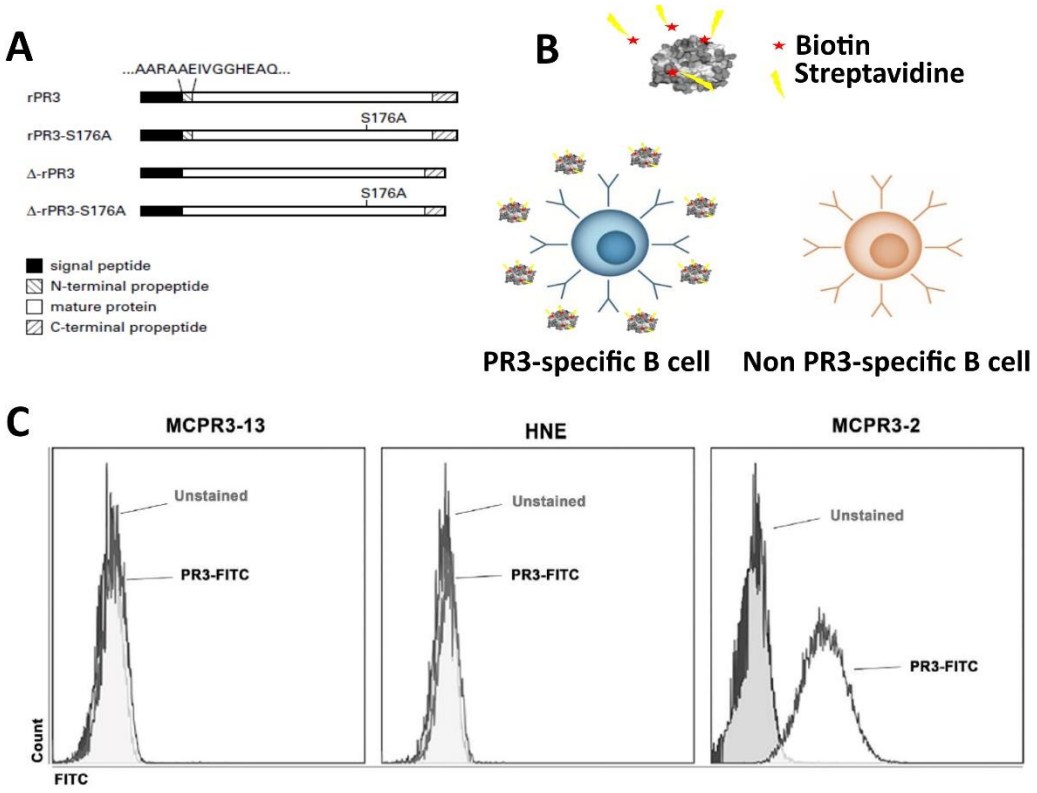

Figure 5. Customized flow cytometry-based assay labeling autoreactive B cells with recombinant PR3 (**A** from Sun J. 1998 *(78)*; **B**), **and validation by staining of hybridoma cell lines** (expressing mouse PR3-IgG, MCPR3-13; expressing human neutrophil elastase (HNE); expressing human PR3-IgG, MCPR3-2) (**C** from Cornec D. 2017 *(75)*).

Other observations of PR3$^+$ B cell detection are scant. Other groups focused on PR3$^+$ B cells *in situ* detection in inflamed tissues, based on the hypothesis that granuloma formation in AAV could represent ectopic lymphoid structures giving rise to autoantibody production *(82)(83)*. Using immunofluorescence staining for IgG and a common PR3-

ANCA idiotype (5/7 Id), the authors detected a few 5/7 Id+/IgG+ B cells in respiratory and kidney tissue of GPA. However, next-generation sequencing of IGHV and IGVL genes derived from respiratory tract tissue of AAV patients showed no identities and few similarities between these and anti-PR3 antibodies, arguing against a presence of B cells that carry PR3-ANCA-prone Ig genes among the clones *(82)*. It is conceivable that these results might have been influenced by technical limitations.

Notably, no data on MPO^+ B cells, the other main autoantigen of AAV, have been published so far, likely due to the significantly larger size of the MPO molecule and the lack of characterization of this protein as compared to PR3.

These preliminary data on autoreactive B cells in AAV call for a more precise elucidation of the mechanisms of the differentiation process leading to maturation of autoreactive B cells in AAV patients compared to healthy and disease controls, as well as for an investigation of the relationship between the frequency of PR3+ B cell subsets and the clinical and biological features of PR3-AAV.

Autoreactive B Cells in ANCA-Associated Vasculitis: A Human Model Of Autoimmune Vasculitis

B cells, ANCA and neutrophils interaction in AAV

B cells represent the source of pathogenic, isotype switched, high-affinity autoantibodies in AAV. Even if the autoreactive B cells have only recently been identified and represent a small fraction of the whole B cell pool *(75)*, the role of B cells has long been recognized

as being of central importance in AAV and going beyond their ability to produce autoantibodies *(84)(29)*. Another important study implicating B cells in AAV demonstrated the activation and the maturation of aggregated B-cells within endonasal inflammatory lesions of patients with granulomatosis with polyangiitis (GPA), one of the clinical subset of AAV, further arguing for a key role of B lymphocytes in the pathogenesis of AAV *(83)*.

From a clinical standpoint, this concept was validated by the results of several prospective randomized trials demonstrating the efficacy of RTX, an anti-CD20 monoclonal antibody, for AAV treatment *(85–88)*. The role of $CD19^+$ B cells as an immunological biomarker for disease monitoring in B cell-depleted patients emerged from these clinical studies, since relapses has been shown to be unlikely when a patient has no circulating B cell *(86)(89)(90)*.

Circulating ANCA, which target either PR3 or MPO, are the hallmark of AAV *(91).* These are the two major antigens of AAV and are usually mutually exclusive (i.e. patients with ANCA directed against PR3 do not have ANCA directed against MPO, and vice versa), while other antigens including bactericidal permeability-increasing protein (BPI), elastase, lysosome-associated membrane protein-2 (LAMP-2), cathepsin G, lysozyme, and lactoferrin are only rarely identified as targets for ANCA *(92)(93)*. The immunofluorescence pattern of ANCA distinguishes cytoplasmic ANCA (c-ANCA), mostly targeting PR3, and perinuclear ANCA (p-ANCA), generally targeting MPO *(94)*. Distinguishing the different types of AAV by autoantigen specificity rather than clinicopathologic items has been proposed for classification purposes because the presence of PR3-ANCA versus MPO-ANCA conveys unique biological and clinically useful information *(94, 95)*.

A number of clinical and basic science studies have supported the hypothesis of the pathogenic role for ANCA in the development of AAV *(94)*. Due to the availability of a murine model for MPO-AAV, the evidence for the pathogenic role of ANCA is stronger for MPO-ANCA than for PR3-ANCA, which has shown nonetheless the same proinflammatory effects in *in vitro* experimentation (92). The disease process, which is best documented for capillaritis (such as glomerulonephritis), happens in two steps *(96)*. First, neutrophils are primed by low-level exposure of proinflammatory cytokines such as tumor necrosis factor (TNF) and Interleukin 1 (IL1), usually as a consequence of an underlying infection. Priming of neutrophils results in surface expression of MPO, PR3 and other substances of neutrophil granules (e.g. lactoferrin, gelatinase, elastase, etc.) and promotes neutrophil adhesion to the endothelial surface of blood vessels. In the second step, neutrophils are activated by interactions with ANCA by binding to neutrophils Fc receptors and/or to antibody substrate, leading to the rapid release of reactive oxygen species (respiratory burst), preformed proteases, mediators of inflammations and chemotactic factors for neutrophils and other cells of the immune system, ultimately leading to inflammation, endothelial injury and tissue damage *(96, 97)*. Hence, neutrophils appear to be the downstream effectors of inflammation in AAV.

ANCA have been shown to have *in vitro* a cytolytic effect on endothelial cells through the activation of neutrophils and the interaction with the alternative pathway of complement system (especially with C5a and the C5a receptor). Charles Jennette's group showed that this occurs also in the mouse model *(98)*, and that there are surrogates of complement activation in renal histologic samples *(99)*. ANCA-stimulated neutrophils can also release chromatin fiber, called neutrophil extracellular traps (NETs), in which

autoantigens MPO and PR3 can be stored, further representing a persistent source of autoantigens and contributing to inflammation maintenance *(100)*.

The histologic hallmark of AAV is a segmental vascular necrotizing inflammation with infiltrate of neutrophils and monocytes, associated with leukocytoclasia and fibrinoid necrosis. This leads often to small-vessel vasculitis and capillaritis, clinically manifesting as purpura (venulitis of the derma), alveolar pulmonary hemorrhage, and hematuria due to crescentic glomerulonephritis *(91, 101)*. Unlike the subset of disease called microscopic polyangiitis (MPA), granulomatosis with polyangiitis (GPA) and eosinophilic GPA (EGPA) are characterized by extravascular granulomatous inflammation, predominantly involving the respiratory tract *(91, 101)*. Immunofluorescence demonstrates minimal deposition of immunoglobulins and complement, hence the so called “pauci-immune” vasculitis, in contrast to immune-complex deposition vasculitides such as SLE or cryoglobulinemic vasculitis, or other small-vessel vasculitides as Henoch-Schönlein purpura or anti-glomerular basement membrane disease *(91, 101)*.

The clinical spectrum of ANCA-associated vasculitis

AAV is defined as a group of systemic, necrotizing vasculitides predominantly affecting small-sized blood vessels *(91)*, encompassing a few major clinic-pathologic variants, i.e. GPA, MPA, and EGPA. The spectrum of clinical manifestations is wide and overlapping, and all the forms of AAV share the clinical features directly due to capillaritis and small-vessel vasculitis (**Figure 6**) *(91)*. The latest annual incidence reported for AAV overall is 3.3 per 100.000, with a prevalence of 42.1 per 100,000, substantially increasing in the last decades *(102)*.

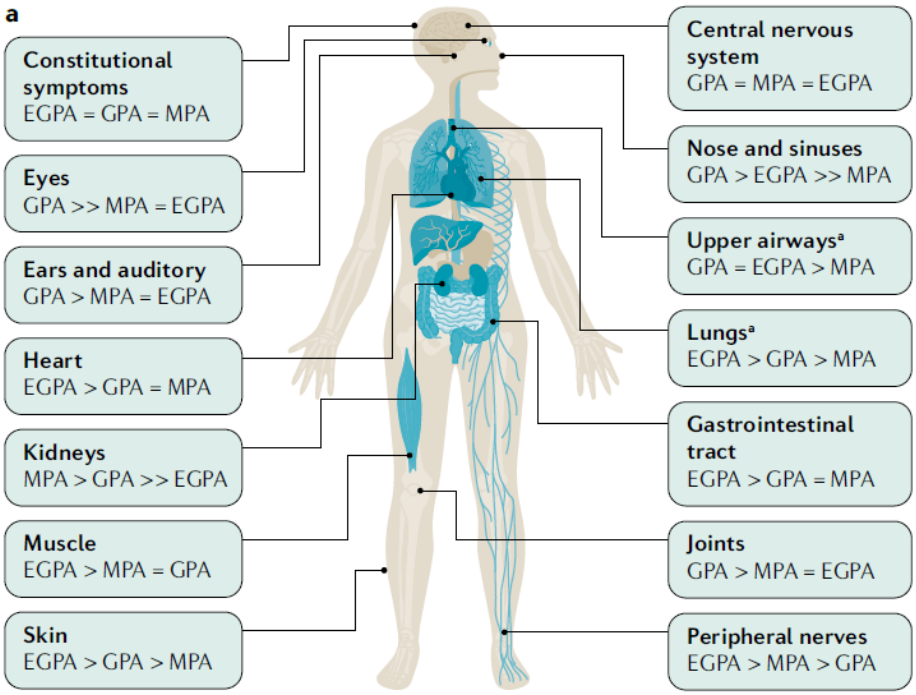

Figure 6. Clinical features of AAV: organ involvement in granulomatosis with polyangiitis (GPA), microscopic polyangiitis (MPA) and eosinophilic GPA (EGPA) (from Kitching RA. 2020 *(91)*).

Clinical manifestations of GPA can be heterogeneous, often affecting the upper and lower respiratory tract, with characteristic destructive lesions in the nasal septum, lung infiltrates, and cavities. Glomerulonephritis is usually more severe and more often detected in patients with MPA, while asthma (often severe) and peripheral hypereosinophilia are unique features of EGPA *(91, 103, 104)*. EGPA represents approximately 10-20% of patients with AAV, and it is treated as a separate entity from GPA and MPA in all the clinical trials and in the latest guidelines *(105)*. Therefore, I will refer from now on only to GPA and MPA when writing on AAV, unless clearly stated otherwise.

All AAV subsets are often associated with the presence of circulating ANCA, and the clinical utility of ANCA serotype stratification (PR3-ANCA versus MPO-ANCA) could provide timely and clinically relevant diagnostic information more readily than clinical syndromes based on current classification systems *(94, 95)*. A higher number of organs are usually involved in PR3-AAV, while renal involvement and pulmonary fibrosis occur more frequently in patients with MPO-AAV *(106)*. Recent data suggest that ANCA specificity seems to have stronger associations with genetic predisposition *(107)*, circulating cytokines *(108, 109)*, response to therapy *(110)*, relapse risk *(111, 112)*, and long-term renal prognosis *(113)* than with clinical diagnoses. Only a relatively small proportion of patients with clinical and pathological features of GPA and MPA show a negative result for ANCA by routine clinical assays (from 10% to 30%) *(94)*, and likely represent a different subset of the disease, with a different pathogenesis *(114)*. The 2012 revision of Chapel Hill Consensus Conference (CHCC) proposed the combination of a prefix indicating the ANCA type, with a suffix indicating the clinical phenotype *(115)*, both contributing to a more precise stratification of patients in mutually exclusive categories (i.e., PR3-GPA, PR3-MPA, MPO-MPA, MPO-GPA, and ANCA negative forms) *(116, 117)*.

The current classification criteria for AAV are not consistent with disease definitions (e.g., American College of Rheumatology (ACR) 1990 criteria exist only for GPA and EGPA, yet not for MPA), and they do not include ANCA testing, which is now routinely used in clinical practice *(115, 118, 119)*. In 2007, to reach a consensus about how to apply the already available nomenclature and classification criteria for AAV, a stepwise algorithm merging the CHCC and ACR criteria was developed by European Medicines Agency

(EMA) *(120)*. Currently, the ACR and the European Alliance of Associations for Rheumatology (EULAR) have undertaken an international effort to develop new diagnostic and classification criteria for systemic vasculitides, the “Diagnostic and Classification Criteria of Vasculitis (DCVAS)” study, the publications of which are expected soon *(121)*.

Disease activity is usually quantified by the Birmingham Vasculitis Activity Score (BVAS), which is a validated tool assessing nine organ systems frequently involved in AAV, and which represents the most widely accepted score for the evaluation of disease activity *(122)*. BVAS for Wegener’s granulomatosis (BVAS/WG) *(123)*, mostly used in USA, and the most recently revised version of the BVAS mainly used in Europe, BVASv.3 *(124)*, have both been consistently shown to be sensitive to change with regard to the activity of disease and are both currently used in clinical trials.

Treatments and outcomes of the disease

With the standard treatment of high-dose glucocorticoids and either cyclophosphamide or RTX, remission is achieved in 70 to 90% of GPA and MPA cases according to the definition of remission *(85)(125)*. However, only a minority of these patients (around 30%) seem to remain relapse-free after 10 years of follow-up *(126)*. Therefore, after remission-induction, a low dose of less toxic immunosuppressive agent with or without glucocorticoids is usually required to avert relapses. Azathioprine, methotrexate, or mycophenolate mofetil have traditionally been used, but recent RCTs have shown that remission maintenance use of RTX is more effective, especially for those patients at higher risk of relapse, although the most appropriate dose and timing of retreatment with

RTX remain unclear (87,105,125,127). These current therapies, however, are associated with an increased risk of infection *(128)* and particularly in the case of glucocorticoids, with progressive damage accrual and complication *(129, 130)*.

A recent metanalysis showed a 2.7-fold increase in mortality among patients with AAV compared with the general population with the latest population-based and cohort studies showing worst survival for renal-AAV and MPA, with a trend toward improvement in survival rate lately, likely due to the improvements in therapy and management of the disease *(131)*. Accordingly, a recent retrospective analysis showed a statistically significant increment of the 5-year survival rate from 72.2% for patients diagnosed before 1980 to 94.5% of those with AAV diagnosed after 2010 *(132)*. Nowadays, the major cause of death are infection and cardiovascular disease, and not disease severity anymore *(128, 132, 133)*.

Despite this remarkable improvement in remission-induction, relapse-free survival remains a major issue, and the main current unmet clinical need. In fact, the relapse rate ranges from 25% to 70% in different studies *(86, 126)*, with a remarkable variability among patients. A clinical diagnosis of GPA, the presence of circulating PR3-ANCA, and having a relapsing course are non-independent risk factors for relapse, and patients with all these features carry the highest risk regardless of the treatment used to keep the disease under control *(86, 95, 111, 112)*.

While the utility of ANCA testing for diagnostic purposes has been widely accepted, the clinical utility of ANCA as a biomarker for relapse prediction remained a matter of debate despite numerous investigations *(112, 134–138)*. Recently, a single-center study found that an increase in ANCA level (PR3-ANCA or MPO-ANCA) was predictive of relapses,

particularly in patients who had presented with renal involvement, and in those with nonrenal severe disease *(136)*, while in the RAVE cohort, PR3-AAV patients treated with RTX who experienced a rise in ANCA titer during complete remission had an increased risk of relapse, particularly severe relapse, especially in those with renal involvement or alveolar hemorrhage *(112)*. However, a clear role for serial ANCA measurements in AAV has not been established, thus is not recommendable to make treatment decisions based only on changes in ANCA titers *(139)*. This inconclusive results regarding longitudinal ANCA measurements might be due to methodological issues (including the sensitivity to change of the various different assays used in different studies), the ANCA serological type, the AAV subset (i.e. GPA versus MPA), and the treatment chosen to induce or maintain remission *(140)*.

Overall, relapse prevention is biggest unmet need nowadays, particularly in patients who are PR3-ANCA positive at diagnosis, i.e. PR3-AAV, which are more prone to relapse. In fact, every relapse increases the damage from disease and treatment toxicity. Accurate relapse prediction requires that patients at high risk of relapse, and therefore in need of preventive therapy, can be distinguished from those that are at low risk, and therefore without the need of prevention therapy. Several studies longitudinally assessed the ANCA titer in patients for monitoring disease activity, but collectively this approach has been found suboptimal. Consequently, a better understanding of the pathogenesis underlying AAV is needed and holds the key to novel biomarkers or predictors of relapse.

Aims of the thesis

Little is known about the autoreactive B cells in AAV. We aimed to investigate the circulating autoreactive PR3$^+$ B cells involved in the development of human AAV.

The aims of this thesis can be summarized as follows:

1. ***Aim #1****: Phenotypic and functional characterization of autoreactive PR3$^+$ B cells*

   To (i) confirm and expand our preliminary observations in a large, well-characterized cohort of patients with PR3-AAV as compared to patients with MPO-AAV as disease controls and HC, (ii) elucidate the peripheral tolerance checkpoints and the mechanisms of the differentiation process leading to mature PR3$^+$ B cell selection in PR3-AAV during the active phase of the disease, as compared to MPO-AAV and HC, and (iii) investigate the relationship between the frequency of PR3$^+$ B cell subsets and the clinical and biological features of PR3-AAV.

2. ***Aim #2****: The ontogeny of PR3$^+$ B cells*

   To investigate the presence and the specific phenotypic features of PR3$^+$ B cells in bone marrow mononuclear cell (BMMC) samples of HC, comparing them to paired PBMC samples of HC and PBMC of PR3-AAV patients, and evaluating the central tolerance checkpoint(s) for PR3$^+$ B cells in the BM.

3. ***Aim #3****: Longitudinal dynamics of PR3$^+$ B cells after B cell depletion*

   To investigate the longitudinal changes of autoreactive PR3$^+$ B cells in PBMC from patients with severe PR3-AAV who had achieved complete remission with RTX and glucocorticoids within 6 months after initiation of remission-induction therapy. We hypothesized that RTX-induced B cell depletion would alter the proportions of

circulating B cell subsets within the autoreactive pool and investigated whether any features of these changes during follow-up were associated with relapse.

This research activity has led so far to the submission of two papers (corresponding to aim #1-3 of the thesis, Berti A et al. “Circulating Autoreactive Proteinase 3^+ B Cells and Tolerance Checkpoints in ANCA-Associated Vasculitis”. *Under revision in JCI Insight*; Berti A et al. “Autoreactive plasmablasts after B cell depletion with RTX and relapses in ANCA-associated vasculitis” under revision at *Arthritis and Rheumatology*), while another additional paper is currently in preparation (corresponding to aim #2 of the thesis, Berti A et al. “Identification of the central tolerance checkpoint for autoreactive proteinase 3^+ B cells in human bone marrow”). In addition to this, I wrote or significantly contributed to other research papers on the biology of circulating B cells and cytokines related to the pathogenesis of AAV, as well as on the epidemiology and the clinical outcomes of AAV (listed in the Appendix).

Aim #1: Phenotypic and functional characterization of autoreactive PR3$^+$ B cells

Summary Aim #1

Background and Rationale: Circulating autoreactive B cells are responsible for autoantibody production in autoimmune diseases, including ANA in lupus, and anti-CCP antibodies in rheumatoid arthritis. Little is known about the autoreactive B cells in AAV. The presence of circulating IgG-secreting cells and their B-cell precursors bearing a BCR specific for PR3 or MPO has been postulated in AAV, but investigation of these cells has been limited by their low frequency in peripheral blood. Using multicolor flow cytometry in combination with bioinformatics and functional studies, we investigated tolerance checkpoints of circulating autoreactive PR3$^+$ B cells in a large cohort of patients with AAV.

Results: The frequency of PR3$^+$ B cells among circulating B cells was higher in PR3-AAV (4.77% [3.98%-6.01%]), than in MPO-AAV (3.16% [2.51%-5.22%]), and in AAV compared to HC (1.67% [1.27%-2.16%], $p<0.001$ for all comparisons), implying a defective central tolerance checkpoint in AAV patients. Only PBMC from PR3-AAV contained PR3$^+$ B cells capable of secreting PR3-ANCA IgG in vitro, and among B cells of PR3-AAV patients only PR3$^+$ B cells secreted PR3-ANCA IgG in vitro, proving to be functionally distinct from those of MPO-AAV and HC. Unsupervised clustering identified subtle subsets of atypical autoreactive PR3$^+$ memory B cells accumulating through the maturation process in PR3-AAV patients. PR3$^+$ B cells were enriched in the memory B cell compartment of PR3-AAV, and were associated with higher serum CXCL13 levels, suggesting an increased

germinal center activity. PR3^{+} B cell maturation correlated with higher systemic inflammation (CRP and ESR, $p<0.05$) and lower remission rate ($p<0.001$).

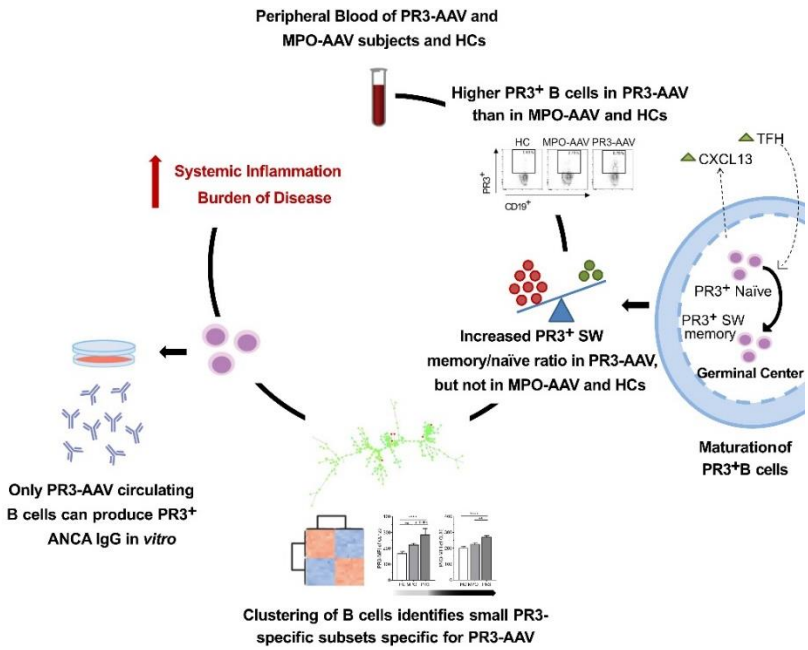

Figure 7. Aim #1 graphical summary. Overview of the set of experiments: phenotypic and functional characterization of autoreactive PR3^{+} B cells in AAV.

Implications: This study suggests the presence of defective central antigen-independent and peripheral antigen-dependent checkpoints in patients in PR3-AAV, elucidating the selection process of autoreactive B cells in this rare autoimmune disease. To our knowledge, this study is the first to decipher the mechanisms of autoreactive B-cell maturation in AAV, analyzing samples of data obtained from a large, well-characterized cohort of patients. Our findings clarified the maturation of B cells bearing the BCR directed towards PR3 that we characterized phenotypically and functionally, and explored biological and clinical associations with autoreactive B cells in PR3-AAV, paving the way for potential novel disease biomarkers and more specific targeted therapy approaches.

Results Aim #1

Perturbations of circulating B cell subsets are similar in patients with PR3-AAV and MPO-AAV

In this first set of experiments, the PBMC of 105 PR3-AAV subjects, 49 MPO-AAV subjects and 27 HC were studied. The characteristics of the participants are shown in **Supplemental Table 1**. Age, sex and other baseline clinical features differed between PR3-AAV and MPO-AAV, as expected and previously reported. In particular, manifestations considered to be expression of capillaritis were more frequent in MPO-AAV subjects, while those clinical manifestations considered to be expression of necrotizing granulomatous inflammation were significantly more represented in PR3-AAV.

We observed that B-cell homeostasis was abnormal in AAV compared to HC (gating strategy **Figure 8A;** percentages of total B cells and B cell subsets in **Figure 8B-C**), confirming previous studies *(90, 141–144)*. The absolute counts of both PR3-AAV and MPO-AAV participants showed higher numbers of circulating B cells and higher numbers of naïve and double negative (DN) B cells than HC (**Supplemental Figure 1A-C**). We further dissected the B-cell pool using the SPADE algorithm (**Supplemental Figure 1D**). Overall, the B-cell clusters segregated PR3-AAV participants from HC when directly compared (principal component analysis in **Figure 8D**, unsupervised hierarchical clustering heat map in **Supplemental Figure 1E**), but not from MPO-AAV participants, meaning that the two groups of patients display similar disturbances in B cell homeostasis compared to HC (**Figure 8E**, **Supplemental Figure 1F**).

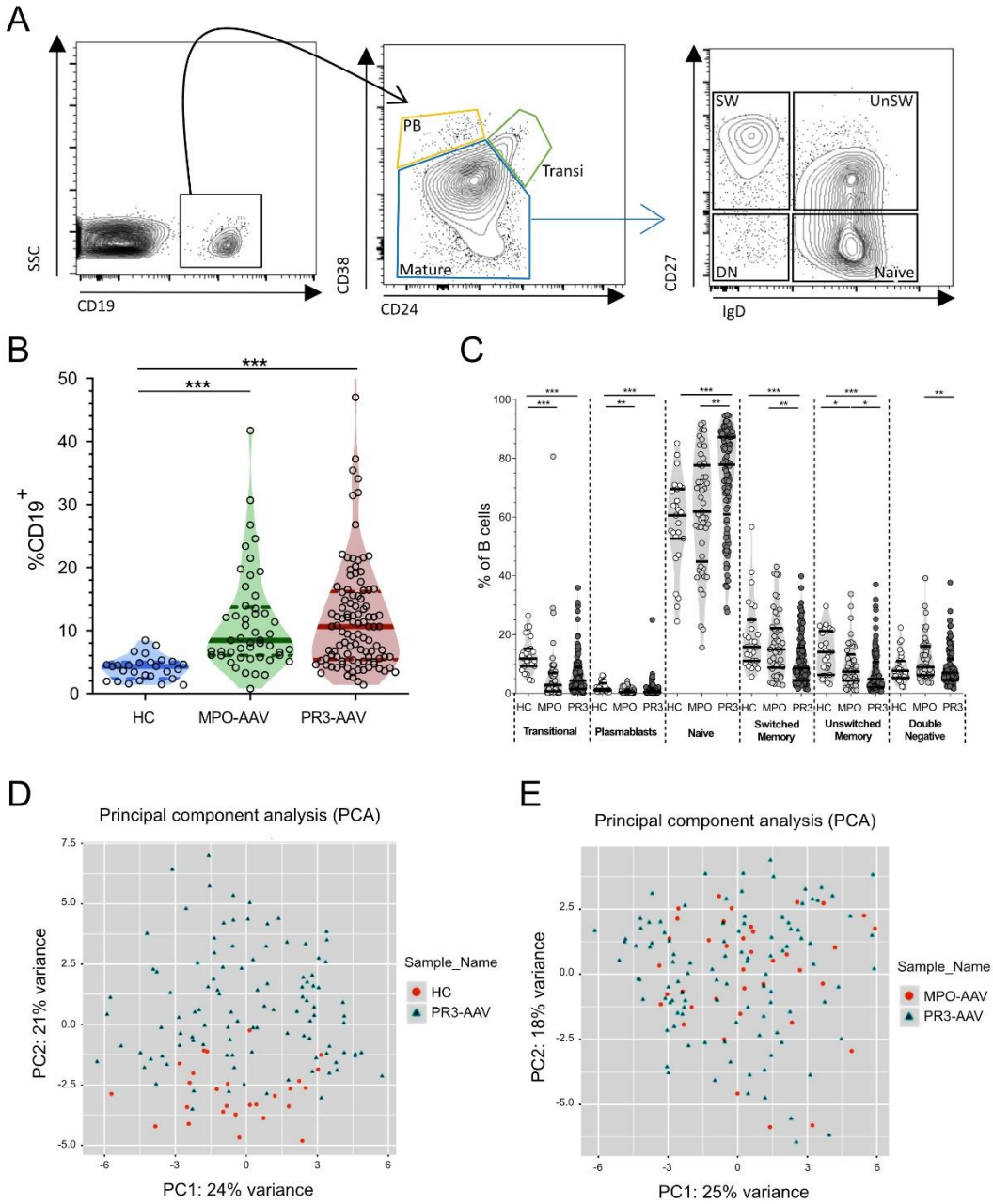

Figure 8. Circulating B cells in patients with PR3-AAV, MPO-AAV and HC subjects. Gating strategy used to define B cell subsets (**A**). CD19^{+} cells were first categorized based on CD24 and CD38 expression, in transitional (transi, CD24^{high}CD38^{high}), plasmablasts (PB, CD24^{-}CD38^{high}), and mature B cells (CD24^{+}CD38^{+}). Mature B cells were further classified into four populations: naïve (CD27^{-}IgD^{+}), unswitched memory (UnSW, CD27^{+}IgD^{+}), switched memory (SW, CD27^{+}IgD^{-}), and double negative (DN, CD27^{-}IgD^{-}). B cells frequency and subset distribution were overall similar in PR3-AAV (n=105) and MPO-AAV (n=49), but different compared to HC (n=27) (**B-C**). Principal component analysis of the 200 B cell clusters obtained with SPADE (Spanning-tree Progression Analysis of Density-normalized Events) representing HC subjects and PR3-AAV trial participants (**D**) and MPO-AAV and PR3-AAV participants (**E**). Data represent median (25-75% IQR). Multiple comparisons between more than 2 groups were performed with Kruskal-Wallis test and P values in the figures are indicated as * $p < 0.05$, ** $p < 0.01$, *** $p < 0.001$ after correction for FDR with Benjamini and Hochberg test.

Circulating PR3$^+$ B cells are higher in patients with PR3-AAV than in controls

PR3$^+$ B cells were detected in PBMC from patients with PR3-AAV and MPO-AAV, as well as HC subjects (representative plots shown **Figure 9A**). Patients with PR3-AAV had higher frequencies and absolute numbers of PR3$^+$ B cells compared to MPO-AAV and HC (median [25-75% IQR], PR3-AAV 4.77% [3.98%-6.01%] *versus* MPO-AAV 3.19% [2.51%-5.22%] *versus* HC 1.67% [1.27%-2.16%], $p<0.001$ for all comparisons; PR3-AAV 5.55 [3.09-9.64] cells/µl *versus* MPO-AAV 3.09 [2.02-8.81], $p<0.05$, and MPO-AAV *versus* HC 0.95 [0.58-1.31] cells/µl, $p<0.001$), confirming and expanding the findings from our previous report *(75)* (**Figure 9B**-**C**). Notably, no significant detectable effect of glucocorticoids on the levels and percentages of lymphocytes, B cells, PR3$^+$ B cells and other T cell specific subsets was observed (**Supplemental Table 2**).

PBMC from patients with PR3-AAV contain PR3$^+$ B cells capable of secreting PR3-ANCA IgG in vitro

Supernatants from PBMC cultures from patients with PR3-AAV contained significantly higher levels of anti-PR3 IgG than those from MPO-AAV and HC subjects ($p<0.001$, **Figure 9D**), showing that PR3$^+$ B cells from patients with PR3-AAV are functionally distinct from their counterparts from MPO-AAV patients and HC.

Then, we sought to assess whether PR3$^+$ B cells that can be detected among PBMC by FACS are responsible for the in-vitro secretion of anti-PR3 immunoglobulin. We measured the frequency of PR3$^+$ secreting cells (IgM and IgG) by ELISPOT after stimulation. After sorting PR3$^+$ and PR3-negative B cells from B cell-enriched PBMC of HC (**Supplemental Figure 2A-B**), we found that circulating PR3$^+$ B cells from HC are

able to produce PR3-ANCA IgM, but not PR3-ANCA IgG. Furthermore, we could not detect any PR3-specific antibody secretion in PR3-negative cells, demonstrating that our detection method ensures a full recovery of circulating PR3$^+$ B cells within the PR3$^+$ B cell pool as detected by FACS.

The significant correlation between anti-PR3 IgG levels from in vitro cultures and in vivo serum levels in PR3-AAV participants (**Figure 9E**, **Supplemental Figure 2C**) suggests that circulating PR3$^+$ B cells from patients with PR3-ANCA can serve as *bona fide* precursors of PR3-ANCA IgG secreting cells in vivo.

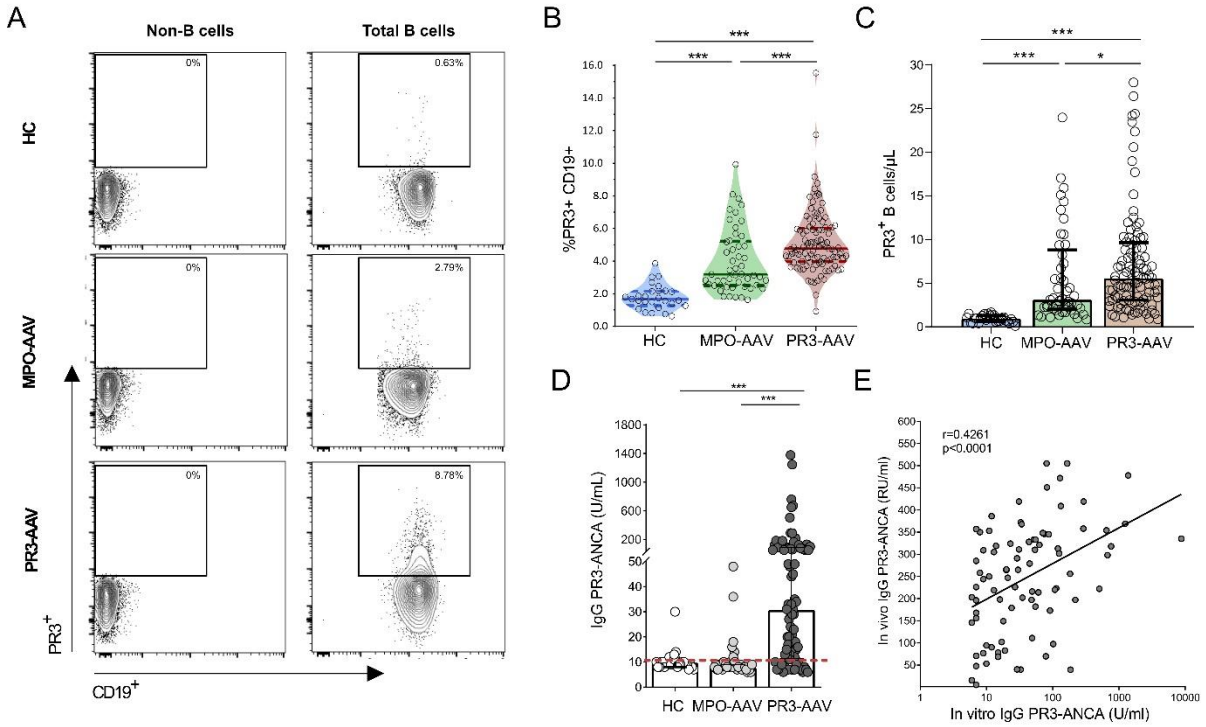

Figure 9. Circulating PR3$^+$ B cells and PR3-ANCA production in patients with PR3-AAV, MPO-AAV and HC subjects. Representative examples of the gating of PR3$^+$ positive B cells among total CD19$^+$ cells in a PR3-AAV patient, a MPO-AAV patient and a HC subject (**A**). PR3$^+$ B cells frequency and count were increased in PR3-AAV (n=105) compared to MPO-AAV (n=49) and HC (n=27) (**B-C**). PBMC were cultured to promote differentiation into antibody-secreting cells, after which PR3-ANCA secretion was analyzed by means of Phadia ImmunoCAP 250 analyzer (**D**). Only PR3-AAV subjects can producePR3-ANCA IgG in vitro. Correlation of circulating (in vivo) PR3-ANCA IgG with secreted (in vitro) PR3-ANCA IgG in PR3-AAV subjects (**E**). Data represent median (25-75% IQR). Multiple comparisons between more than 2 groups were performed with Kruskal-Wallis test. P values in the figures are indicated as * $p < 0.05$, ** $p < 0.01$, *** $p < 0.001$ after correction for FDR with Benjamini and Hochberg test.

Functional validation of autoreactive PR3$^+$ B cells by flow cytometry

To prove that autoreactive PR3$^+$ B cells identified by flow cytometry bear BCR that recognize the PR3$^+$ antigen, we performed a functional validation. We sorted PR3$^+$CD19$^+$ and PR3$^-$CD19$^+$ cells from PBMC obtained from 3 PR3-AAV patients at the time of active disease, cultured for 4 days with CpG, CD40L, IL-2, IL-10 and IL-15 to promote B cell maturation and Ig production, after which antigen-specific antibody secretion in the supernatant was analyzed by means of enzyme-linked immunosorbent assay (ELISA) (**Figure 10**). Significantly, we detected PR3-ANCA IgG only in the supernatant of the PR3$^+$CD19$^+$ cell culture**.** We also performed histological staining of B cells harvested at day 4 for a qualitative assessment, showing signs of B cell activation and initial cytoplasmic IgG accumulation, suggestive of an initial differentiation towards antibody-secreting cells in both PR3$^+$CD19$^+$ and PR3$^-$CD19$^+$ cells.

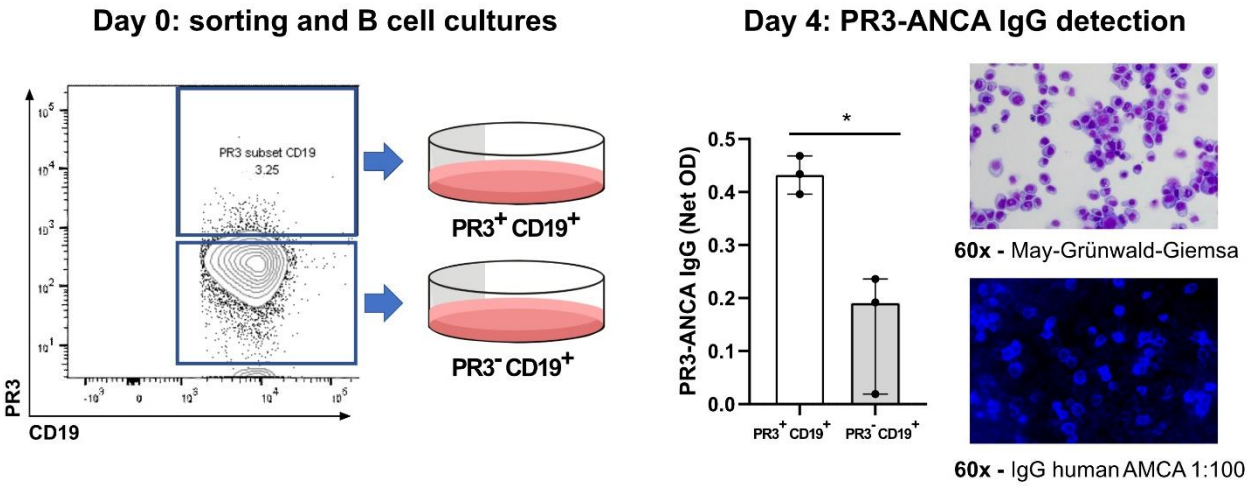

Figure 10. Functional validation of autoreactive PR3$^+$ B cells by sorting PR3$^+$ and PR3$^-$ B cells. PR3$^+$ and PR3$^-$ B cells were sorted and cultured for 4 days (**A**). PR3-ANCA IgG from sorted PR3$^+$ and PR3$^-$ B cells as measured by ELISA (**B**), and representative staining of cytospin smears at day 4 with May-Grünwald Giemsa to assess B cell activation and with anti-human IgG AMCA in immunofluorescence to assess initial cytoplasmic IgG accumulation. P values were determined by 2-tailed Wilcoxon matched-pairs signed rank test. P values in the figure is indicated as * for $p < 0.05$.

Autoreactive PR3$^+$ memory B cells accumulate through the maturation process only in patients with PR3-AAV.

The frequency of PR3$^+$ B cells within each of the different B-cell subsets was higher in PR3-AAV than in MPO-AAV, and in AAV overall compared to HC, implying a defective central tolerance checkpoint in patients compared to HC (**Figure 11A**; representative plots are shown in **Supplemental Figure 3)**. B-cell subsets within the PR3$^+$ B-cell pool were similarly distributed in PR3-AAV, MPO-AAV, and HC, except higher levels of mature B cells in PR3-AAV and MPO-AAV compared to HC ($p<0.001$) (**Figure 11B**).

To better understand whether rare subsets of PR3$^+$ B cells were specifically enriched in patients with PR3-AAV compared to controls, we identified PR3-reactive B cell clusters defined by the SPADE algorithm significantly more represented or activated in PR3-AAV. Among the 200 B-cell nodes, 6 clusters of cells displayed a stable increased reactivity for PR3 across all the samples in HC, MPO-AAV and PR3-AAV participants (**Figure 12A-B,** phenotypic characterization in **Table 3**). Among these 6 stable PR3$^+$ clusters, we observed a significant enrichment of PR3$^+$ cells in CL57, CL93, CL160 and CL185 (Bm2/naïve and transitional clusters) in PR3-AAV subjects compared to MPO-AAV and HC (**Figure 12C**), confirming a deficient central checkpoint (controlling the maturation of immature B cells towards transitional and naïve mature B cells).

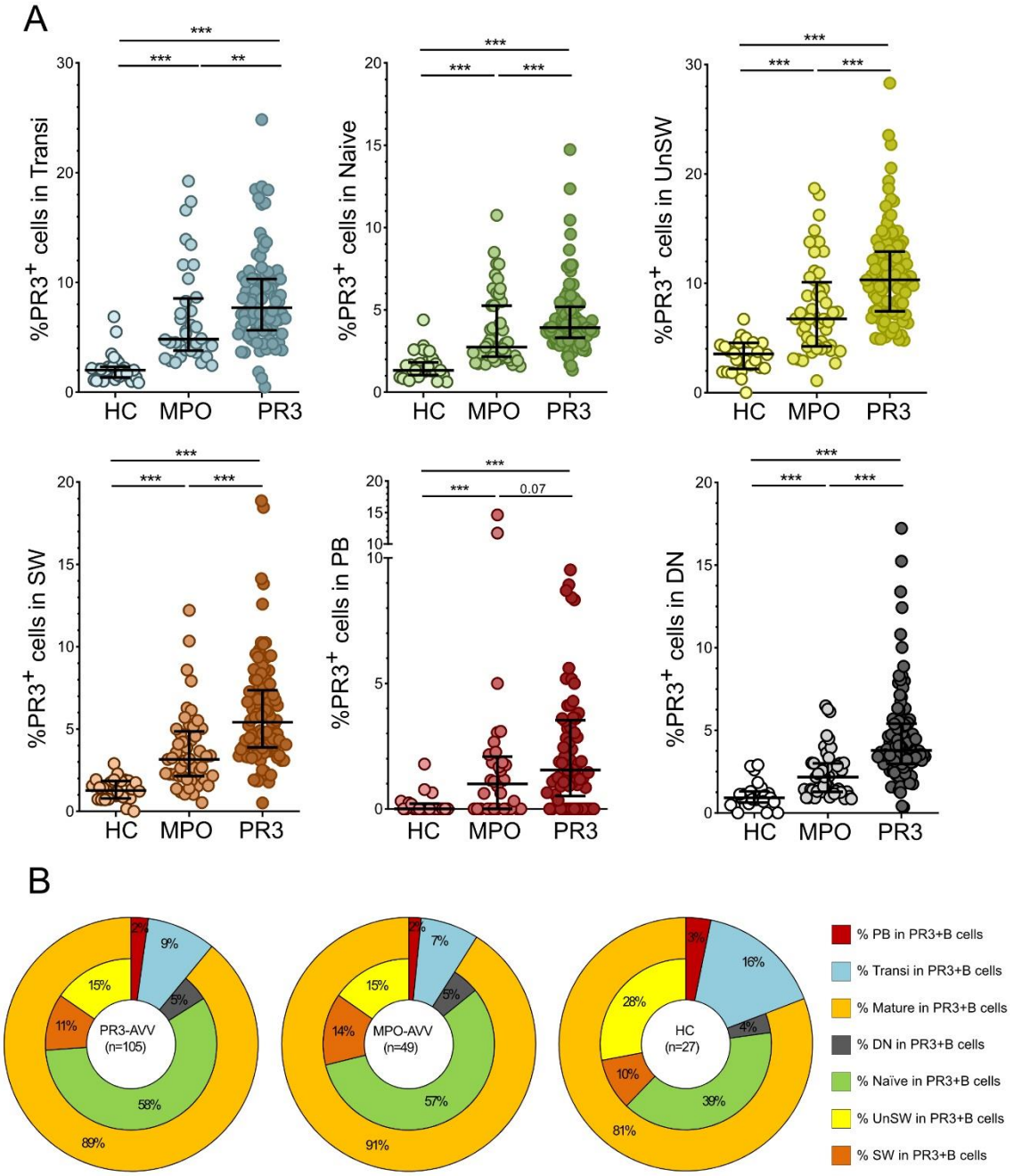

Figure 11. Frequency of PR3⁺ B cells within each B cell subset. Scatterplots depicting the frequency of PR3⁺ B cells within each B cell subset in HC (n=27), MPO-AAV subjects (n=49), and PR3-AAV subjects (n=105) (**A**). B cell subset distribution within PR3⁺ poll in PR3-AAV and MPO-AAV patients and HC subjects (**B**). Data represent median (25-75% IQR). Multiple comparisons between more than 2 groups were performed with Kruskal-Wallis test. P values in the figures are indicated as * $p < 0.05$, ** $p < 0.01$, *** $p < 0.001$ after correction for FDR with Benjamini and Hochberg test.

The investigation of the MFI of the PR3 BCR in these transitional/naïve clusters (**Figure 12D, Supplemental Figure 4A**) revealed a marked reduction in CL160, CL187, CL93, and CL140 in patients with AAV, a hallmark of chronically activated or anergic cells. In contrast, the PR3 BCR MFI was significantly higher in five other clusters (CL86, CL129, CL104, CL132, CL155), belonging to the memory compartments, suggesting the presence of defective peripheral checkpoints in AAV. Clusters CL104 and CL132 (corresponding to switched activated memory cells) and CL155 (corresponding to plasmablasts, PB) were increased in AAV subjects with no significant differences between PR3-AAV and MPO-AAV (**Figure 12E**), and a PR3-specific defect was identified in the clusters CL86 and CL129 (corresponding to the DN $IgD^{-}CD27^{-}CD38^{-}$ subset) only in PR3-AAV patients (**Figure 12F**).

We therefore repeated the manual gating analysis using a more conservative strategy to identify $PR3^{+}$ B cells with the highest reactivity ($PR3^{high}$) (gating strategy **Figure 12G, left**), and observed that similar to the frequency of total $PR3^{+}$ B cells (**Figure 9B**), the frequency of $PR3^{high}$ B cells was significantly increased in PR3-AAV compared to MPO-AAV and HC (**Figure 12G, central**). Consistent with the unsupervised cluster analyses, enrichment of $PR3^{high}$ B cells among the peripheral pool of DN B cells distinguished PR3-AAV from both MPO-AAV and HC (**Figure 12G, right; Supplemental Figure 4B).**

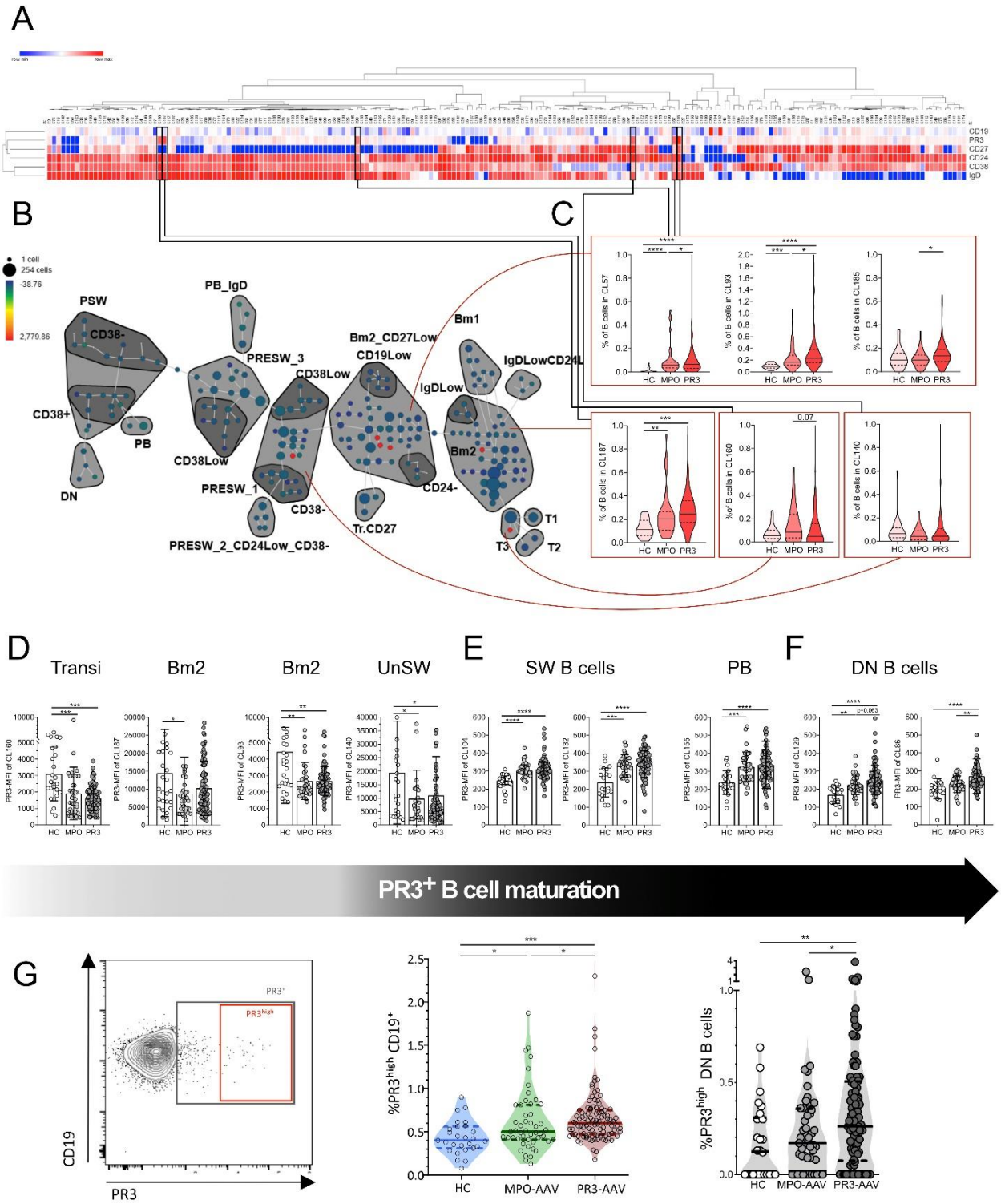

Figure 12. Selected PR3⁺ B cell clusters significantly more represented or activated in PR3-AAV patients. Six out of 200 clusters showed a stable expression of PR3 on the membrane of the B cells (**A**). A processed SPADE explanatory image of one PR3-AAV subject showing the most relevant clusters grouped by conventional subsets (**B**). In red, the six clusters of B cells with a stable increased reactivity for PR3 across all the samples, and their frequencies (**C**). The MFI of 4 out of these 6 clusters is reduced in

AAV compared to HC (**D**). Additional 5 clusters that significantly varied MFI between HC and AAV: the MFI of clusters within the SW memory and PB are increased in AAV compared to HC (**E**), and 2 clusters within the DN showed a relative MFI increase in PR3-AAV compared to MPO-AAV and HC (**F**). A more conservative gating approach ($PR3^{high}$) (**G**, left), showing the increase of $PR3^{high}$ B cells in PR3-AAV compared to MPO-AAV participants and HC (**G**, central). Among B cell subsets, $PR3^{high}$ B cells were significantly increased only in the DN subset in PR3-AAV participants compared to MPO-AAV participants and HC (**G**, right). Each point represents the frequency in an individual subject; horizontal lines show the median with 25-75% IQR, each histogram represents mean (± SD). Multiple comparisons between more than 2 groups were performed with one-way ANOVA or Kruskal-Wallis test, where appropriate. P values in the figures are indicated as * $p < 0.05$, ** $p < 0.01$, *** $p < 0.001$, **** $p < 0.0001$ after correction for FDR with Benjamini and Hochberg test. MFI stands for mean fluorescence intensity.

Table 3. Phenotypic characterization of selected $PR3^+$ B cell clusters.

Cluster ID	Phenotype	Main Population
Stable Clusters		
CL 160	IgD^+ $CD24^{high}$ $CD38^{high}$ $CD27^-$	Transitional
CL 187	IgD^+ $CD24^+$ $CD38^+$ $CD27^-$	Bm2
CL 185	IgD^+ $CD24^+$ $CD38^{low}$ $CD27^{low}$	Bm2 $CD27^{low}$
CL 93	IgD^+ $CD24^+$ $CD38^+$$CD27^{low}$	Bm2 $CD27l^{ow}$
CL 57	IgD^+ $CD24^+$ $CD38^{low}$ $CD27^{low}$	Bm2 $CD27^{low}$
CL 140	IgD^+ $CD24^+$$CD38^{low}$ $CD27^+$	UnSW 1
Variable Clusters		
CL 104	IgD^- $CD24^+$ $CD38^+$ $CD27^+$	SW $CD38^+$
CL 132	IgD^- $CD24^{low}$ $CD38^+$ $CD27^+$	SW $CD38^+$
CL 155	IgD^- $CD24^-$ $CD38^{++}$ $CD27^{++}$	PB
CL 129	IgD^- $CD24^+$ $CD38^-$ $CD27^-$	DN $CD38^-$
CL 186	$IgD^-$$CD24^+$ $CD38^+$ $CD27^-$	DN $CD38^+$

Selection of mature PR3$^+$ B cells and determinants of the maturation of autoreactive B cells

When comparing the frequencies of PR3$^+$ B cells in each B-cell subset within each disease group, we observed a significant decrease in the frequencies of PR3$^+$ B cells from transitional to naïve, from unswitched (UnSW) to switched (SW), and from SW to PB in all the groups, illustrating the different layers of control of the peripheral checkpoints (**Figure 13A**).

PR3-AAV participants showed a higher frequency of PR3$^+$ B cells in the SW compartment compared to the naïve one, while MPO-AAV subjects and HC did not (**Figure 13B**).

To illustrate the differential enrichment of PR3$^+$ B cells during the maturation process, we computed a ratio of the frequency of PR3$^+$ within SW B cells over the frequency of PR3$^+$ within naïve B cells. The median ratio was < 1 in HC and MPO-AAV subjects but was > 1 in PR3-AAV participants (**Figure 13C**), with approximately one third of HC, half of the MPO-AAV and almost three quarters of the PR3-AAV participants with a ratio >1 (**Supplemental Figure 5A**).

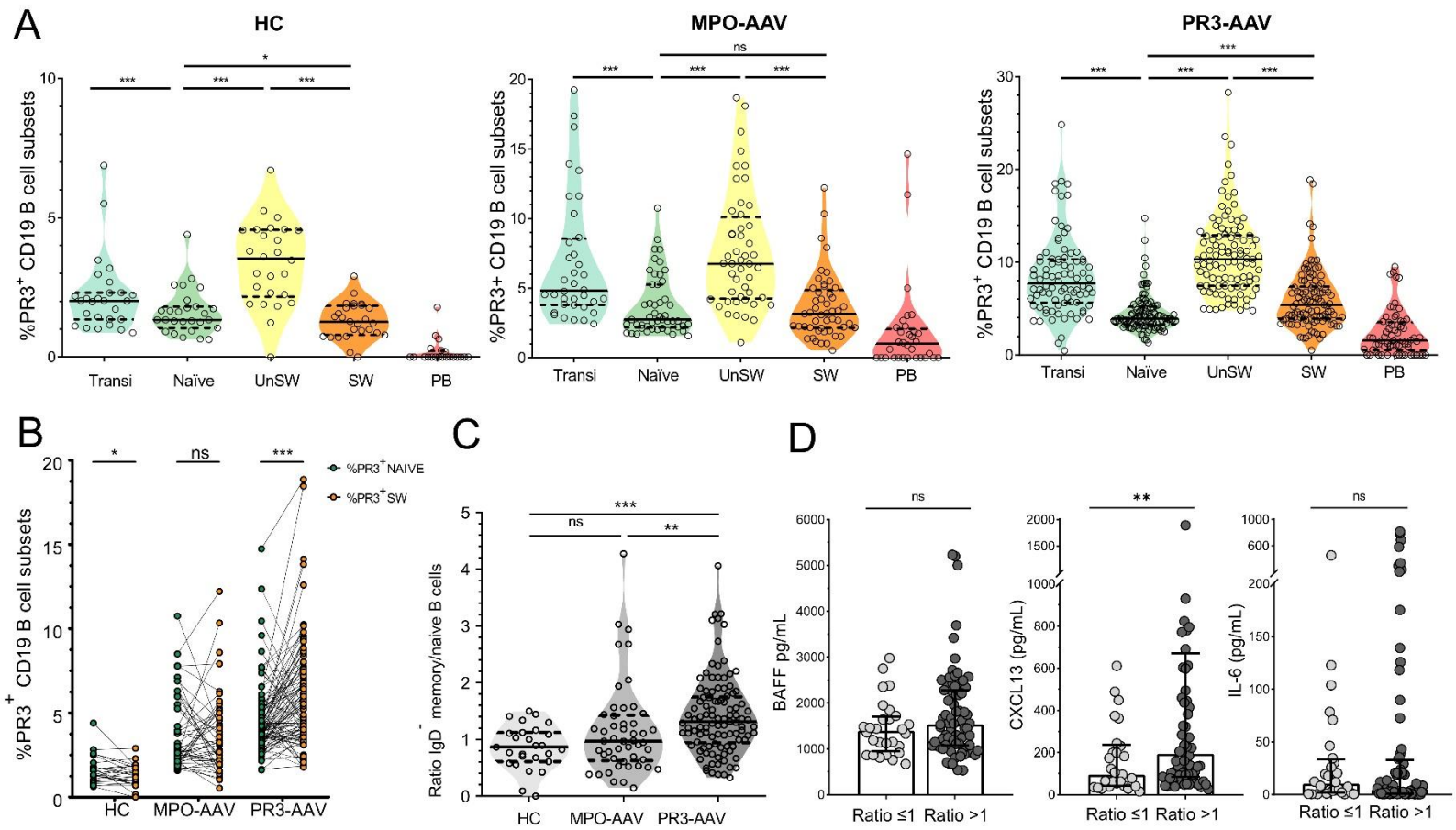

Figure 13. Maturation of PR3⁺ B cells among different participant groups. Scatterplots depicting the different frequency of PR3⁺ B cells within each B cell subsets through the maturation process in HC subjects (n=27), in MPO-AAV (n=49) and in PR3-AAV participants (n=105). The multiple comparisons on B cell maturation were analyzed by using mixed-effects modelling. (**A**). Paired comparisons between PR3⁺ naïve and SW mature PR3⁺ B cells showing the enrichment of memory B cells in PR3-AAV, but not in participants with MPO-AAV and HC (**B**). Ratio between the frequency of PR3⁺ B cells among IgD⁻ switched memory and the frequency of PR3⁺ B cells among naïve B cells (**C**). Each point represents the frequency in an individual subject; horizontal lines show the median with 25-75% IQR**.** Multiple comparisons among more than 2 groups were performed with Kruskal-Wallis test. Selected cytokine (BAFF, CXCL13, IL-6) levels by SW memory/naïve PR3⁺ B cell ratio in PR3-AAV patients. P values were determined by 2-tailed Mann-Whitney test (**D**). P values in the figures are indicated as * $p < 0.05$, ** $p < 0.01$, *** $p < 0.001$ after correction for FDR with Benjamini and Hochberg test.

In addition to having higher proportions of PR3$^+$ SW B cells relative to the proportions of PR3$^+$ naïve B cells (accounting for a higher ratio), PR3-AAV participants with a ratio >1 compared to those ≤1 had higher levels of circulating PR3$^+$ PB and DN B cells and lower levels of transitional B cells, suggesting that the ratio reflects an overall higher degree of PR3$^+$ B cells maturation (**Table 4**).

Table 4. Baseline PR3$^+$ B cell subsets by switched memory/naïve B cell ratio in PR3-AAV.

PR3$^+$ B cell subsets	Ratio ≤1	Ratio >1	p value
Transitional, median % (25-75% IQR)	8.95 (6.79; 13.54)	7.28 (5.26; 10.02)	**0.031**
Naïve, median % (25-75% IQR)	4.55 (3.70; 7.49)	3.82 (3.11; 4.68)	**0.005**
Unswitched memory, median % (25-75% IQR)	9.77 (7.00; 13.46)	10.63 (8.03; 12.86)	**0.538**
Switched memory, median % (25-75% IQR)	3.39 (2.39; 4.42)	6.41 (4.38; 8.29)	**<0.001**
Plasmablasts, median % (25-75% IQR)	0.96 (0; 1.89)	1.88 (0.91; 3.64)	**0.029**
Double Negative, median % (25-75% IQR)	3.18 (2.42; 3.49)	4.23 (3.29; 6.16)	**<0.001**

PR3: proteinase 3; AAV : ANCA-associated vasculitis; IQR: interquartile range.

Data represent median (25-75% IQR). P values were determined by 2-tailed Mann-Whitney test.

We measured the relationship between PR3$^+$ B cell maturation and serum cytokine levels potentially implicated, which were similar between MPO-AAV and PR3-AAV subjects (**Supplemental Figure 5B**). While B-cell activating factor (BAFF) and interleukin

(IL)-6 did not show any association with PR3$^+$ B-cell maturation in PR3-AAV subjects, C-X-C motif ligand 13 (CXCL13) levels were higher in those with a SW memory/naïve ratio >1 compared to those with a ratio ≤1 (**Figure 13D**), suggesting a higher germinal center reaction *(145)* for PR3-AAV participants with a SW memory/naïve ratio >1.

The absolute numbers of chemokine receptor 5 (CXCR5), programmed cell death-1 (PD-1), T follicular helper cells (CXCR5$^+$PD-1$^+$ Tfh) were significantly elevated in PR3-AAV and MPO-AAV compared to HC (**Supplemental Figure 5C-D**), in line with observations made by others *(146)*, and we observed that circulating Tfh count and frequency were lower in participants with PR3-AAV with a SW memory/naïve ratio >1 compared to those with a ratio ≤1 (**Supplemental Figure 5E**). Together, these results support the activation of the germinal center machinery to promote PR3-reactive B cell maturation in participants with PR3-AAV *(147)*.

Maturation of PR3$^+$ B cells and clinical manifestations in PR3-AAV subjects

The PR3$^+$ SW memory/naïve B cell ratio did not show significant correlations with clinical and demographic features (**Figure 14A-C** and **Supplemental Figure 6A-E**). However, subjects with ratio >1 had higher markers of inflammation, i.e. C-reactive protein (CRP) serum levels and a erythrocyte sedimentation rate (ESR) compared to those with a ratio ≤1 (**Figure 14D**), but disease activity assessed by BVAS/WG did not show an association with this ratio (**Figure 14E**).

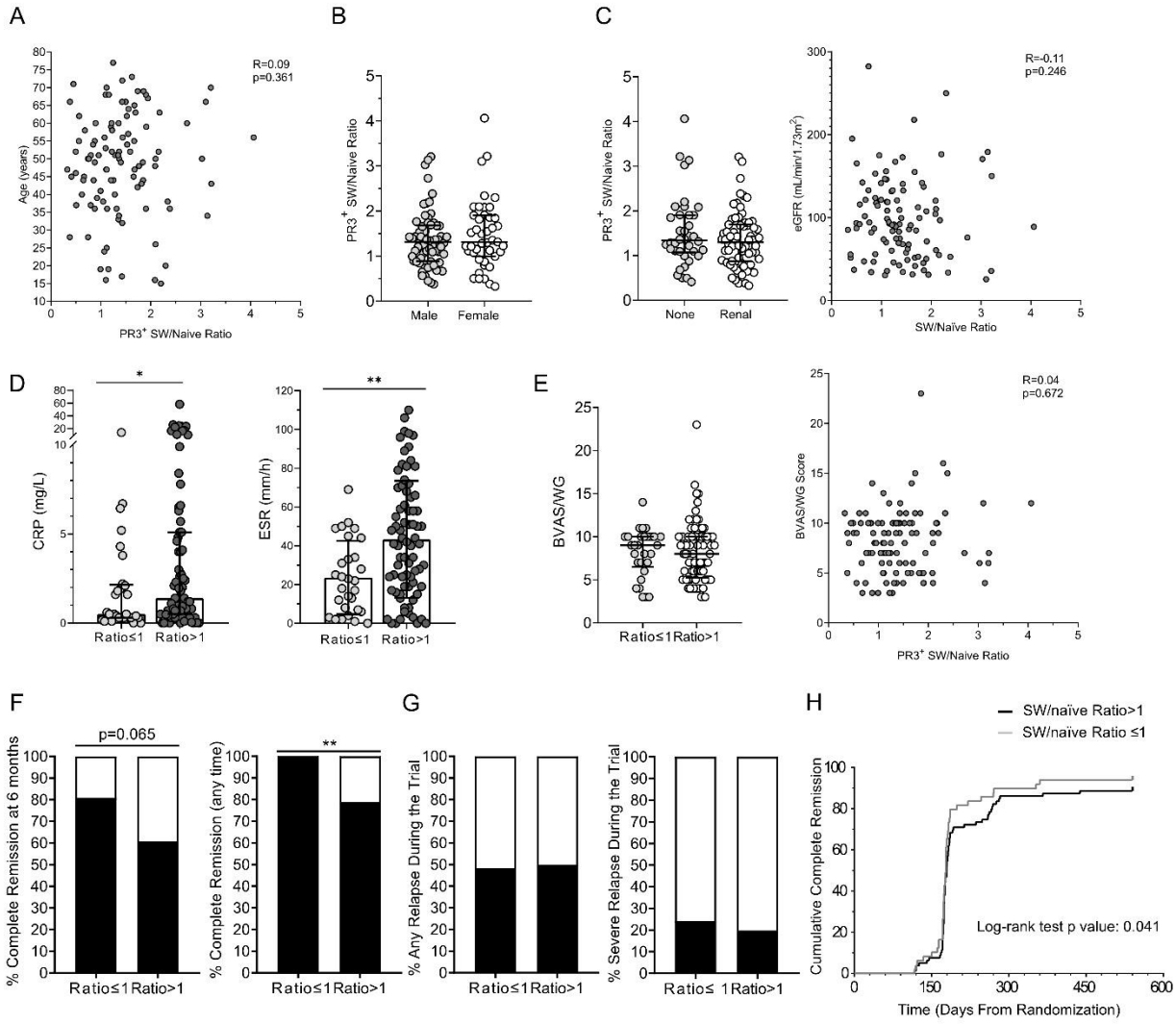

Figure 14. SW memory/naïve PR3⁺ B cell ratio and clinical manifestations in PR3-AAV patients. In PR3-AAV participants (n=105), SW memory/naïve PR3⁺ B cell ratio did not correlate with age (**A**), sex (**B**), or renal manifestations (**C**), but higher levels of CRP and ESR were associated with a ratio >1 (**D**). The ratio did not correlate with disease activity as assessed by BVAS/WG (**E**). Associations with complete remission definitions (**F**), future relapse and severe relapse (**G**), and time to complete remission (**H**) are represented. When evaluating associations with remission, the patients that underwent cross over (n=7) or experienced early treatment failure (n=6) during the trial time were excluded from the analysis.
Data represent median (25-75% IQR), while histograms represent proportions. P values were determined by 2-tailed Mann-Whitney test or Fisher's test, where appropriate. Spearman's test and the Kaplan–Meier method with the log-rank test was used to test correlations and time to event, respectively. P values in the figures are indicated as * $p < 0.05$, ** $p < 0.01$, *** $p < 0.001$.

Whereas participants with ratio ≤1 tended to achieve complete remission at 6 months more frequently than those >1 (80.8% vs. 60.6%, respectively, p=0.0649; primary endpoint of the trial, defined as BVAS/WG=0 and Prednisone=0), 100% of participants

with ratio ≤1 achieved complete remission at any time during the observation period compared to less than 80% in those with ratio > 1 ($p \leq 0.001$) (**Figure 14F**). Time-to-complete remission (**Figure 14H**) and time-to-first remission (BVAS/WG=0) (**Supplemental Figure 6F**) were significantly shorter in subjects with ratio ≤1 compared to ratio >1. Future relapse and severe relapse were not associated to this ratio (**Figure 14G**). No striking correlations between the frequency of $PR3^+$ B cells and the demographic, disease activity, and major clinical features was observed (**Supplemental Figure 7**).

Taken together, a $PR3^+$ SW memory/naïve B cell ratio >1 seems to be associated with higher degrees of systemic inflammation and slower response to treatment.

Discussion Aim #1

Here, we confirm our previous findings *(75)* in a large well-characterized cohort of patients with AAV with active disease, and show that patients with PR3-AAV have higher circulating levels of $PR3^+$ B cells compared to healthy and disease controls, suggesting a general defect in B-cell tolerance in AAV compared to HC. Notably, only circulating B cells from PR3-AAV secrete PR3-ANCA IgG under appropriate stimulation, reflecting their in vivo activity. While the frequency of $PR3^+$ B cells decrease as B cells progress through the maturation checkpoints in AAV and HC, there appears to be a preferential enrichment of $PR3^+$ B cells in the memory B-cell subsets of patients with PR3-AAV. This phenomenon is accompanied by signs of germinal center activation, suggesting an antigen-specific breach in this layer of control of peripheral B-cell maturation. The selection of these autoreactive B cells through the different B cell compartments results in an accumulation of autoreactive $PR3^+$ memory B cells, particularly in $PR3^+$ DN subsets. The association between the maturation of $PR3^+$ B cells, as reflected by the IgD^- memory/naïve ratio, with CRP, ESR and complete remission suggest a link between autoimmunity and systemic inflammation in AAV.

Interestingly, when focusing on the frequency of $PR3^+$ B cells within each cell subset, the frequency of $PR3^+$ B cells was also elevated in patients with MPO-AAV compared to HC, suggesting a defect in an early central tolerance checkpoint due to impaired selection of B cells before the transitional stage in both PR3- and MPO-AAV patients. Self-reactive human pre- or pro-B cells are usually eliminated before reaching the naïve B cell stage by receptor editing or clonal deletion, while antigen-experienced B cell populations are further excluded by induction of anergy and follicular exclusion*(35,*

148–151). A possible mechanism contributing to the increase of PR3$^+$ B cells in MPO-AAV might be a non-specific defect in clonal anergy predisposing to autoimmunity*(152)*, since levels of the circulating PR3 antigen are increased in both PR3-AAV and MPO-AAV compared to HC as a consequence of neutrophil activation. A possible explanation of the subsequent tolerance failure in PR3-AAV, but not in MPO-AAV patients, might be the interplay between different genetic factors and autoreactive PR3$^+$ B cells. It is well documented that MPO-AAV and PR3-AAV have different HLA and non HLA-gene associations, i.e. for PR3-AAV the HLA-DP and the genes encoding for α1-antitrypsin (SERPINA1) and PR3 (PRTN3) *(153)*. Even though both MPO-AAV and PR3-AAV patients have increased levels of autoreactive PR3$^+$ B cells, only those from PR3-AAV patients are able to maturate and produce PR3-ANCA IgG possibly because of the genetic predisposition conferred by these genes. Beside the HLA, mutations of the genes coding for the PR3 antigen, the PR3-specific B cell receptor (i.e. an ANCA immunoglobulin) and possibly the α1-antitrypsin inhibiting PR3, might increase the affinity of this tripartite interaction leading to a breach in immune tolerance. However, despite this mild increase of PR3$^+$ B cells in MPO-AAV, only circulating B cells of patients with PR3-AAV can produce PR3-ANCA IgG, suggesting that only patients with PR3-AAV can provide adequate T-cell help that may be instrumental to bypass anergy mechanisms.

From a methodological perspective, our customized flow cytometry-method using rPR3 as a ligand was already proven to be specific for human PR3-BCR expressed by hybridoma cell lines *(75)*. In contrast with studies of other disease such as SLE or RA, characterized by autoreactive B cells recognizing nuclear extracts, dsDNA, and CCP that are usually more difficult to detect for different reasons, studies in patients with AAV may

be easier because PR3 is a very well characterized protein of moderate size (29-33 kDa), allowing the use of the whole protein as antigen source *(75, 80)*. This is of relevance considering that most PR3-ANCA target conformational surface epitopes of the molecule *(80)*. To further validate that the B cells identified by FACS as $PR3^+$-specific B cells indeed represent autoreactive B cells, we isolated and cultured among the PBMC of a small group of patients with active AAV the $PR3^+$-$CD19^+$ and $PR3^-$-$CD19^+$ populations by FACS. After 4 days, all the $PR3^+$ and $PR3^-$-$CD19^+$ cells showed initial differentiation towards antibody-secreting B cells, but PR3-ANCA IgG were detected by ELISA exclusively in the supernatant of the $PR3^+$ B cells. These data prove that $PR3^+$ B cells genuinely represent B cells capable of producing ANCA upon stimulation, thus confirming specificity of the staining, similarly to what has been documented for other diseases *(36, 67)*.

The hierarchical B-cell clustering provided evidence of qualitative differences among the different patient groups. Patients with AAV seem to display a more permissive microenvironment, leading to the emergence of autoreactive B-cell clones while $PR3^+$ B cells progress through the maturation stages. Importantly, we identified rare subsets of atypical autoreactive $PR3^+$ memory B cells accumulating through the maturation process in PR3-AAV as compared to MPO-AAV and HC subjects. A similar Ag-specific defect has recently been identified for ANA secreting B cells as a source of pathogenic antibodies in SLE*(32)*. DN B cells have characteristics of memory B cells and are thought to represent a source of autoreactive antibody-secreting plasmablasts in SLE*(32)*.

Patients with PR3-AAV showed a higher degree of maturation of $PR3^+$ B cells compared to both disease and healthy controls, as represented by a significantly higher

PR3$^+$ IgD$^-$ memory/naïve ratio and a higher frequency of subjects with ratio >1 compared to MPO-AAV subjects and HC. Serum CXCL13 levels were significantly increased, and the proportion of Tfh cells was decreased in patients with PR3-AAV with a PR3$^+$ ratio >1 compared to those with ratio ≤1, suggesting an increased germinal center activity in patients with PR3-AAV with a higher PR3$^+$ IgD$^-$ memory/naïve ratio. B-cell maturation takes place in germinal centers of secondary lymphoid tissue or in tertiary lymphoid organ structures in inflamed target tissues in patients with autoimmune diseases, where the interaction of the recruited antigen-specific B cells with cytokines and cells (i.e. activated Tfh cells) leads to expansion, differentiation, and ultimately positive selection of antibody-secreting B cells and memory B cells*(7, 154–156)*. One limitation of our study is that lymphoid tissue from patients with AAV was not available, which impaired a direct assessment of the germinal center microenvironment. Therefore, we measured selected circulating cytokines, such as CXCL13, previously shown to reflect germinal center activation in lymph nodes in clinical and preclinical models of autoimmune and infectious diseases, as well as circulating Tfh *(145, 157)*. Altogether, these data support the maturation process of PR3$^+$ B cells ultimately leading to a preferential enrichment of PR3$^+$ B cells in the memory compartment of patients with PR3-AAV as compared to those with MPO-AAV and HC subjects.

From a clinical perspective, the PR3$^+$ SW memory/naïve B cell ratio seems to correlate with the degree of systemic inflammation as measured by the serological markers of inflammation used in clinical practice, CRP and ESR, and by the time to achieving complete remission, but not with disease activity scored by the BVAS/WG, an instrument that iterates all disease manifestations affecting a patient within a 28 day

period leading up to the date of the biological sampling. BVAS/WG has sensitivity to measure disease activity to guide the need of immunosuppressive treatment, but it is probably a suboptimal gauge of systemic inflammation at a specific point in time when serum, plasma and PBMC are collected. Overall, our findings suggest a possible link between the maturation of $PR3^+$ B cells and the burden of systemic inflammation of the disease, an observation that requires confirmation in future clinical studies.

This work has also several potential limitations. First, glucocorticoids were allowed by the trial protocol prior to obtaining the baseline samples, and therefore this could have potentially influenced the results of the analyses. However, we observed no significant detectable effect of glucocorticoids on the levels and percentages of lymphocytes, $CD19^+$B cells, $PR3^+$ B cells, and Tfh cells, as shown. Second, all the samples studied were frozen (most of the samples, those from the clinical trial, from 2010) and therefore are at least a decade old. Previously published studies suggested that cryopreserved cells can be stored for at least 12 years with no general tendency toward cell loss over time *(158)*. Furthermore, no statistically significant changes in the percent cell viability according to the length of time frozen have been reported, regardless of HIV serostatus or the level of CD4+ lymphocytes, and without changes in fluorescence intensity in subsequent flow cytometry for most of the subsets (including CD19 cells) *(159, 160)*. As mentioned, another limitation of the study is that lymphoid tissue from patients with AAV was not available, impairing a direct assessment of the germinal center microenvironment. We also we did not use disease controls other than MPO-AAV, such as lupus, pemphigus, rheumatoid arthritis, or other autoantibody-mediated autoimmune diseases that would indeed be of interest, especially for the assessment of the antigen-

independent, central checkpoint. However, this require a very costly and time-consuming dedicated effort which unfortunately is beyond the scope of this study; furthermore, no other study that has identified antigen-specific autoreactive B cells in other autoimmune diseases had access to and has used disease controls.

In conclusion, with this first set of experiments we elucidate for the first time the positive selection of autoreactive $PR3^+$ B cells in PR3-AAV responsible for generating a distinct subset of mature autoreactive B cells in the peripheral circulation which are likely the source of PR3-ANCA IgG in vivo, beginning to unravel the layers of control that are deficient in patients with AAV and that promote the development of PR3-ANCA.

Aim #2: The ontogeny of PR3$^+$ B cells

Summary Aim #2

Background and Rationale: We observed that, as compared to HC, the frequency of circulating PR3$^+$ B cells was elevated in patients with PR3-AAV and MPO-AAV, even if only PR3$^+$ B cells of PR3-AAV were able to produce PR3-ANCA IgG. This suggests a defect in an early central tolerance checkpoint, before the transitional B cell stage in both AAV forms. We were intrigued by this unexpected finding, hence we investigated this central tolerance checkpoint controlling immature PR3$^+$ B cells in the BM, before B cells migrate into the peripheral blood as transitional B cells. We investigated the presence and the specific phenotypic features of PR3$^+$ B cells in BMMC samples of non-vasculitis controls (No-AAV), comparing them to paired PBMC samples of No-AAV and PBMC of PR3-AAV patients, and to evaluate the central tolerance checkpoint for PR3$^+$ B cells.

Results: The proportion of PR3$^+$ B cells within BMMC of No-AAV subjects (median [IQR25-75%]; 1.98% [1.77-2.75]) was similar to their proportion within PBMC of PR3-AAV patients (1.82% [1.66-3.21]; $p>0.05$), while it was significantly higher than within PBMC of No-AAV subjects (0.9% [0.63-1.44], $p<0.01$ by paired comparison). PR3-BCR membrane expression on total B cells was higher in PBMC of AAV patients as compared to BMMC and PBMC of No-AAV subjects ($p<0.05$). When focusing on immature/transitional CD24^{++}CD38^{++} B cells only in No-AAV subjects, we observed distinct phenotypes within BMMC versus PBMC (i.e. higher proportion of CD27$^-$CD10$^+$ cells and lower expression of CD21, IgD, IgM within BMMC versus PBMC), representing two separate developmental stages of B cell maturation. BMMC contained the greatest proportion of PR3$^+$ B cells within CD24^{++}CD38^{++} B cells, as compared to PBMC (3.35%

[1.99-4.92] versus 1.23% [0.62-1.55], p<0.01). Within this population in BMMC, we observed a significant decline of the PR3$^+$ fraction from T1-like/immature subset (IgD$^-$ IgM$^+$; 2.80% [1.23-4.02]) to T2-like/early transitional subset (IgD$^+$IgM$^+$; 1.76% [0.96-2.68], p<0.01), while no significant reduction was observed between the latter subset and the transitional compartment of PBMC (1.26% [0.62-1.56], P>0.05).

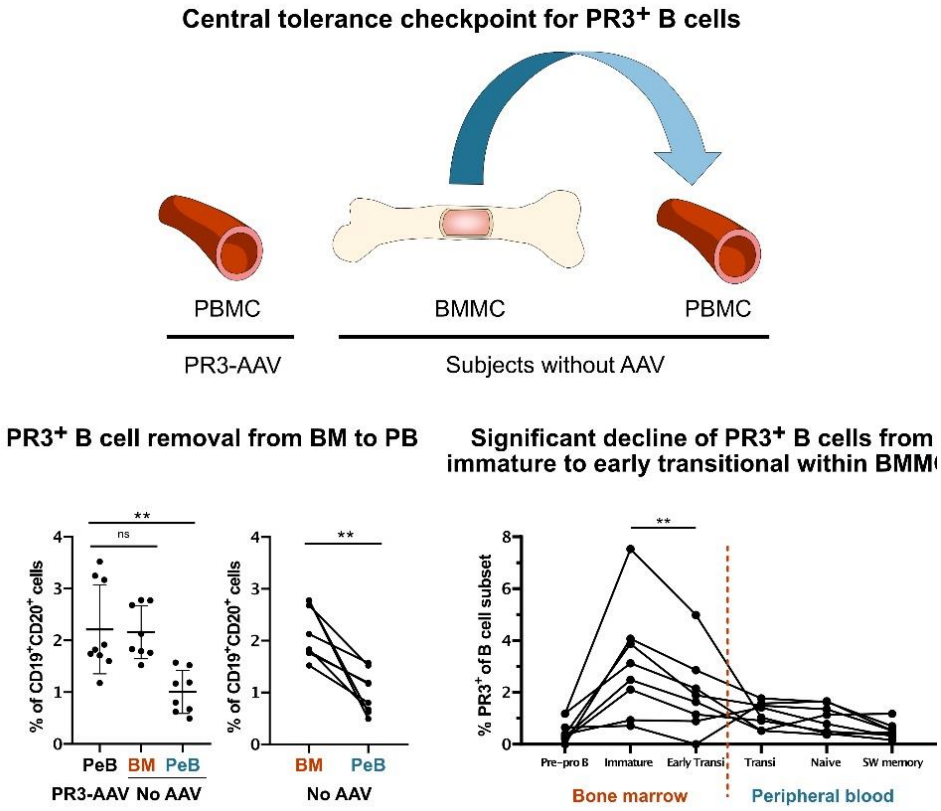

Figure 15. Aim #2 graphical summary. Overview of the set of experiments: The ontogeny of PR3$^+$ B cells**.** *PeB: Peripheral Blood, BM: bone marrow (blood), AAV: ANCA associated vasculitis, PR3: proteinase 3.*

Implications: Autoreactive B cells need to pass a stringent selection in the BM of No-AAV subjects. We illustrated for the first time how PR3$^+$ B cells are removed by central tolerance mechanisms in BMMC under homeostatic conditions in individuals without AAV, showing that the removal of autoreactive B cells mainly occurs between T1-like/immature to T2-like/early transitional B cells, thus preventing PR3-related autoimmunity.

Results Aim #2

Study cohorts

We compared BMMC and PBMC of a cohort of subjects without AAV (No-AAV) (n=8), in which BM blood and peripheral blood were collected the same day, and PBMC of a cohort of patients with PR3-AAV (n=9). We included 8 consecutive No-AAV subjects that underwent BM aspirate, eventually resulted normal (2 healthy controls and 2 subjects with previous acute myeloid leukemia in prolonged remission) or with a chronic neoplasm of the myeloid lineage without signs of acute disease and not requiring any immunosuppressive treatment (2 subjects with a diagnosis of myelodysplastic syndrome, 1 with chronic myeloid leukemia, 1 with hypereosinophilic syndrome).

Nine PR3-ANCA positive AAV patients were selected among consecutive subjects with AAV seen in our Unit, seven were GPA and two were MPA. Of those, three patients had active disease (median [25-75% IQR] BVAS.v3: 20 [13-21]) and six were in remission when the blood was drawn; two of three patients with active disease were only on prednisone 1mg/kg and four out of six of those in remission were on azathioprine, 2 of which were also receiving low dose prednisone (5 mg daily or less). Further details on these two cohorts are summarized in **Supplemental Table 3 and 4**.

$PR3^+$ B cells are increased in BMMC in non-vasculitis subjects and in PBMC of PR3-AAV patients

Using our customized flow cytometry-based assay, we studied the proportion of $PR3^+$ B cells of BMMC in No-AAV subjects, and compared them to their paired PBMC

and to the PBMC of PR3-AAV patients. The proportion of total B cells ($CD19^+CD20^+$) were higher in BMMC as compared to PBMC of both AAV and No-AAV subjects (**Table 5**, p<0.01). Gating strategy in **Supplemental Figure 8**.

Table 5. Lymphocytes and B cell subsets of BMMC and PBMC of non-vasculitis controls (n=8), and PBMC of AAV patients (n=9).

Characteristics	AAV PBMC (n=9)	HC PBMC (n=8)	HC BMMC (n=8)
Lymphocyte, %	62.9 [55.8,75.45]	81.50 [77.43,82.75]	54.25 [46.25 64.08]
Total B cells ($CD19^+CD20^+$), %	4.97 [2.36,5.90]	5.20 [3.00, 6.51]	7.78 [4.98, 8.12]
Transitional ($CD19^+CD20^+CD38^{++}CD24^{++}$),%	6.96 [1.14,13.95]	6.14 [1.59 8.91]	19.50 [12.38, 30.43]
T1 or T1-like* (IgD^- IgM^+), %	24.50 [7.88, 29.70]	16.65 [10.53, 37.58]	36.05 [22.93, 44.08]
T2 or T2-like* (IgD^+ IgM^+), %	43.30 [28.10, 70.95]	61.05 [23.28, 66.13]	15.10 [13.20, 17.33]
T3 or T3-like* (IgD^- IgM^-), %	23.10 [9.54, 54,70]	19.15 [9.63, 50.65]	48.30 [38.98, 60.38]
Mature/Non transitional ($CD19^+CD20^+CD38^{low}CD24^{low}$),%	91.50 [81.20, 95.50]	91.85 [87.15, 96.45]	73.50 [62.53, 84.65]
Naïve ($CD19^+CD20^+CD27^-IgD^+$),%	57.00 [43.55, 72.00]	61.20 [51.45, 76.23]	-
Switched Memory ($CD19^+CD20^+CD27^+IgD^-$),%	14.40 [3.38, 17.85]	8.54 [4.08, 11.80]	-
Unswitched Memory ($CD19^+CD20^+CD27^+IgD^+$),%	5.75 [4.27,18.90]	5.99 [2.71, 13.93]	-
Double Negative ($CD19^+CD20^+CD27^-IgD^-$),%	17.30 [17.30, 31.00]	14.20 [10.69, 27.73]	-

Values are presented as median [25%-75% Interquartile Range]
** T1, T2, T3 refer to $CD24^{++}CD38^{++}$ B cell subsets within PBMC, while T1-like, T2-like, T3-like refer to $CD24^{++}CD38^{++}$ B cell subsets within BMMC*
Abbreviations: PR3=proteinase-3; ANCA=anti-neutrophil cytoplasmic antibodies; AAV=ANCA-associated vasculitis, No AAV=non-vasculitis controls.

The proportion of circulating $PR3^+$ B cells within BMMC of No-AAV subjects (median [IQR25-75%]; 1.98% [1.77-2.75]) was similar to their proportion within PBMC of PR3-AAV patients (1.82% [1.66-3.21]; p>0.05) (**Figure 16A**), while it was significantly

higher than within paired PBMC of non-vasculitis subjects (0.9% [0.63-1.44], p<0.01 by paired comparison) (**Figure 16B**). Notably, PR3-BCR membrane expression on total B cells was higher in PBMC of AAV patients as compared to BMMC and PBMC of non-vasculitis subjects (**Figure 16C**). PR3-ANCA IgG were detectable only in AAV patients' sera (**Supplemental Table 3**). Altogether, since the proportion of PR3$^+$ B cells declined from BMMC to PBMC in non-vasculitis subjects whereas in AAV patients the proportion of PR3$^+$ B cells was as elevated in PBMC as in the BMMC from No-AAV patients, we hypothesized a central tolerance checkpoint active for PR3$^+$ B cells at the level of immature B cells/transitional B cells in HCs, before their migration to the peripheral compartment.

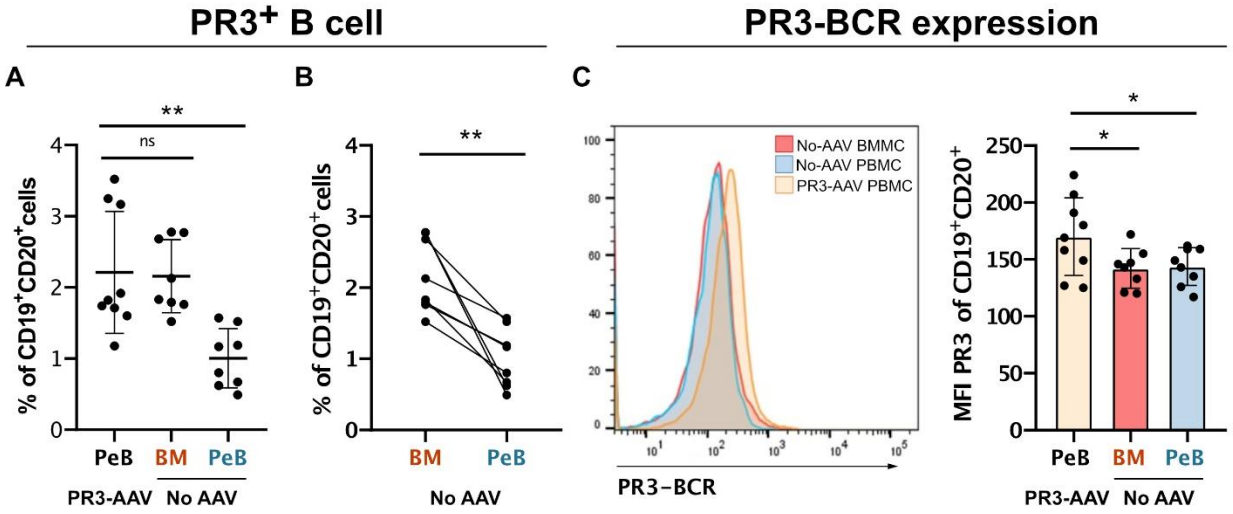

Figure 16. PR3+ B cells in BMMC and PBMC non-vasculitis (No-AAV) subjects and PR3-AAV patients. The proportion of circulating PR3$^+$ B cells in BMMC and PBMC of No-AAV subjects and PBMC of PR3-AAV patients (**A**). Paired comparisons between BMMC and PBMC of No-AAV subjects (**B**); and PR3 membrane expression on total B cells of BMMC and PBMC of No-AAV subjects and of PBMC of PR3-AAV patients (**C**). Each point represents the frequency in an individual subject; horizontal lines show the median with 25-75% IQR; each histogram represents mean (± SEM). P values were determined by 2-tailed Mann-Whitney test or Student T test, where appropriate. Multiple comparisons between more than 2 groups were performed with Kruskal-Wallis test. P values in the figures are indicated as * $p < 0.05$, ** $p < 0.01$, *** $p < 0.001$ after correction for FDR with Benjamini and Hochberg test. *PeB: Peripheral Blood, BM: bone marrow (blood), AAV: ANCA associated vasculitis, PR3: proteinase 3.*

Immature/Transitional B cells in bone marrow and peripheral blood

We thus focused on immature/transitional B cells, identified as the $CD24^{++}CD38^{++}$ subset of the $CD19^{+}CD20^{+}$ cells, and further categorized them by IgM and IgD expression (**Figure 17A**), as previously described *(28)(161)*. It is accepted that among PBMC T1 ($IgM^{+}IgD^{-}$) and T2 ($IgM^{+}IgD^{+}$) transitional B cells represent subsequent steps of maturation, while T3 ($IgM^{-}IgD^{-}$) transitional B cells have an intermediate profile of activation constituting a resting state *(28)*. In BMMC, T1-like represents a truly "immature" B cell phenotype, T2-like shows a more advanced pattern of differentiation representing "early transitional" B cells, while T3-like represents the initial steps of B cell maturation corresponding to "pre/pro B cells" *(161)*.

Total $CD24^{++}CD38^{++}$ B cells were significantly higher in BMMC than PBMC of AAV and non-vasculitis controls (**Figure 17B**) (19.50% [12.38-30.43] versus 6.96% [1.14-13.95] versus 6.14% [1.59-8.91], $p<0.01$ in both comparisons), reflecting the immaturity of B cells in the BM before transitioning to the peripheral compartment. The distribution of isotype-defined subsets within the $CD24^{++}CD38^{++}$ compartments between BMMC and PBMC differed as well, with $IgM^{+}IgD^{-}$ being predominantly present in BMMC as compared to PBMC of non-vasculitis controls and AAV subjects, and $IgM^{+}IgD^{+}$ being predominant in PBMC as compared to BMMC (**Figure 17, Table 5**). These results were consistent with those previously published *(162)*.

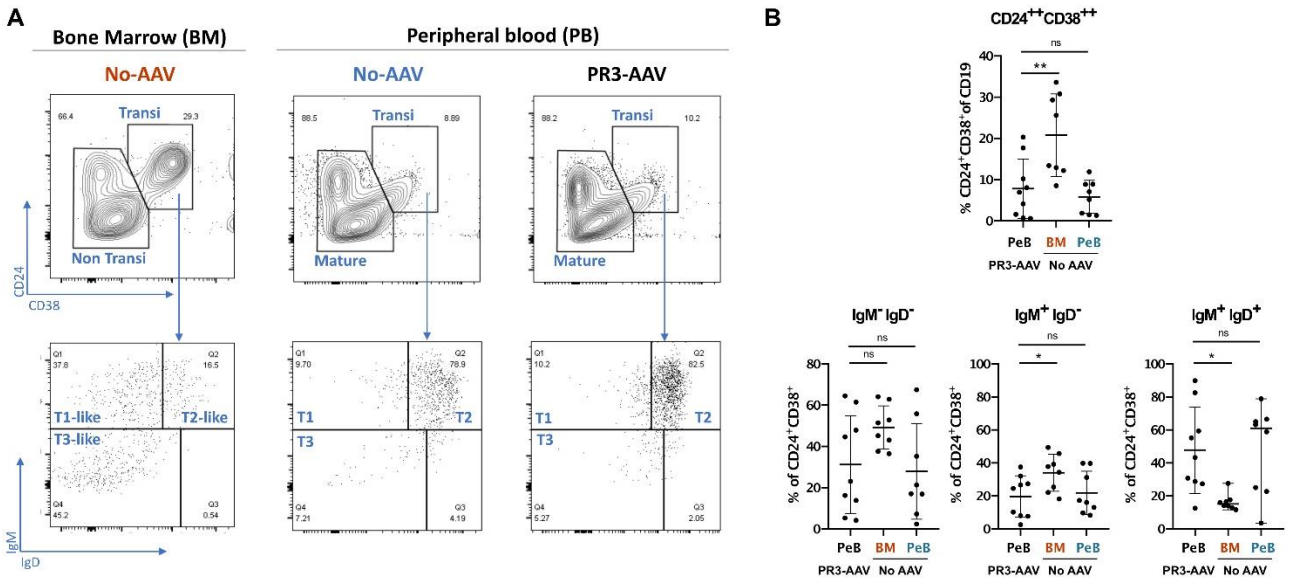

Figure 17. Immature/Transitional B cells in bone marrow and peripheral blood. Gating strategy of $CD24^{++}CD38^{++}CD19^{+}CD20^{+}$ cells, further plotted by IgM and IgD (**A**); proportion of $CD24^{++}CD38^{++}$ within each subsets, i.e. T1 (or T1-like in BM), T2 (or T2-like in BM), and T3 (or T3-like in BM) (**B**). Each point represents the frequency in an individual subject; horizontal lines show the median with 25-75% IQR. Multiple comparisons between more than 2 groups were performed with Kruskal-Wallis test. P values in the figures are indicated as * $p < 0.05$, ** $p < 0.01$, *** $p < 0.001$ after correction for FDR with Benjamini and Hochberg test. *PeB: Peripheral Blood, BM: bone marrow (blood).*

We further characterized $CD24^{++}CD38^{++}$ B cells in BMMC and PBMC of non-vasculitis controls. First, we plotted $CD24^{++}CD38^{++}$ B cells for CD27 (a marker of memory B cells) and CD10, expressed at high levels on B cell progenitors in the BM and then progressively disappearing with maturation *(163)*. This confirmatory gate showed low-to-absent expression of CD27 in $CD24^{++}CD38^{++}$ B cells of both BMMC and PBMC, while the proportion of $CD27^{-}CD10^{+}$ cells was significantly higher in $CD24^{++}CD38^{++}$ B cells among BMMC as compared to those among PBMC (**Figure 18A**) ($CD27^{-}CD10^{+}$: 72.50% [21.18-84.28] versus 40.10% [5.94-53.48], $p<0.01$). In addition, the expression of CD21, a marker of maturation, IgM and IgD was consistently higher on $CD24^{++}CD38^{++}$ B cells in PBMC as compared to $CD24^{++}CD38^{++}$ B cells in BMMC (**Figure 18B**). Altogether, these

findings confirm that CD24^{++}CD38^{++} B cells in BMMC and PBMC of non-vasculitis subjects represents two distinct developmental stages of B cell maturation rather than a single population in different compartments.

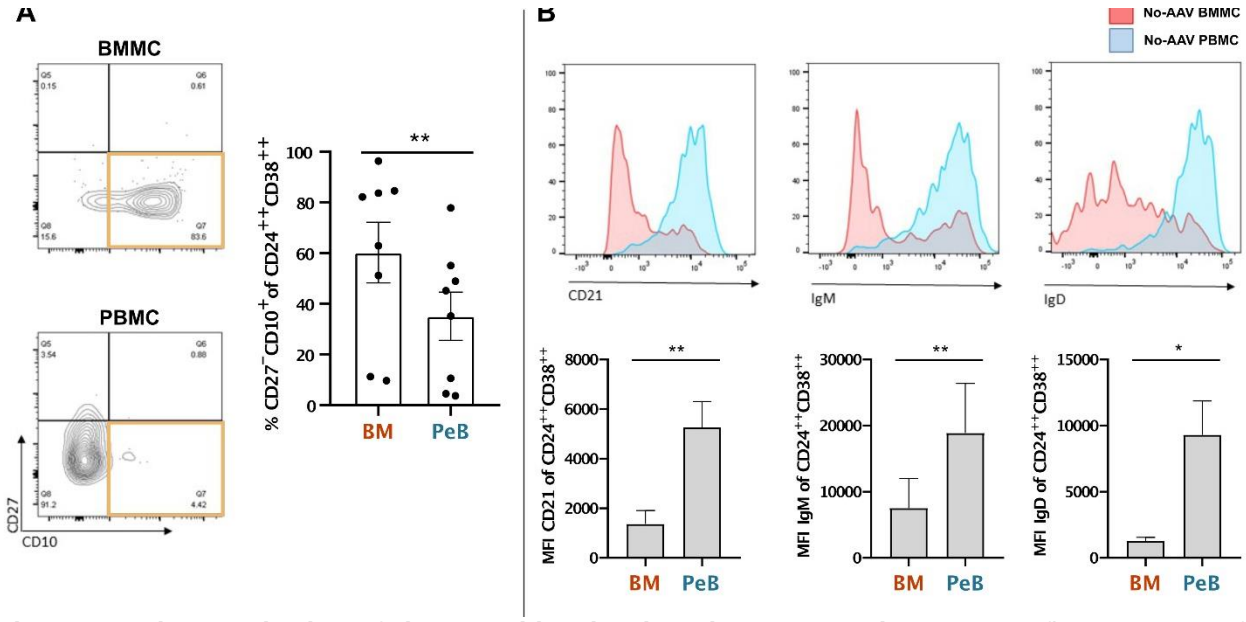

Figure 18. Characterization of the Transitional Subset in BMMC and PBMC. Confirmatory gate of CD27$^-$CD10$^+$ on CD24^{++}CD38^{++} (**A**). Expression of markers of maturity on transitional B cells, CD21, IgM and IgD (**B**). Each point represents the frequency in an individual subject; each histogram represents mean (± SEM). P values were determined by 2-tailed Mann-Whitney test or T test, where appropriate. P values in the figures are indicated as * $p < 0.05$, ** $p < 0.01$, *** $p < 0.001$. *PeB: Peripheral Blood, BM: bone marrow (blood), BMMC: bone marrow mononuclear cells; PBMC: peripheral blood mononuclear cells.*

Maturation of PR3$^+$ B cells from BM to periphery in non-vasculitis subjects and AAV patients

When frequencies of PR3$^+$ B cells were enumerated within CD24^{++}CD38^{++} B cells in non-vasculitis patients, it was found that BMMC contained the greatest proportion of PR3$^+$ B cells, as compared to PBMC (3.35% [1.99-4.92] versus 1.23% [0.62-1.55], p=0.0078), while no significant difference was found between the PR3$^+$ fraction within the latter subset and the one within total mature B cells (CD24^{dim}CD38^{dim}) of non-vasculitis subjects (0.91% [0.58-1.58], p=0.742) (**Supplemental Figure 9A-C**). The membrane

expression of PR3-BCR on $CD24^{++}CD38^{++}$ B cells was similar between BMMC and PBMC (**Supplemental Figure 9D**). Notably, the $PR3^{+}$ proportions within mature B cells of PBMC were higher in AAV patients compared to non-vasculitis subjects (**Supplemental Figure 9C**). By compiling these descriptive data, the results provide evidence that the main tolerance checkpoint activity for $PR3^{+}$ B cells in non-vasculitis subjects occurs early in the BM, before B cell transition to the peripheral compartment, and suggests that this mechanism may be defective or at least less efficient in AAV patients.

To further investigate with more precision at which level the immune checkpoint activity occurs in BMMC, we tracked the frequencies of $PR3^{+}$ B cells through the developmental stages of $CD24^{++}CD38^{++}$ B cells in BMMC, followed by the main subsets in PBMC known to represent immune checkpoints in AAV patients, as previously described *(75)*. In all the samples the proportion of $PR3^{+}$ B cells was close to 0% in the $IgD^{-}IgM^{-}$ $CD24^{++}CD38^{++}$ B cell subset (likely reflecting the absence of expression of a functional BCR at the developmental stage), then was greatest in the $IgD^{-}IgM^{+}$ subset (2.80% [1.23-4.02]), significantly declined as B cells mature into the $IgD^{+}IgM^{+}$ subset (1.76% [0.96-2.68], $p<0.01$), while no significant reduction was observed between the latter subset and the transitional compartment of PBMC (1.26% [0.62-1.56], $p=0.2500$) (**Figure 19**). In contrast, parent gates of B cell subsets reduced progressively from $IgD^{-}IgM^{+}$ to $IgD^{+}IgM^{+}$ in the BMMC ($p<0.01$), and from $IgD^{+}IgM^{+}$ of BMMC to transitional B cells of PBMC ($p<0.01$) (**Supplemental Figure 10, Table 5** for the median values). In other words, since $PR3^{+}$ B cells reduced from “immature” to “early transitional” B cell

compartments in BMMC, the early central tolerance checkpoint mostly contributing to the deletion of PR3^{+} B cells in non-vasculitis subjects appears to be at this level.

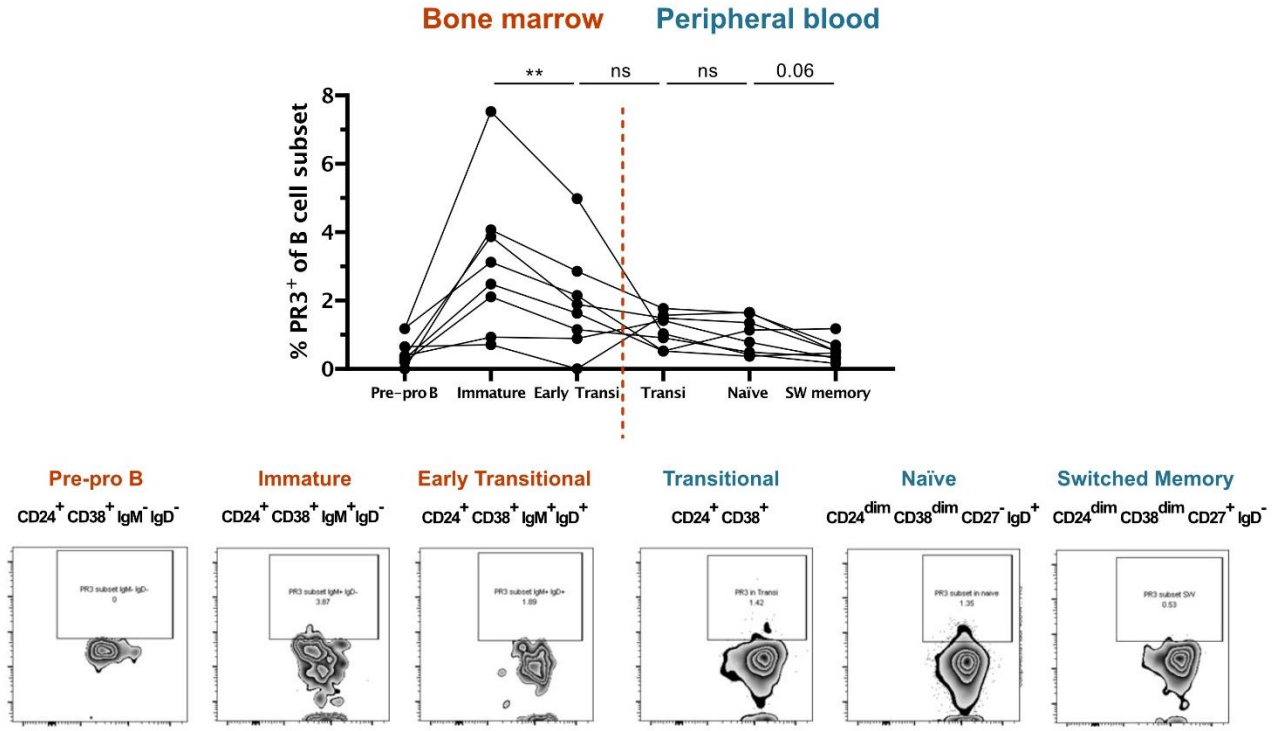

Figure 19. Comparison of the proportions of PR3+B cells among the different bone marrow B-cell subsets to peripheral B cell subsets in non-vasculitis (No-AAV) subjects. PR3^{+} B cells are significantly vetted from the T1-like to T2-like B cells compartments in non-vasculitis controls, and not after, indicating that the central immune checkpoint for PR3^{+} B cells mostly contributing to deletion of these autoreactive B cells occurs at that level (upper figure). Proportion of PR3^{+} B cells in these different B-cell subsets (bottom). Each point represents the frequency in an individual subject. The multiple comparisons on B cell maturation were analyzed by using mixed-effects modelling. P values in the figures are indicated as * $p < 0.05$, ** $p < 0.01$, *** $p < 0.001$ after correction for FDR with Benjamini and Hochberg test. *SW memory: Switched memory (B cells), PR3: proteinase 3.*

Discussion Aim #2

As second aim of this work, we investigated the central tolerance checkpoint, occurring early, before B cell become mature.

Autoreactive B cells need to pass a stringent selection in the BM in healthy subjects. Virtually, all the autoreactive B cells are eliminated before B cells migrate to the peripheral compartment. However, a small percentage of these self-reactive B cells are still migrating to the periphery, a phenomenon described as natural autoimmunity, and they will release polyreactive, generally IgM idiotype, natural autoantibodies *(41, 42, 164)*. In contrast to autoreactive B cell BM precursors in murine models *(13, 151)*, our knowledge on the biology of the human ones is still scarce. In particular, nothing is known about the BM development of $PR3^+$ B cells, the precursors of autoreactive B cells secreting PR3-ANCA IgG involved in the pathogenesis of AAV.

Our study reveals that $PR3^+$ B cells within BMMC of non-vasculitis controls are as high as within PBMC of AAV patients, while they are significantly lower in PBMC of non-vasculitis controls, suggesting a central tolerance checkpoint for autoreactive B cells at this level. We then confirmed that immature/transitional B cells, i.e. the subset of $CD24^{++}CD38^{++}$ B cells that migrate from BM to peripheral blood, have different phenotypic features in BM than in periphery (i.e. a higher proportion of $CD10^+$ cells and lower surface expression of CD21, IgD, and IgM in the BMMC cells versus PBMC), representing two separate developmental stages of B cell maturation *(163)(165)*. We further explored the maturation of natural autoreactive $PR3^+$ B cells focusing on these $CD24^{++}CD38^{++}$ B cell subsets in BM and periphery. We observed that the central tolerance checkpoint mostly contributing to the deletion of $PR3^+$ B cells in non-vasculitis subjects occurred between

“T1-like/immature” and “T2-like/early transitional” B cells within BMMC (i.e. from $IgD^{-}IgM^{+}$ to $IgD^{+}IgM^{+}$ $CD24^{++}CD38^{++}$ B cells), and not later, such as between BM “T2-like/early transitional” and peripheral transitional B cells. Since transitional $PR3^{+}$ B cells within PBMC are higher in AAV in than in non-vasculitis subjects, this data suggests that the checkpoint at this level can be defective or at least less efficient in AAV patients, independently from the antigen specificity of the autoimmune reaction (PR3 or MPO).

Even though only circulating autoreactive $PR3^{+}$ B cells of PR3-AAV are able to produce PR3-ANCA IgG detectable by conventional ELISA, the proportion of $PR3^{+}$ B cells was higher in BMMC than in PBMC of non-vasculitis controls. This is not surprising to us, since the overall frequency of autoreactive B cells in the BM starts at 50-80%, and then decreases progressively to 10% of mature naïve B cells in human adults *(64, 166)*. Consistently, our findings on PR3-autoimmunity showed that PBMC of PR3-AAV patients had significantly higher $PR3^{+}$ mature ($CD24^{dim}CD38^{dim}$) B cells than PBMC and BMMC of non-vasculitis controls. Several tolerance mechanisms operate in pre-immune B cells, before the acquisition of immunocompetence that occurs in the naïve stage *(13)(167)*.

Here, BCR editing and clonal deletion occur at the stage of pre/pro B cells to immature B cells, while additional checkpoints at the level of early transitional stage can occur, leading to apoptosis or anergy of autoreactive B cells. In our experiments, pre/pro B cells ($CD24^{++}CD38^{++}$ B cells of BMMC) were not reactive for PR3, since no functional Ig are present on the B cell surface at this stage, and therefore tolerance checkpoints cannot be studied at this level. To address which tolerance checkpoints might be defective, we tracked the $PR3^{+}$ B cells in BMMC after pre/pro B cell stage. We found a significant reduction of $PR3^{+}$ B cells from T1-like/immature to T2-like/early transitional B

cells, meaning that at this level there is the checkpoint contributing the most to the removal of PR3$^+$ B cells in non-vasculitis controls, a checkpoint likely less efficient in AAV patients.

Several central mechanisms balancing positive and negative selection of autoreactive B cells have been identified (summarized in *(13)*). In BALB/c and C57BL/6 mice, a positive selection for ANA$^+$ autoreactive B cell at this level has been reported by some authors *(39)*, but evidence is limited for BM, while there is a well-documented peripheral splenic positive selection of B cells at the transitional T1 and T2 stages, recent immigrants from the BM to the spleen *(39, 168)*. In the BM, the BCR tonic signaling in immature B cells promotes the positive selection of cells with unligated receptors through a phosphoinositide 3-kinase-dependent pathway, whereas BCR ligation promotes negative selection, by hindering this pathway and likely by downregulating BCR levels *(13)*. Consistently, our findings showed a downregulation of PR3-BCR expression on the surface of B cells in the non-vasculitis BMMC as compared to AAV patient PBMC, which might reflect this process. Overall, while central tolerance is probably responsible of the loss of (poly)autoreactive B cells through the tolerance checkpoints, the increased level of autoantigen-specific reactivity in autoimmune diseases is associated with less efficient negative selection in the BM and germinal maturation in the periphery.

We illustrated how PR3$^+$ B cells are removed by central tolerance mechanisms in BMMC under homeostatic conditions in non-vasculitis individuals. Despite this well-structured system of central tolerance checkpoints to avoid autoimmunity, functionally active PR3$^+$ B cells clones still emerge in PR3-AAV patients, indicating overall that pathogenic autoimmunity configures as a dysregulation of natural homeostatic

autoimmunity rather than the new onset of a previously absent self-recognition*(169)*. More in general, defects in the early removal of autoreactive B cells do not only occur in autoimmune disease, but also in primary immunodeficiency *(64)*. In this regard, alterations of BCR and Toll-like receptor signaling pathways results in a defective central checkpoint resulting failing to counterselect immature autoreactive B cells in the BM *(6, 64, 170, 171)*. These phenomena have been shown in humans, resulting in a high frequency of autoreactive transitional B cells in patients with either autoimmune diseases or several immunodeficiencies.

This work has strength and limitations. One strength is that the ontogeny of human autoreactive B cells is usually a neglect area, probably due to the difficulty to obtain BMMC samples of healthy/non-vasculitis patients for research purposes. Our findings, therefore, provide new insights into the mechanisms of controlling PR3-autoimmunity occurring in pre-immune cells. Another strength is that we used a wide panel of antibodies for the flow cytometry analysis, for instance considering double positive $CD19^{+}CD20^{+}$ as B cells. In fact, considering all the $CD19^{+}$ as B cells as usual for PBMC would have been imprecise for BMMC, since this would have led to the inclusion in the immature B cell pool of mature plasma cells, usually $CD20^{-}$ and residing in the BM *(37)*, and some early precursor of B cells without surface BCR, as pro-B cells *(13)*.

This work has also several potential limitations. One is that the number of BMMC samples was relatively small, and this could have potentially influenced the results of the analyses. Second, we did not have access to BMMC of patients with AAV, which would have proven the central checkpoint defect likely present in AAV. The BM blood is an invasive maneuver quite painful, and without a defined clinical reason would have been

unethical to draw AAV patients for research purposes only. In addition, some of the PR3-AAV patients had active disease and other were in remission, and were under different immunosuppressive agents, including glucocorticoids, potentially interfering with B cells (and $PR3^+$ B cells).

To summarize this second set of experiments, the negative selection of $PR3^+$ B cells at the level of T1-like/immature to T2-like/early transitional B cells in BMMC of non-vasculitis controls showed that the removal of autoreactive B cells occurs mainly at this level under normal circumstances, thus preventing PR3-related autoimmunity. The major limitation is that we cannot repeat these experiments on BM of AAV patients that would have definitely proven a defect of the B-cell tolerance machinery at this level.

Aim #3: Longitudinal dynamics of PR3$^+$ B cells after B cell depletion

Summary Aim #3

Background and Rationale: Our previous findings clarified the tolerance checkpoints of autoreactive PR3$^+$ B cells that we characterized phenotypically and functionally in AAV and HC. However, the reconstitution of circulating PR3$^+$ B cells after RTX-induced depletion of B cells, their repartition between the different B cell subsets within the PR3$^+$ pool, and their relationship with long-term outcomes remain unknown. We investigated these changes and associations of the circulating autoreactive B cell pool following RTX with disease relapse.

Results: Sequential flow-cytometry was performed on 148 samples of PBCS from 23 PR3-AAV patients treated with RTX for remission-induction and monitored off-therapy during long-term follow-up in a prospective clinical trial. At B cell recurrence, i.e. the first blood sample with ≥10 B cells/µL after RTX, autoreactive B cell frequency among B cells was higher than at baseline ($p<0.01$). Frequencies of transitional and naïve subsets were higher, while memory subsets were lower at B cell recurrence than baseline within both autoreactive and total B cells ($p<0.001$ all comparisons). At B cell recurrence, frequencies of B cells and subsets did not differ between relapsers and non-relapsers. In contrast, the frequency of plasmablasts within the autoreactive B cell pool was higher in relapsers, associated with a shorter time-to-relapse, and levels higher than baseline were more likely to be found in patients who relapsed within the following 12 months compared to non-relapsers ($p<0.05$).

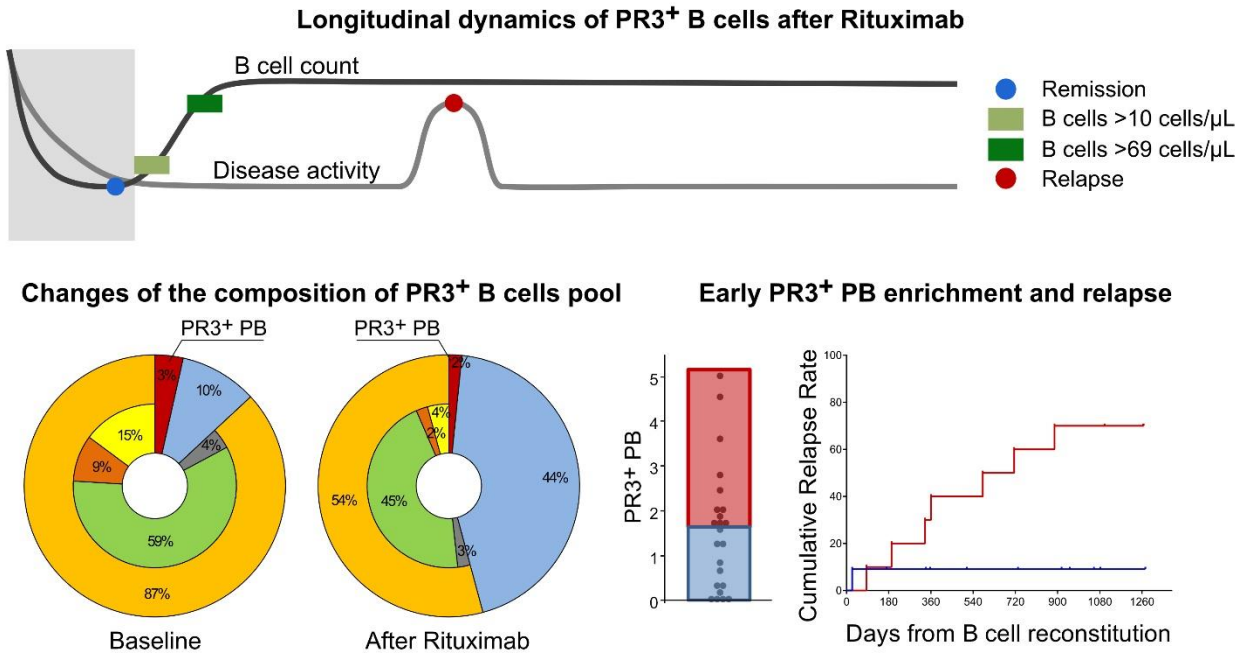

Figure 20. Aim #3 graphical summary. Overview of the set of experiments: Longitudinal dynamics of PR3+ B cells after B cell depletion. *PB: plasmablasts, PR3: proteinase 3.*

Implications: The composition of autoreactive B cell pool varies significantly following RTX treatment in AAV, and early plasmablast enrichment within the autoreactive pool is associated with future relapses. This study contributes to a better understanding of the mechanisms governing the reconstitution of autoreactive B cells in AAV with implications for maintenance of long-term remission after RTX, and potentially leading in the next future to the development of better biomarkers to predict relapse.

Results Aim #3

Remission, relapse and B cell recurrence in PR3-AAV

Clinical and demographic features of the study participants are reported in **Supplemental Table 5**. All patients were treated with RTX and glucocorticoids for the induction of remission, achieved complete remission prior to month 6 after randomization and were off therapy (including glucocorticoids) after month 6 unless a relapse occurred (**Figure 21**).

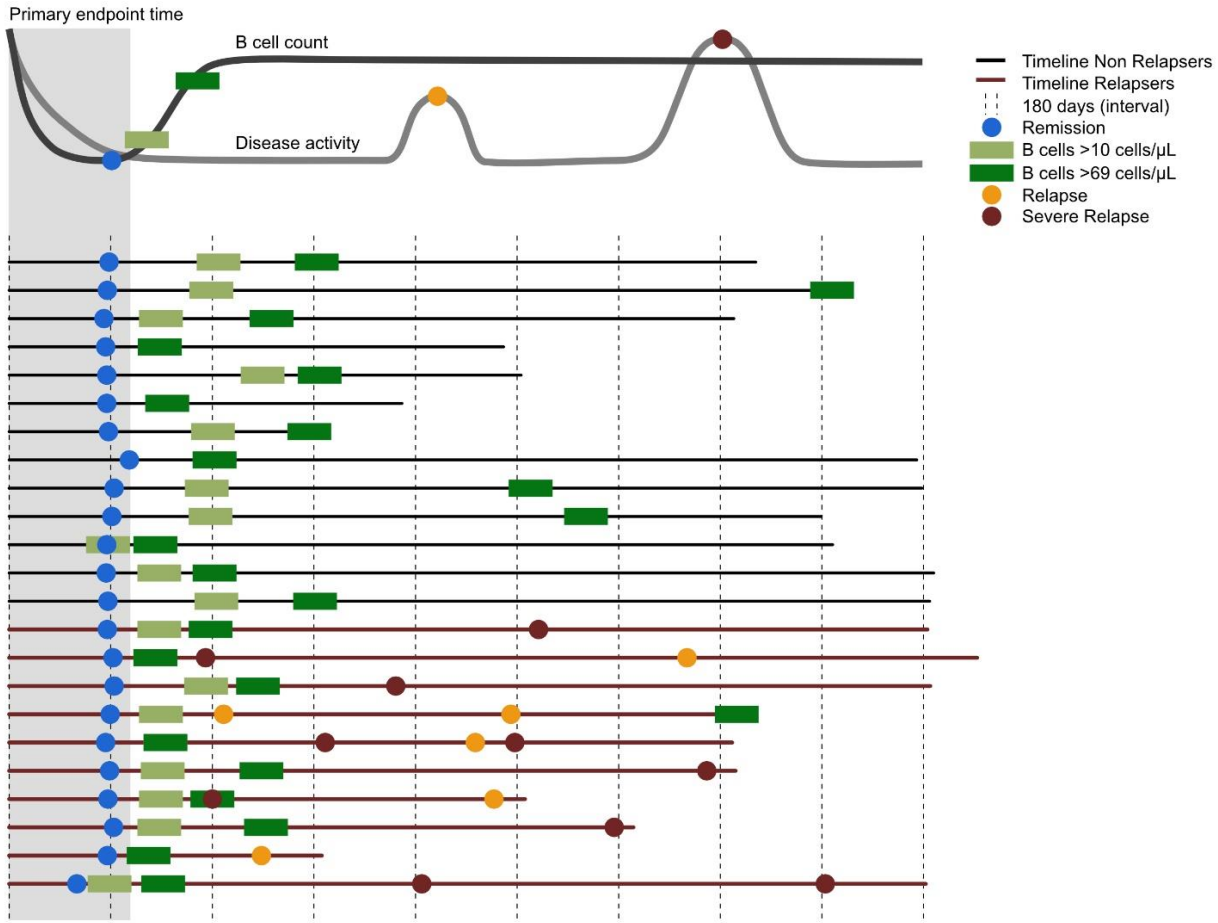

Figure 21. Swimmer plot showing response to RTX, relapse and B cell dynamics in PR3-AAV trial participants during follow-up. After the induction of remission with RTX and glucocorticoids, complete remission off therapy including glucocorticoids was achieved by all subjects (blue dots), before month 6th after randomization (grey shadow). Ten subjects relapsed during follow-up (red timelines), eight of them had severe relapse (red dots; non-severe-relapse, yellow dots), and five of them had multiple relapses during the observation period. All the patients repopulated B cell during follow up (green bars), in all relapsing patients and no patient relapse before B cells repopulated (B cells > 69 cells/ µL).

Total median follow-up was 44 months (25-75% IQR, 31-54); 43 months (25-75% IQR, 35-54) for patients who suffered a relapse after achieving complete remission, and 48 months (25-75% IQR, 30-54) for patients who remained in complete remission for the duration of the trial (p=0.975). Ten subjects relapsed during follow-up (red timelines), eight of them had severe relapses, and five of them had multiple relapses during the observation period (**Figure 21**).

We compared the circulating PBMC samples collected at baseline with those collected at B cell recurrence. The median time point of B cell recurrence was month 12 (range, month 6-24). At B cell recurrence, B cell counts and frequencies were significantly lower compared to baseline (**Figure 22A**). Among B cell subsets, the frequencies of transitional (Transi, $CD19^{+}CD24^{high}CD38^{high}$) and naïve B cells were significantly higher, while the frequencies of the memory B cell subsets were significantly lower at B cell recurrence than at baseline (subsets and gating strategy shown in **Figure 22B-D).**

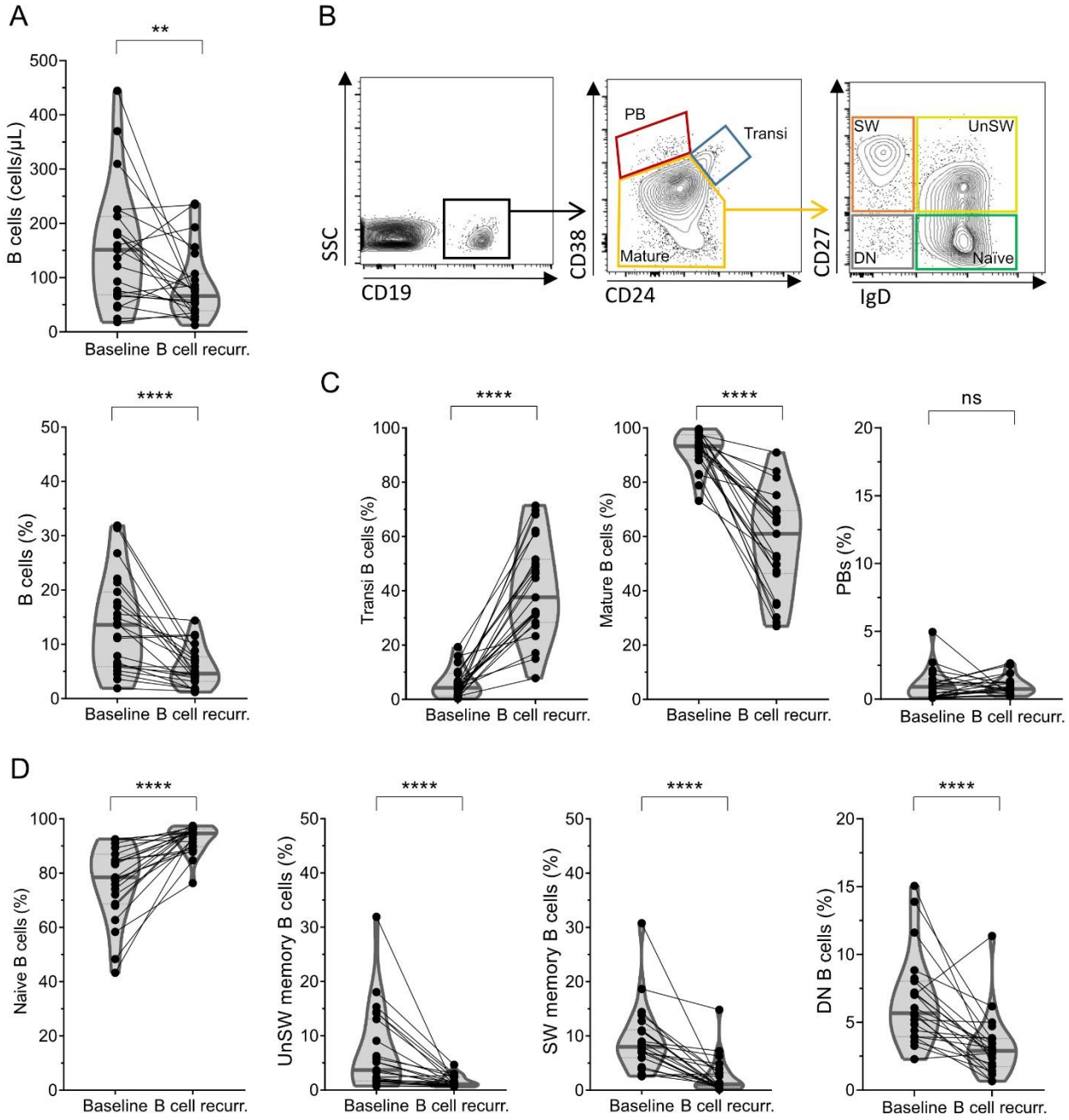

Figure 22. B cells comparisons of absolute count and frequency of B cells and B cell subsets at baseline and at B cell recurrence. Pairwise comparisons of absolute count (top panel) and frequency (lower panel) of B cells among cryopreserved PBMC between baseline and B cell recurrence **(A)**. B cell subset gating strategy **(B)**. Pairwise comparisons of the frequency of subsets within circulating B cells between baseline and B cell recurrence **(C-D)**: at B cell recurrence, a median of 37.56% (25-75%IQR, 28.35%-51.56%) of circulating B cells expressed a transitional phenotype. PB ($CD19^{+}CD24^{-}CD38^{high}$) did not significantly change from baseline (**2C**). Within the mature B cell pool ($CD19^{+}CD24^{low/high}CD38^{low}$), the frequency of naïve ($CD27^{-}IgD^{+}$) cells was significantly higher; the frequency of unswitched (UnSW, $CD27^{+}IgD^{+}$), switched (SW, $CD27^{+}IgD^{-}$), and double negative (DN, $CD27^{-}IgD^{-}$) memory subsets was significantly lower at B cell recurrence compared to baseline (**2D**). P values in the figures are indicated as * $p < 0.05$, ** $p < 0.01$, *** $p < 0.001$, and **** $p < 0.0001$.

Recurrence and subset redistribution of circulating autoreactive B cells following RTX-induced remission in PR3-AAV

The frequency of autoreactive B cells was significantly higher at B cell recurrence compared to baseline (median (25-75%IQR), 5.82%, (4.11-7.87) vs. 4.25% (3.77-5.30), p=0.025; gating strategy **Figure 23A,** $PR3^+$ as % of B cells in **Figure 23B**). Similar to what was observed for total B cells, the composition of the B cell subsets within the autoreactive pool at B cell recurrence was substantially different from baseline, with an increase in Transi (in blue, **Figure 23C**) and a decrease in mature naïve subsets (in green **Figure 23C**), a decrease in mature switched (SW) and unswitched (UnSW) memory subsets (in orange and yellow, respectively; p<0.001 in all cases except UnSW, p=0.002), and no significant change in the median frequency of mature double negative (DN) or plasmablast (PB) subsets (in grey and red, respectively **Figure 23C**).

Pairwise comparisons showed that the frequency of circulating transitional and naïve subsets were higher, and the frequency of mature, UnSW and SW memory subsets were lower within the autoreactive pool at B cell recurrence compared to baseline (p<0.001 for all comparisons; **Figure 23D**).

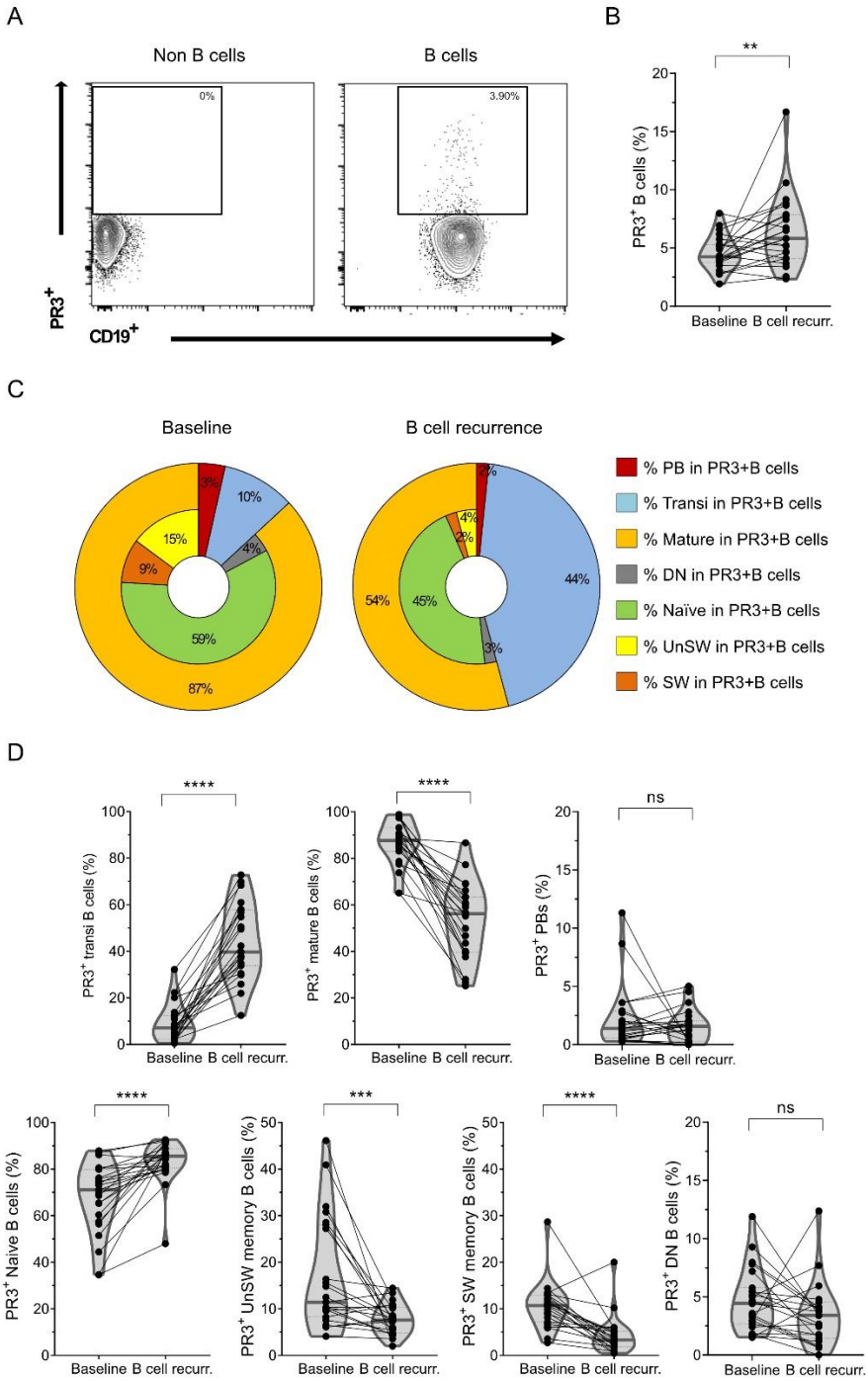

Figure 23. B cells comparisons of frequency of autoreactive PR3⁺B cells and subsets at baseline and at B cell recurrence. Gating strategy for autoreactive PR3⁺B cell subset **(A)**. Pairwise comparisons of frequency of PR3⁺B cells between baseline and B cell recurrence **(B)**. Frequencies of B cells subsets within PR3⁺B cell pool at baseline and B cell recurrence **(C).** Pairwise comparisons of circulating PR3⁺B cell subsets between baseline and B cell recurrence **(D)**. P values in the figures are indicated as * $p < 0.05$, ** $p < 0.01$, *** $p < 0.001$, and **** $p < 0.0001$.

Dynamics of total B cells and autoreactive B cells and relapse during long-term follow-up

Overall, the dynamics of total B cell and autoreactive B cell counts in peripheral blood of AAV participants that achieved complete remission following RTX-induction were similar between relapsers and non-relapsers throughout the time points evaluated (*p>0.05* in comparisons) (**Figure 24A-B**, **Supplemental Figure 11A-C**). After RTX, total B cells and autoreactive B cells were depleted (<10 cells/μL) in all participants (**Figure 24A-B**). Total and autoreactive B cells repopulated during follow-up in all participants, but only two participants had detectable total B cells and autoreactive B cells at month 6; of those, one relapsed, and one maintained remission throughout the follow up. Of note, all participants that relapsed repopulated total and autoreactive B cells before the relapse occurred.

The composition of subsets within autoreactive B cells and total B cells was similar at baseline between relapsers and non-relapsers (**Supplemental Figure 11C-D**). At B cell recurrence, no differences in the frequency of total B cells were observed between relapsers and non-relapsers (median (25-75%IQR); 5.44% (3.65-10.45) vs. 4.11% (2.30-7.17), p=0.410) or of total autoreactive B cells (median (25-75%IQR), 4.65% (3.18-7.02) vs. 6.5% (5.34-8.44), p=0.121). The frequency of all subsets evaluated within B cells at B cell recurrence were similar between these two disparate long-term outcome groups (**Figure 24C**); in particular, the frequency of Transi and PB were similar between relapsers and non-relapsers. However, a significantly higher frequency of PB was observed within the autoreactive pool at B cell recurrence in relapsers compared to non-relapsers (**Figure 24D**), and this subset was further enriched in severe relapsers

compared to non-severe relapsers (**Supplemental Figure 11E**). Overall, enrichment of PB within the autoreactive pool at recurrence was the only B cell biomarker that differed between relapsers and long-term non-relapsers.

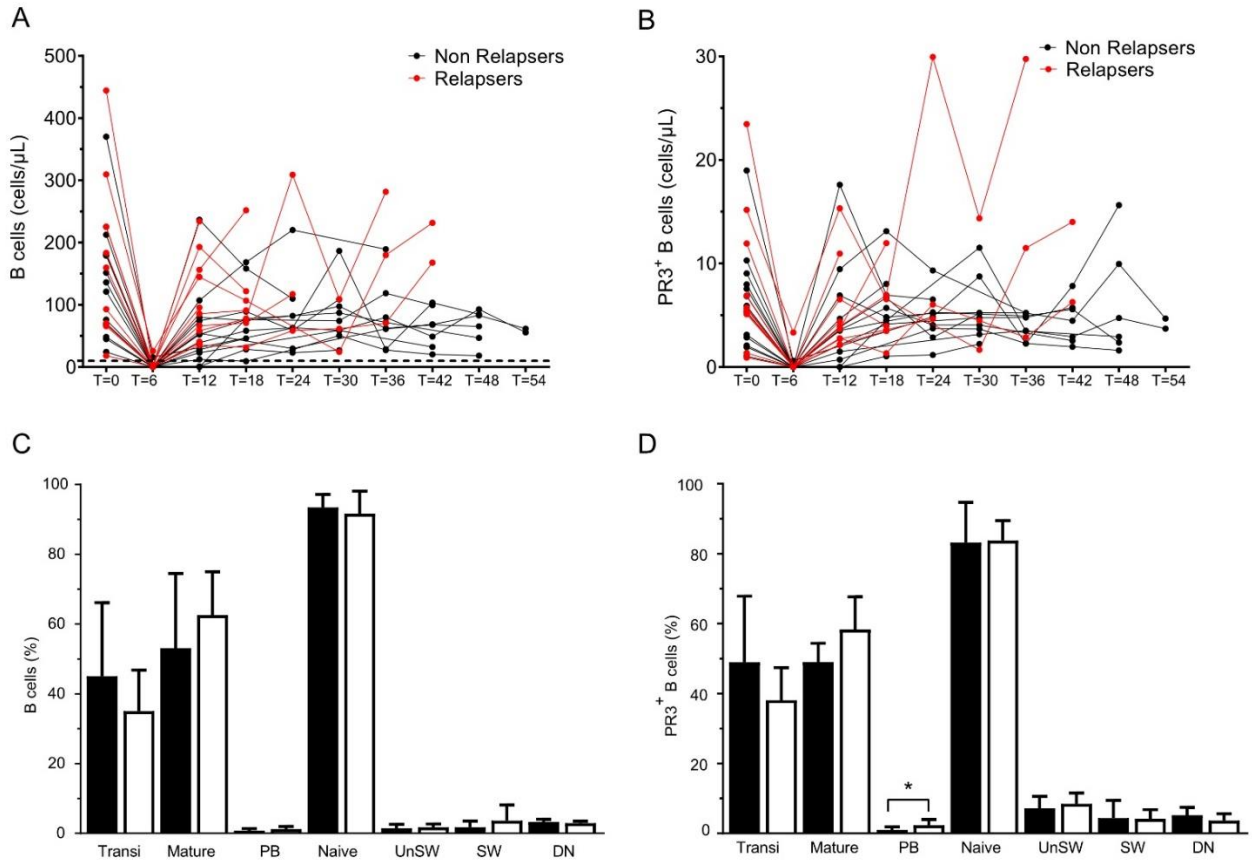

Figure 24. B cells and autoreactive PR3+ B cells during follow up. Counts of total B cells (cells/10^6L) and autoreactive $PR3^+$ B cells (cells/10^6L) at baseline and during follow up (relapsers in red; non-relapsers in black) (**A-B**). All the patients repopulated total B cells and autoreactive B cells during follow up; two patients had detectable total B cells and autoreactive B cells at month 6. Frequency at B cell recurrence of subsets within total B cells **(C)** and autoreactive B cells **(D)** in subjects that relapsed (open bars) or maintained long-term remission (black bars)**.** P values in the figures are indicated as * $p < 0.05$, ** $p < 0.01$, *** $p < 0.001$, and **** $p < 0.0001$.

Relationship of enrichment of plasmablasts within circulating autoreactive B cells with relapse

Since PB were enriched within the autoreactive PR3$^+$ B cell pool in relapsers compared to long-term non-relapsers at B cell recurrence, we wanted to determine a metric of PB frequency within autoreactive B cells associated with relapse risk. The median follow-up from B cell recurrence to the last clinical evaluation was 31 months (25-75% IQR, 18-42) for the entire group; 31 months (25-75% IQR, 23-42) for future relapsers and 32 months (25-75% IQR, 15-40) for non-relapsers (p=0.574).

At B cell recurrence, the frequency of PB within the autoreactive B cell pool ranged from 0.0% to 5.0%, with a median of 1.6% (**Figure 25A**). The ROC curve showed that the optimal levels of PB within autoreactive PR3$^+$B cells at B cell recurrence to discriminate relapsers from long-term non-relapsers was 1.6% (AUC=0.79, p=0.013, **Supplemental Figure 12**). Study participants with ≥ 1.6% of PB within autoreactive B cells at B cell recurrence had a significantly shorter time to first relapse and time to first severe relapse (**Figure 25B**; log-rank test p-value=0.026; **Figure 25C,** log-rank test 0.007, respectively).

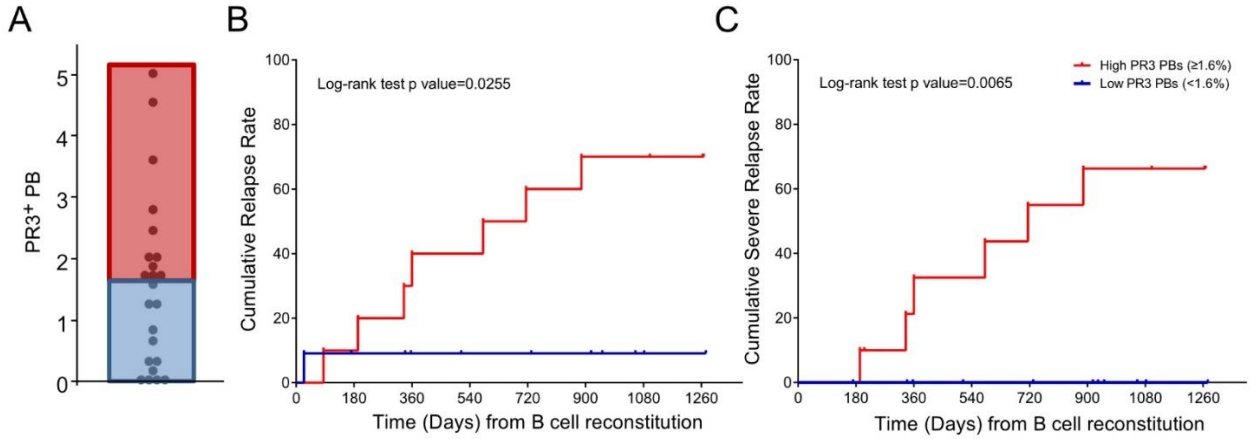

Figure 25. Relapse, severe relapse and autoreactive PR3$^+$ plasmablasts. Distribution of PB frequency within autoreactive PR3$^+$B cell pool at B cell recurrence by the median value of the cohort (blue <1.6%; red≥1.6%) **(A).** Time-to-relapse and time-to-severe relapse in AAV by PB within autoreactive PR3$^+$B cell levels (blue <1.6%; red≥1.6%) **(B-C)**.

To explore whether an increased frequency of PB among autoreactive B cells occurs before each relapse, we performed a case-crossover analysis to evaluate if each relapse was preceded by a rise of PB in autoreactive B cells within the previous 12 months. After B cell depletion, PBs within autoreactive B cells were redetected in all participants at some point during the follow up. Sixteen relapses occurred in 10 of the 23 participants studied (**Figure 21**). Among relapsers, the increase of PBs within the autoreactive pool in the 12 months preceding each relapse was approximately 2-fold and significantly more likely (OR 2.10; 95%CI 1.07-4.11, p=0.031). In contrast, the increase of PB within the autoreactive pool was smaller and non-significant among non-relapsers (OR 1.40; 95%CI 0.76-2.59, p=0.278), resulting in a case time-control OR for the autoreactive PB increase of 1.50.

Since the increase of PR3-ANCA has previously been shown to anticipate severe relapses in patients treated with RTX*(112)*, we repeated the previous analysis with PR3-ANCA. At baseline, PR3-ANCA was detectable in all the subjects regardless the future relapsing status (210RU/mL, 95%IQR: 70.9-327; versus 266RU/mL, 95%IQR: 86.35-366, p=0.403). Although PR3-ANCA levels were increased in relapsers compared to non-relapsers at B cell recurrence (p<0.05, **Supplemental Figure 11**), PR3-ANCA titer higher than the median at B cell recurrence (36.1 RU/mL; range, 3.4 to 331) was not associated with shorter time to relapse or severe relapse at time-to-event analyses (log-rank test p=0.157 and p=0.414, respectively). Consistently, after B cell depletion, increases of PR3-ANCA levels (if the assay had previously become positive) or reappearance (detectable from undetectable levels, if the assay was previously negative) did not anticipate the autoreactive PB increase or reappearance **(Supplemental Table 6).**

Discussion Aim #3

Here we evaluated the association between longitudinal perturbations of autoreactive PR3$^+$ B cells and the major outcome of AAV: disease relapse.

This third set of experiments shows a major change in the composition of B cell subsets within the autoreactive pool after RTX-induced B cell depletion in patients with AAV that achieved complete remission, and supports the hypothesis that an early enrichment of the PB fraction within autoreactive B cells during the reconstitution process is indicative of future relapse off therapy. This finding significantly contributes to clarifying the biological mechanisms underpinning disease relapse and prolonged remission in AAV, further providing mechanistic insights of the dynamics of B cells and autoreactive B cells in response to B cell targeted therapy in AAV. These results may lead to the development of better biomarkers to predict relapses and of more specifically targeted therapies.

We performed a detailed longitudinal analysis of autoreactive, antigen-specific PR3$^+$ B cells before and after B cell depletion in patients with PR3-ANCA positive AAV who were successfully treated with RTX and did not receive any other potentially confounding treatment after remission induction. We compared baseline with the B cell recurrence time-point, which is characterized by a relative increase of transitional and reduction of mature B cells. The depletion of B cells after RTX lasted for approximately 1 year in the majority of patients, and B cell counts remained lower than baseline at B cell recurrence. Clinically, the prolonged depletion of B cells after RTX treatment in AAV is well recognized *(86, 126, 172, 173)*, and it may impact on the B cell ontogeny at reconstitution, as shown by the expansion of the transitional B cell compartment after

RTX in patients with rheumatoid arthritis, lupus and pemphigus, and during reconstitution after hematopoietic stem cell transplantation *(71, 162, 174)*.

Autoreactive B cells were detectable in all the AAV subjects following B cell recurrence. The composition of B cell subsets within the autoreactive pool differed significantly between B cell recurrence and baseline, as for total B cells, with a relative increase of the transitional and naïve subsets and a reduction of the memory subsets at B cell recurrence. Relapsers exhibited an enrichment of the autoreactive PBs fraction (i.e. the precursor of the cells producing PR3-ANCA) compared to non-relapsers. Previous data have suggested that increased total PBs during remission is related to higher frequency of disease relapse in GPA patients *(175)*. In contrast, our study shows that total PBs were not different between relapsers and non-relapsers at B cell recurrence, and only a small minority of total PBs were $PR3^+$ at this stage (between 0 and 5%). Among these, it is likely that only a fraction of them will be able to terminally differentiate into plasma cells and produce high affinity PR3-ANCA IgG. An alternative explanation for the diverging findings by von Borstel et al. is that those patients received a variety of different additional conventional immunosuppressive treatments which may have affected the final results *(175)*. For all those reasons, we believe that changes in PB-$PR3^+$ could be more biologically meaningful than changes in total PBs in PR3-$ANCA^+$ AAV.

Consistently, a higher frequency of PB in autoreactive $PR3^+$ B cells at B cell recurrence was associated with shorter time to relapse. Additionally, increased levels of autoreactive PB were more likely to be found in subjects that relapsed in the following 12 months, and this increase was 50% more likely to occur when compared to non-relapsers, strongly linking autoreactive PB to relapse. In addition, the return of PR3-ANCA or

increases in PR3-ANCA levels did not anticipate the return or increase of the autoreactive PB subset. In other words, autoreactive PBs are significantly higher in relapsers compared to non-relapsers, further increasing in the 12 months before each relapse, anticipating or presenting in concomitance with PR3-ANCA titer increase. Because of these associations in relation to the relapse timeline, one could speculate that expansion of PB within the circulating autoreactive B cell pool may provide a source of high affinity antibody secreting cells that initiate relapses in AAV.

One strength of our work is that it is based on the analysis of data and samples obtained during the conduct of a clinical trial; and subjects included in this study underwent standardized prolonged clinical monitoring and systematic blood sampling, and were treated with what is now considered standard-of-care*(86)*. By means of the novel flow cytometry method that we used to detect autoreactive B cells in this longitudinal analysis, we were able to identify the repopulating autoreactive $PR3^+$ B cells throughout the course of the disease, providing new insights into the mechanisms of relapse, as shown by enrichment of PBs within the autoreactive pool.

This study has limitations. First, the number of patients studied is small and limited to PR3-ANCA positive AAV. A precise, longitudinal characterization of antigen-specific B cells in different samples would require a lot of effort from both individual subjects and the study team. The subjects included were all treated with RTX to effectively induce remission and were off-treatment during the follow-up according to the trial protocol, including glucocorticoids, which is known to be lymphocytolytic and to interfere with B cells *(176, 177)*, representing an exceptional model to study B cell dynamics.

To summarize, our findings relative to the third set of experiments show the restructuring of circulating B cell and autoreactive B cell compartments after B cell depletion in AAV patients successfully treated with RTX, and demonstrate that early changes within the autoreactive B cell pool are associated with the future outcome. Our results indicate that enrichment of PB within the autoreactive pool after successful treatment with RTX is linked to subsequent relapse, identifying a potential mechanistic target for more durable treatment strategies in AAV.

Conclusion and Future Perspectives

Autoreactive B cells are responsible for autoantibody secretion, ultimately triggering the immune response in B cell mediated autoimmune conditions. By means of our customized flow cytometry-based method using labeled rPR3 as a ligand to target autoreactive B cells, we were able to identify autoreactive $PR3^+$ B cells in PBMC of AAV patients and BMMC and PBMC of HC. Herein, we phenotypically characterized autoreactive B cells in active AAV, proving their functional ability to produce autoantibodies in *vivo* and in *vitro*. We also identified the main central and peripheral tolerance checkpoints throughout their maturation from the BM to the peripheral compartment, leading to an accumulation of atypical autoreactive $PR3^+$ memory B cells only in PR3-AAV patients and not in MPO-AAV and HC, and showed the association of disease relapse with the return of autoreactive after B cell depletion with RTX.

The identification of autoreactive B cells and the better definition of their roles in AAV may have several mechanistic and clinical implications, such as disclosing the molecular mechanisms underlying immune-tolerance defects in AAV, expanding their use as disease biomarkers, and potentially developing specific treatments targeting these cells. Mechanistically, this study supports the presence of defective central antigen-independent and peripheral antigen-dependent checkpoints in patients in PR3-AAV, elucidating the selection process of autoreactive B cells. Class-switched IgG autoantibodies arise through defects occurring initially in immature and thereafter in antigen-experienced B cells, in the latter depending on antigen and BCR affinity for the antigen. By our customized flow cytometry method used to identify autoreactive $PR3^+$ B cells, however, we do not assess the level of affinity nor the precise specificity (i.e. at the

epitope level) of the BCR for the antigen, and therefore we cannot completely prove that these “autoreactive” B cells in disease and healthy controls (usually low-affinity, polyreactive) are different from PR3-AAV (usually high affinity, oligoreactive). Single-autoreactive-B-cell sorting by FACS analysis (from patients and HC) could clarify this point, that must be undertaken in the future. There is still much to be done in understanding autoreactive B cells in humans, and in the context of AAV, the identification and initial characterization of the PR3^{+} B cells are just the beginning of a potential line of research that we want to exploit. Specifically, novel tools can be used to better dissect phenotype, gene-expression programs and functions of autoreactive B cells in health and disease. For instance, single-cell RNA-Seq of the PR3-Ig genes of circulating cells and tissue-eluted cells can help to identify if the same B cells clones reappear after B cell depletion in the blood of relapsing patients, or if different B cell clones are present within the inflamed tissues as compared to the blood. RNA-Seq could contribute to a better understanding of the B cell Ig repertoire. More subtle B cell subsets of autoreactive cells based on their transcriptomic programs can be discovered, and these genetic data could be further integrated at the protein level. In addition, the checkpoint(s) controlling the terminal differentiation of autoreactive plasma cells need to be studied further to determine if at this level the defect generating autoreactive PC occurs through an additional antigen-specific tolerance defect, or through other mechanisms, such as the generalized expansion of the PC leading to an aberrant B-cell differentiation, as demonstrated for instance for SLE. Finally, tissue-infiltrating autoreactive B cells could be studied as well. Mass cytometry-based technologies, like Hyperion platforms, are able to simultaneously measure the expression of more than 40 different biomarkers in a single

biopsy. This could complement the work we have done so far, finally permitting a more comprehensive understanding of the GC reaction and the B cell intrafollicular maturation. The potential applications following the identification of autoreactive B cells in AAV could have an impact in routine practice. If proven in an independent population, the clinical implications of the association with systemic inflammation and proportion and time to complete remission would include both prognosis and identification of an at-risk AAV subset for more intensive therapy. Notably, our preliminary results may lead to the development of better biomarkers to predict relapse, and possibly more specific targeted therapies. Furthermore, prospective confirmatory clinical studies on the role of autoreactive $PR3^{+}PB$ should be undertaken, possibly with a high-sensitive flow cytometry approach, and the ability of circulating $PR3^{+}PB$ to guide RTX retreatment explored.

In addition to these observational studies, more explorative analyses on the PR3 epitopes more frequently recognized by the BCR of PR3-autoreactive B cells, or more closely linked to disease relapse or disease severity can be identified by bioinformatic approaches combined with RNA-seq followed by the cloning of the Ig genes from autoreactive B cells.

Conventional disease-modifying anti-rheumatic drugs (DMARDs) for AAV suppress the immune system cells and partially inhibits antibody production, but are associated with frequent serious adverse effects. More recently, the use of biological DMARDs have been developed, and among these the use of RTX in AAV has shown satisfactory therapeutic efficacy, depleting B cells and circulating ANCA to undetectable levels in most of the cases. This pointed out that short-living PB are the main source of autoantibodies in AAV, and the strategy to target $CD20^{+}$ precursors could also indirectly

reduce autoantibody-secreting $CD20^-$ PB. Our results further integrate this concept, by showing that an early autoreactive PB redetection after anti-CD20 treatment was associated with relapse and shorter time to relapse in AAV. On the other hand, the depletion of B cells may transiently increase the risk of severe infection and reduce the possibility of immune response to vaccination in AAV patients. Therefore, treatments specifically targeting $PR3^+$ B cells are likely the future, like engineering patient immune cells to react against their autoreactive B cells, as done with chimeric antigen receptor (CAR)-T cells for hematological neoplasms or as preliminarily tested in pemphigus. In fact, the chimeric autoantibody receptor (CAAR)-T cells are modified from CAR-T cells where chimeric autoantibody receptors are harbored by T cells instead of chimeric antigen receptors to target antibody-producing cells (i.e. autoreactive cells), as shown for mice with pemphigus vulgaris and as studied in ongoing phase I/II trials for human systemic lupus erythematosus and myasthenia gravis. This approach specifically targets autoreactive B cells, avoiding the risk of general immunosuppression. In addition to this, conventional and biological DAMRDs (including RTX) cannot restore immune tolerance permanently, while adoptive cellular therapy as CAAR-T cells might be able to achieve this by eradicating autoreactive clones.

Altogether, starting from these preliminary findings, future efforts will be aimed at providing a more comprehensive understanding of the autoreactive B cells and their role in the pathogenetic processes underlying AAV, and on their potential to guide current treatment and to develop new personalized immunotherapy for AAV.

Materials and Methods

Study Populations and definitions

For aims #1 and #3, all available baseline cryopreserved PBMC samples from the Rituximab in ANCA-Associated Vasculitis (RAVE) (*NCT00104299(178)*) were collected and used for our analysis.

For aim #1, we analyzed 181 subjects, 105 with PR3-AAV, 49 with MPO-AAV, and 27 HC. Initially, 110 PR3-AAV trial participants and 53 MPO-AAV participants were included in the current study, while 27 age-matched volunteers were used as HC. A total of 9 participants were excluded from the final analysis because B cell depleted, i.e. <10 cells/µL (n=6; 4 PR3-AAV and 2 MPO-AAV) or because of artifacts/technical problems with the staining (n=3; 1 from PR3-AAV, 2 from MPO-AAV). In total, we analyzed 181 subjects, 105 with PR3-AAV, 49 with MPO-AAV, and 27 HC.

For aim #3, 23 subjects with PR3-ANCA positive AAV from the RTX arm of the RAVE trial (*NCT00104299)(178)* who reached the primary endpoint of the study (BVAS=0 off glucocorticoids at month 6) with available baseline and follow-up PBMC samples were selected for our analysis and provided 148 unique serial PBMC samples. PBMC had been collected and cryopreserved upon enrollment, at month 6 and every 3 months until month 18, and annually after month 18, according to the trial protocol*(86)*. Trial participants were followed until the last enrolled patient had completed 18 months of follow-up, ensuring an extended follow-up for the majority of enrolled patients.

According to the trial definition, B cell recurrence (or redetection) in RTX-treated trial participants was defined as at least 10 but less than 69 $CD19^+$ cells per microliter, and reconstitution as 69 or more $CD19^+$ cells per microliter or a return to baseline levels.

All clinical data were obtained from the trial database. To ensure comparability of the subsets of B cells and autoreactive cells between baseline and B cell return (i.e. assuring a minimum number of B cells at B cell recurrence, allowing an accurate assessment of B cell subsets), we considered the biological time-point “B cell recurrence” as the first blood sample at or after month 6 in which study participants had ≥10 B cells/μL

The RAVE study (*NCT00104299*, *(178)*) was a multicenter, double-blind, placebo-controlled trial that randomized 197 participants (all ANCA positive) in a 1:1 ratio to receive either RTX (375 mg/m^2 intravenously each week for 4 weeks) or cyclophosphamide (CYC) (2 mg/kg for 3–6 months) followed by azathioprine (AZA) (2 mg/kg, up to 150 mg/day). All clinical data were obtained from the RAVE database. Disease activity was measured using the Birmingham Vasculitis Activity Score for Wegener’s Granulomatosis (BVAS/WG) *(123)*. The primary outcome of the trial was defined as complete remission (BVAS/WG=0 and prednisone=0) within 6 months from randomization, other outcomes were complete remission, defined as BVAS/WG=0 and prednisone=0 at any time of the follow-up; complete response, defined as BVAS/WG=0 and prednisone ≤10mg/day; first remission, defined as a BVAS/WG=0, regardless the dose of glucocorticoids. Disease relapse was defined as any new disease activity, with an increase in BVAS/WG≥1 point after achievement of complete remission. Severe relapse was defined as a BVAS/WG≥3 or the occurrence of at least one major BVAS/WG item following disease remission requiring re-treatment with either RTX or CYC.

For aim #2, non-vasculitis adult subjects were selected among consecutive subjects undergoing BM aspirate to exclude hematologic conditions of myeloid origin and eventually resulted healthy or in long-term complete remission during follow-up of myeloid

neoplasms at S. Chiara Hospital of Trento (Italy). To avoid any possible interference, those that were on conventional immunosuppressive therapy or in remission for less than 12 months were excluded. Eight subjects were enrolled. Both BMMC and PBMC were collected from these patients the same day, and these subjects were evaluated in conjunction from the hematologist and the rheumatologist the day of the sampling.

Adult PR3-ANCA positive AAV (PR3-AAV) patients with a clinical diagnosis of granulomatosis with polyangiitis (GPA) or microscopic polyangiitis (MPA) were selected among consecutive subjects with AAV seen at the Rheumatology Unit of the S. Chiara Hospital of Trento (Italy). To be enrolled, they needed to be PR3-ANCA positive at both disease onset and at sampling, regardless the treatment received. Only PBMCs were collected from these patients. BMMC and PBMC of non-vasculitis subjects and AAV patients were collected and cryopreserved upon enrollment. All clinical data were extracted from medical files. In AAV, disease activity was measured using the Birmingham Vasculitis Activity Score version 3 (BVASv.3) *(124)*. In this subset, disease remission was defined as the stable absence of clinical and laboratory sign of disease (BVAS=0 for vasculitis) for at least 12 months after finishing the induction treatment. For those patients treated with the B depleting agent RTX, B cells needed to be more than 69 $CD19^{+}$ cells per microliter, as previously reported *(86)(179)*.

Recombinant proteinase 3 production and labelling

A recombinant PR3 (rPR3) was expressed in an epithelial cell line as previously described *(78)*. This variant consisted of the mature form of the protein (deletion of the N-terminal pro-dipeptide, allowing a mature conformational state), enzymatically inactive (S195A

point mutated to avoid the protease activity which could digest different proteins including immunoglobulins), and produced by stable transfection of HEK-293 cells *(180)*. This rPR3 is well recognized by PR3-ANCA from patients with AAV *(181)*. Culture supernatants were harvested after a 48h starvation, and rPR3 was purified using a column loaded with the anti-human PR3 monoclonal antibody (Ab) MCPR3-2 *(79)* following recommendations from the supplier (CNBr-Activated Sepharose 4 Fast Flow, GE HealthCare), concentrated, and quantified by Coomassie Plus (Pierce, Rockford, IL). We biotinylated rPR3 using a commercial biotinylation kit (Lightning-Link Rapid Biotin Conjugation Kit, Innova Biosciences, Cambridge, UK), as previously published *(75)*.

PR3$^+$ B cell detection and flow cytometry analysis

BMMC and PBMC from trial participants with AAV and HC were 10%-DMSO cryopreserved PBMC. Cryopreserved PBMC were stained and PR3$^+$ B cells and Tfh detected by flow cytometry analysis. In aim #1 and #3, for PR3$^+$ B cell detection, cells were counted, and 1x10^6 cells were incubated on ice for 20 min with rPR3-biotin and a cocktail of different antibodies (anti-CD19-APC-Alexa Fluor 700 cat# A78837 clone J3-119, Anti-Human IgD-APC cat# B30651 clone IA6-2, anti-CD27-PC7 cat# A54823 clone 1A4CD27, CD38-PC5.5 cat# A70205 clone LS198.4.3, and anti-CD24-APC-Alexa Fluor 750 cat# B10738 clone ALB9, all from Beckman Coulter, Inc.), washed 3 times, incubated for 15 min with streptavidin-FITC (cat# 554060), washed, and fixed. In aim #2, 500.000 cells were incubated on ice for 20 min with rPR3-biotin and a cocktail of different antibodies (anti-CD19-PC7 cat# 560911 clone SJ25C1, anti-Human IgD-BV786 cat# 740997 clone IA6-2, anti-CD27-APC-Alexa fluor 750 cat# 561786 clone M-T271, CD38-

PerCp 5.5 cat# 561106 clone HIT2, CD21-PE cat# 561768 clone B-ly4, CD24-BV480 cat# 746278 clone ML5, IgM BV421 cat# 562618 clone G20-127, CD20 APC-Alexa Fluor 700 cat# 560734 clone 2H7, CD10-BV650 cat# 563734 clone HI10a, all from Becton Dickinson, Inc.), followed by the same staining procedure.

For each experiment, unstained cells as well as single color controls were included. This customized flow cytometry assay, based on recombinant (r)PR3-FITC staining to identify the PR3-reactive B cells, was developed and validated by using anti-PR3 and anti-human neutrophil elastase antibody-producing hybridoma cell lines as positive and negative controls, as previously published by our group *(75)*.

For Tfh detection, cells were counted, and $1x10^6$ cells were stained with antibodies against human CD4 (Clone: RM4-5, Biolegend, San Diego, CA, USA), CD45RO (Biolegend, San Diego, CA, USA), PD-1 (Clone: 29F.1A12, Biolegend, San Diego, CA, USA), and CXCR5 (Clone: 2G8, BD Biosciences, San Jose, CA, USA).

Cell analysis was performed on a FACS Canto (BD Bioscience) or Attune NxT system (Life Technologies). FACS data were analyzed and graphed using KALUZA (Beckman Coulter, Inc., Indianapolis IN) and FlowJo (Ashland, Oregon) softwares.

The unsupervised clustering of flow cytometry data was performed using the SPADE (Spanning-tree Progression Analysis of Density-normalized Events) algorithm*(182)* based on the level of expression of 6 markers on each B cell (PR3, CD19, CD27, IgD, CD38 and CD24) on each cell. The analysis was performed on 27 HC, 105 PR3-AAV and 49 MPO-AAV participants. Briefly, after an initial downsampling, the SPADE was performed using 200 nodes for the clustering. SPADE trees were initially visually investigated to identify and regroup nodes that exhibit similar phenotype. Then, data

accompanying each SPADE tree (cluster abundance and MFI of each cluster for each sample) was downloaded from Cytobank, followed by hierarchical representation or testing for statistical significance.

In vitro PR3-ANCA production by PBMC and detection of PR3$^+$ B cells with ELISPOT

PBMC were cultured for 10 days to promote differentiation into antibody secreting cells, after which PR3-ANCA secretion was measured in the supernatant by the EliA PR3S test (ThermoFisher Scientific, Waltham, MA, USA) on a Phadia ImmunocaCAP 250 analyzer*(52)*.

Experiments were performed in duplicates in all trial participants with AAV and HC subjects. For each sample, one million PBMC per well were cultured in 1 ml of RPMI 1640 supplemented with 10% fetal calf serum and 50 mg/ml gentamycin (Gibco, Invitrogen, Carlsbad, CA, USA), in the presence of 3.2 µg/ml CpG-ODN 2006 (Hycult Biotechnology, Uden, The Netherlands), 100 ng/ml BAFF (PreproTech, Rocky Hill, NJ, USA) and 100 ng/ml of IL-21 (PreproTech, Rocky Hill, NJ, USA). PBMC were cultured for 10 days to promote differentiation into antibody secreting cells, after which PR3-ANCA secretion was measured in the supernatant.

PR3-ANCA IgG and IgM were measured by ELISPOT in peripheral blood of HC. To determine the ability of circulating PR3$^+$ B cells to secrete in vitro immunoglobulins of different isotypes against PR3, we measured PR3-ANCA IgG and IgM by ELISPOT in peripheral blood of HC. Briefly, enriched B cells from PBMC of a healthy subject were

FACS-sorted based on streptavidin expression to isolate $PR3^+$ B cells and $PR3^-$ B cells. The $PR3^+$ B cells, $PR3^-$ B cells and total B cells were cultured for 24h with 1 µg/ml R848 (Mabtech) and 10 ng/ml recombinant human (rh) IL-2 (Mabtech). After 24 hours, pre-stimulated cells were added to the plate with 100µl cell suspension/well (10,000 cells/well, 30,000 cells/well and 15,000 cells/well for $PR3^+$ B cells, $PR3^-$ B cells and total B cells, respectively). The ELISPOT was conducted according to the manufacturer's instructions (Mabtech, Nacka Strand, Sweden).

This could not be performed in the AAV trial participants, since the PBMC required to obtain $PR3^+$ B cells were in the order of $500x10^6$, much more than the frozen PBMC available for every AAV participant.

For the functional validation, PBMC of 3 active PR3-AAV were FACS-sorted based on streptavidin expression to isolate $PR3^+CD19^+$ and $PR3^-CD19^+$, as described above. Culturing and differentiating B-cells were done using modifications of previously published protocols *(183–186)*. All cultures were done in Iscove's modified Dulbecco's medium (IMDM), with GlutaMax-I (Gibco/ Thermo Fisher Scientific, Waltham, MA) and further supplemented with 50 µg/ml human transferrin, 5 µg/ml insulin (both from Sigma-Aldrich, St. Louis, MO) and 10% fetal calf serum (Atlanta Biologicals, Flowery Branch, GA). B-cells were cultured for 4 days in this media with the following cytokines: soluble CD40L (0.1 µg/ml), enhancer for ligands (1.0 µg/ml; both from Enzo Life Sciences, Farmingdale, NY), CpG-ODN 2006 (Hycult Biotechnology, Uden, The Netherlands), IL-2 (50 ng/ml), IL-10 (50 ng/ml) and IL-15 (10 ng/ml; all from Peprotech, Rocky Hill, NJ). Cells were plated at a density of 250,000 cells/ml in 96 well round bottom plate in 250µl per well, after which PR3-ANCA IgG secretion was measured in the supernatant by an in-house direct ELISA.

Cytospin smears of B cells harvested at day 4 were stained for qualitative assessment with May-Grünwald Giemsa, and with AMCA (7-amino-4-methylcoumarin-3-acetic acid) goat anti-human IgG 1:100 (Jackson ImmunoResearch, Ely, UK) after cell permeabilization, as previously described *(184)*.

ANCA testing

In patient sera, PR3-ANCA IgG levels were determined by enzyme-linked immunosorbent assay (ELISA) (supplied by Euroimmun, Inc.) in all serum samples from all the subjects, tested at a 1:20 dilution, as previously described *(112)*.

In culture supernatants, for the 10 day-cultures, PR3-ANCA IgG in the supernatants was measured by the EliA PR3S test (ThermoFisher Scientific, Waltham, MA, USA) on a Phadia ImmunocaCAP 250 analyzer *(52)*. For the 4 day-culture, the presence of PR3-IgG was assessed in the supernatants by an in-house direct ELISA based on reactivity against the rPR3. Plates were coated with 2 ug/ml purified rPR3, culture supernatant (with primary PR3-ANCA antibodies) were added, followed by biotinylated goat anti-human IgG 1:5000 and streptavidin-horseradish peroxidase (HRP, DAKO) 1:10.000. Culture supernatants were tested undiluted. Purified PR3-IgG and MPO-IgG from patients were used as positive and negative controls, respectively.

Data availability

Clinical data from the RAVE clinical trial are publicly available on the Immune Tolerance Network website (https://www.immunetolerance.org/researchers/trialshare). Experimental data are available upon reasonable request.

Statistics

Ordinal data are presented as N (%), continuous data as median (interquartile range) or mean (SD). Groups were compared using parametric or non-parametric tests when appropriate, Student T test or Mann-Whitney test (2 tailed) for continuous data.Chi^2 or Fisher's test were used as appropriate for categorical data.

Clinical outcomes were correlated with B cells and autoreactive B cells and their subsets. Multiple comparisons between more than 2 groups were performed with one-way ANOVA or Kruskal-Wallis test, as appropriate. The multiple comparisons on B cell maturation were analyzed by using mixed-effects model. Findings in all the analyses were considered significant at $p < 0.05$ after adjustment for multiple comparisons by calculating the false discovery rate as described by Benjamini and Hochberg*(187)*. Spearman's test was used to test correlations. The estimated distributions of time to remission, of relapse and severe relapse were performed with the Kaplan–Meier method and the log-rank test. The adjusted P values in the figures are indicated as * $p < 0.05$, ** $p < 0.01$, *** $p < 0.001$.

To further assess the ability of the frequency of plasmablasts (PBs) within the autoreactive B cell pool to distinguish between relapsers and patients remaining in long-term remission, a receiver operating characteristic (ROC) curve was constructed using logistic regression, with the % of the circulating biomarker as the predictor variable and

relapse versus remission during follow-up as the dichotomous outcome. The area under the ROC curve (AUC or C-statistic) was calculated.

To assess a possible association between an increase of peripheral blood autoreactive PBs and relapse, we performed a case-time-control analysis. It comprises a regular case-crossover of cases (relapsers) and a case-crossover of controls (non-relapsers). For this analysis, 148 samples, i.e. all available samples from the 23 patients studied, were used. For each individual study participant, the increase in the PB-PR3$^+$ frequency after B cell depletion was defined as a PB-PR3$^+$ level during follow-up equal or higher than the individual baseline level. For the patient to be considered at risk ("exposed"), the increase of PB-PR3$^+$ level had to occur within the 12 months preceding the relapse. In order to calculate the effect of autoreactive PR3$^+$ PB increase, we used conditional logistic regression. The ratio between the odds ratio (OR) from the case arm of the study and the OR obtained in the control arm generated the case-time-control study OR risk for relapse if a autoreactive PR3$^+$ PB increase occurred.

A vector graphic editor program was used to build the Swimmer-plot (Affinity Designer, Serif (Europe) Ltd, UK). Conditional logistic regression was calculated using STATA (STATA-Corp LP, version 13.1). All other statistical analyses were performed using the GraphPad Prism (San Diego, California) or JMP (Version 8, SAS Institute Inc) software.

Study approvals

The RAVE trial was approved by the institutional review board at each participating site. All patients consented for participation to the RAVE study and for subsequent mechanistic

studies, providing a written informed consent. The trial protocol, including all provisions for the future use of biospecimens collected during the trial, was approved by the institutional review board of each participating trial site. The institutional review board of the S. Chiara Hospital of Trento (Italy) approved the use of blood mononuclear cells of patients and healthy controls, and both were asked to sign a written informed consent.

Supplemental Material

Supplemental Figures

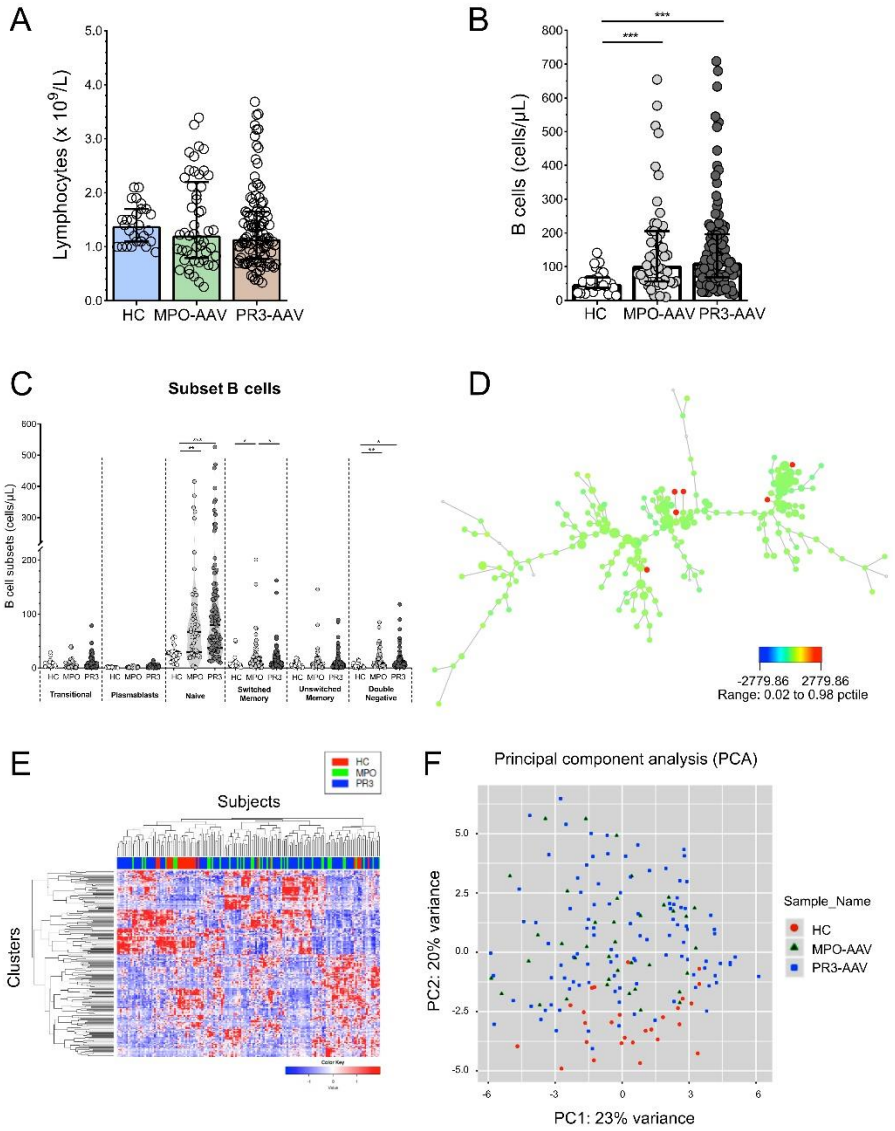

Supplemental Figure 1. B cells and distribution of B cells among different subsets in HCs, MPO-AAV and PR3-AAV. Lymphocyte count (**A**), B cell count (**B**), and distribution of B cell count among the different B cell subsets (**C**). An explanatory example of the 200 B cell clusters obtained with SPADE (Spanning-tree Progression Analysis of Density-normalized Events) in a PR3-AAV patient (**D**). Heat Map of the 181 patients (x axis, HCs in red, MPO-AAV in green and PR3-AAV in blue) showing the different expression of each one of the 200 B cell clusters (y axis) (**E**). Principal component analysis of the B cell clusters representing HC subjects, MPO-AAV and PR3-AAV participants (**F**). Data are represented as mean ± SEM. Data are represented as median (25-75% IQR). Multiple comparisons between more than 2 groups were performed with Kruskal Wallis test and P values in the figures are indicated as * $p < 0.05$, ** $p < 0.01$, *** $p < 0.001$ after correction for FDR with Benjamini and Hochberg test.

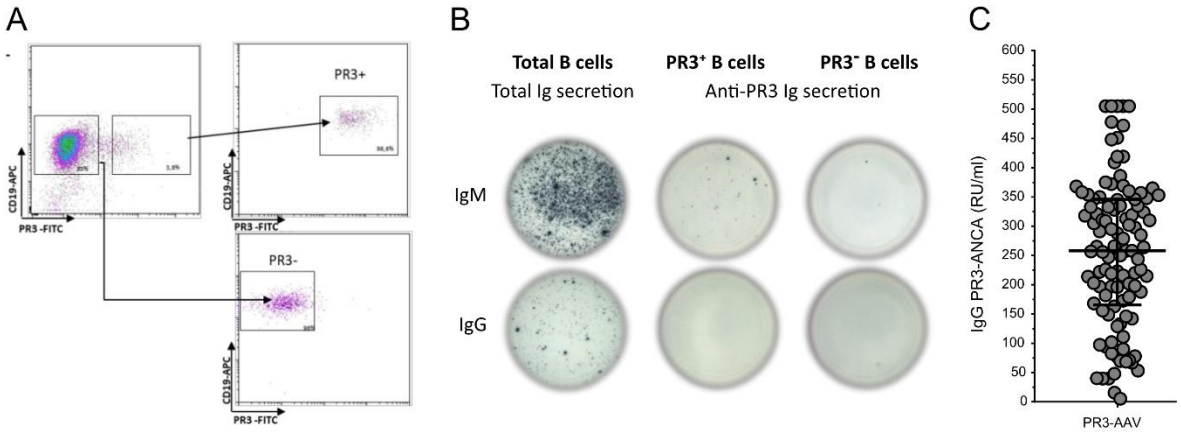

Supplemental Figure 2. Circulating PR3⁺ B cells and PR3-ANCA production. Purification of PR3⁺ B cells and PR3⁻ B cells for the ELIspot analysis in HCs (**A**). PBMCs isolated from a healthy subject were enriched for B cells by anti-CD19 antibody-linked magnetic bead selection. The B cell enriched fraction was FACS-sorted based on streptavidin expression to isolate PR3⁺ B cells and PR3⁻ B cells. Purity was 99% for PR3⁺ B cells and 96% PR3⁻ B cells, respectively.

Despite the production of total IgG and IgM by B cells (shown in **B**, left), PR3-ANCA IgM, but not PR3-ANCA IgG, can be secreted by PR3⁺ B cells (shown in **B**, central).

Circulating (*in vivo*) PR3-ANCA IgG in PR3-AAV participants by ELISA (**C**).

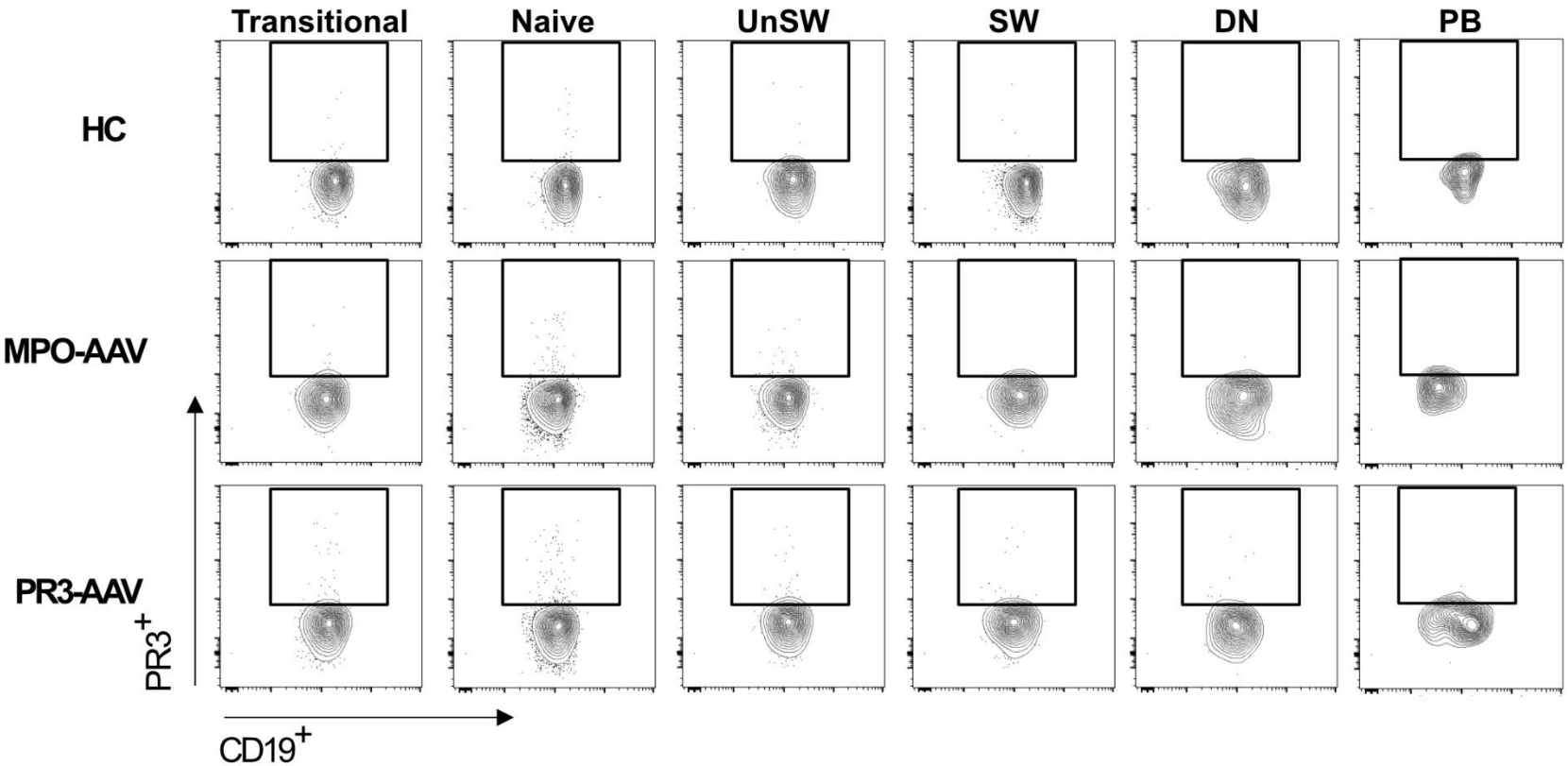

Supplemental Figure 3. Representative B cell subset plots of a HC subject, a MPO-AAV patient and a PR3-AAV patient. $PR3^+$ B cells recognizing nuclear antigens were identified within each B cell subset in AAV and HC.

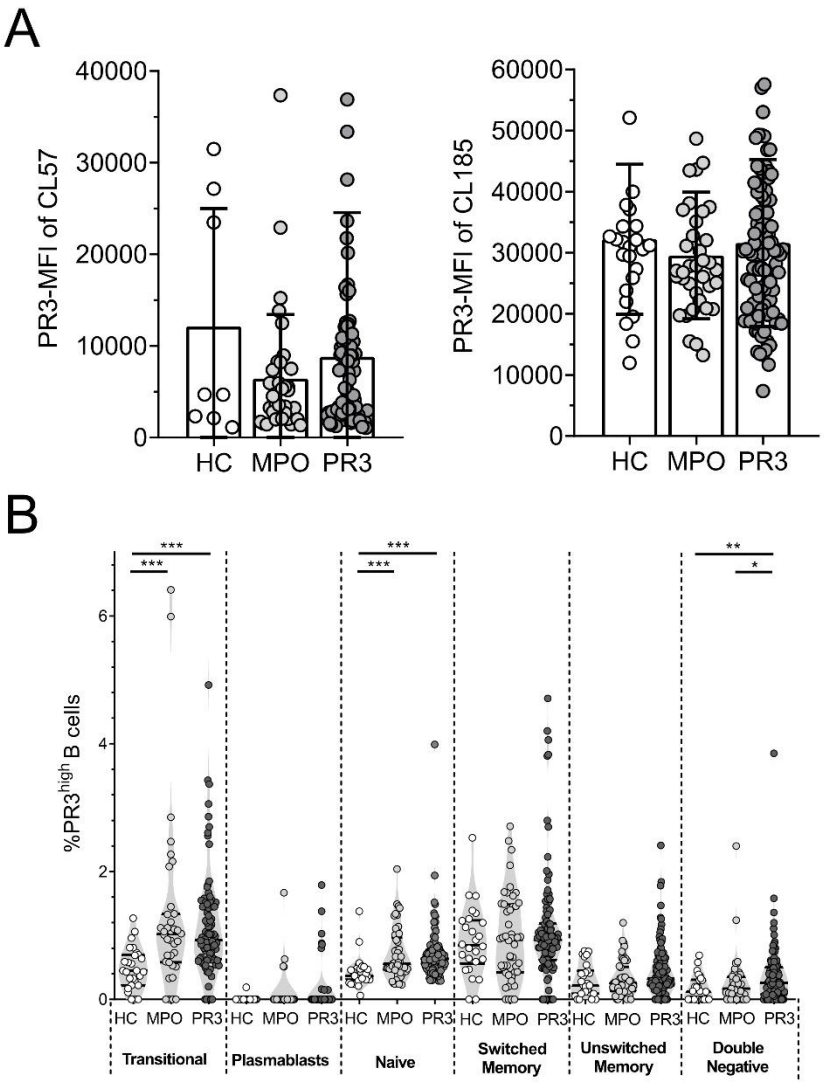

Supplemental Figure 4. Unsupervised clustering of circulating PR3+ B cells. Mean fluorescence intensity (MFI) of 2 out of 6 clusters with stable expression of PR3 across the samples (CL185 and CL57) (**A**), the others are represented in Figure 5. $PR3^{high}$ B cell distribution in the B cell subsets (**B**); frequencies of $PR3^{high}$ in transitional and naïve B cells are higher in AAV participants compared to HCs, but only the frequencies of $PR3^{high}$ in DN B cells were higher in PR3-AAV participants compared to both MPO-AAV participants and HCs. Data represent median (25-75% IQR) in violin plots or mean ± SD in histograms. Multiple comparisons between more than 2 groups were performed with one-way ANOVA or Kruskal-Wallis test, where appropriate. P values in the figures are indicated as * $p < 0.05$, ** $p < 0.01$, *** $p < 0.001$ after adjustment for FDR as described by Benjamini and Hochberg.

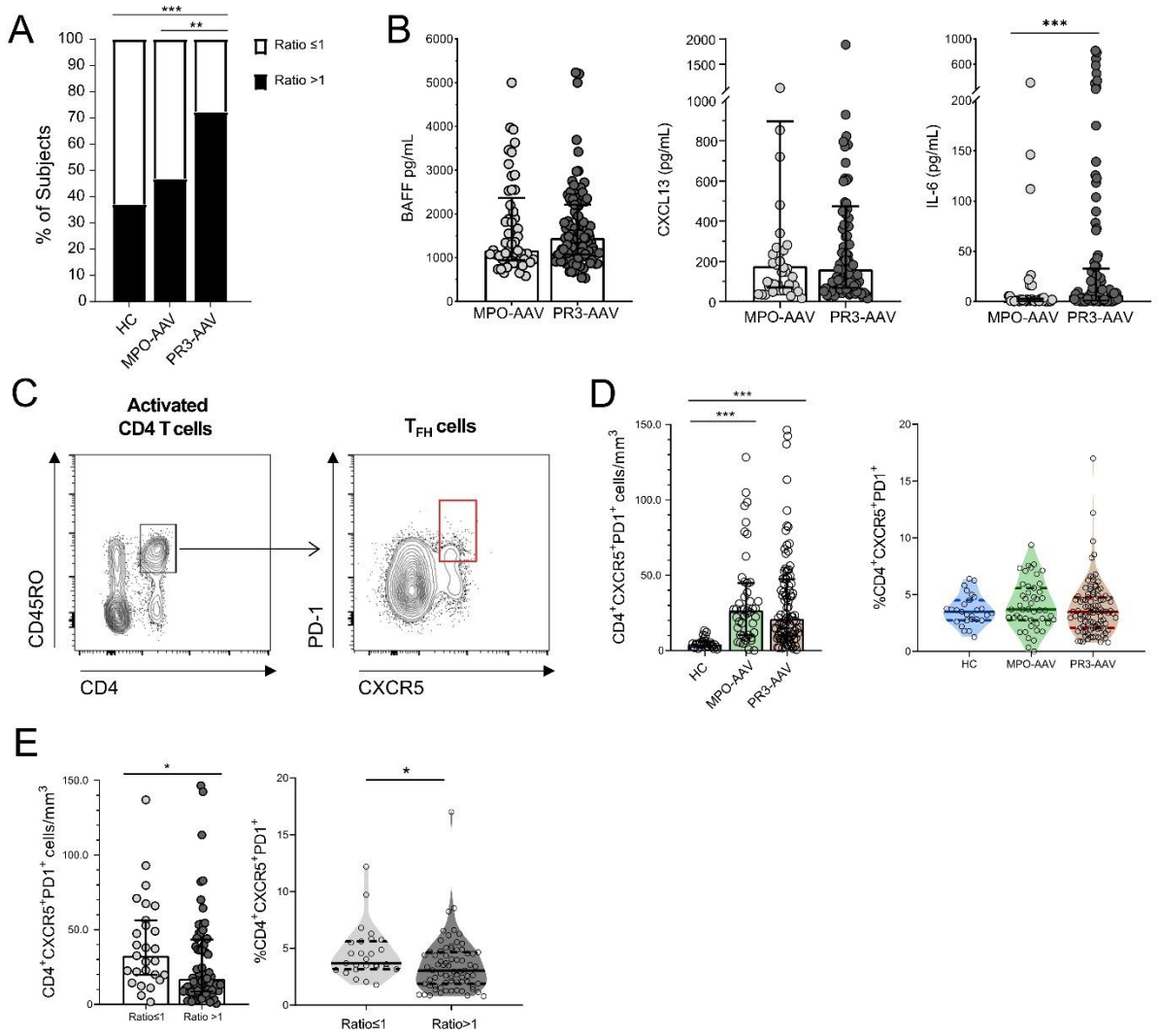

Supplemental Figure 5. Determinants of PR3⁺ B cell maturation. Frequency of AAV participants and HC subjects with a positive PR3+ B cell memory/naïve ratio (**A**). Levels of BAFF, CXCL13, IL-6 and in MPO-AAV and PR3-AAV participants (**B**). Gating strategy used for TFH identification (the reference population for the frequency is $CD4^+CD45RO^+CXCR5^+PD\text{-}1^+$) (**C**), TFH cell count and frequency in HCs, MPO-AAV and PR3-subects (**D**), and association of TFH higher levels with ratio ≤ 1 in PR3-AAV participants (**E**). Each point represents the frequency in an individual subject; horizontal lines show the median with 25-75% IQR. P values were determined by 2-tailed Mann-Whitney test. Multiple comparisons between more than 2 groups were performed with Kruskal-Wallis test. P values in the figures are indicated as * $p < 0.05$, ** $p < 0.01$, *** $p < 0.001$ after adjustment for FDR as described by Benjamini and Hochberg.

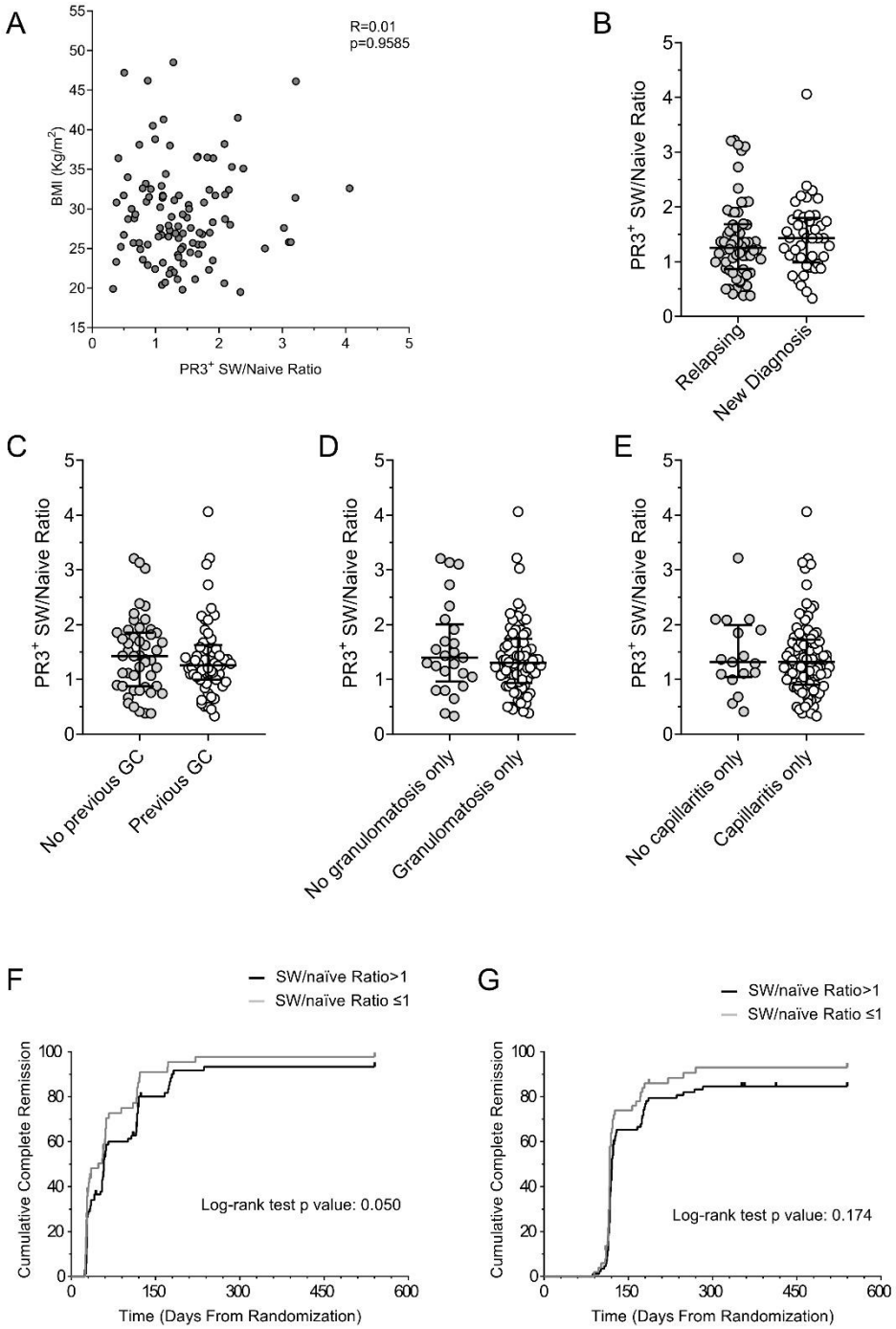

Supplemental Figure 6. SW memory/naïve PR3⁺ B cell ratio and clinical manifestations in PR3-AAV patients. In PR3-AAV patients (n=105), SW memory/naïve PR3⁺ B cell ratio did not correlate with Body Mass Index (BMI) (**A**), relapsing versus new diagnosis (**B**), previous use of glucocorticoids (**C**), the presence of manifestations reflecting granulomatous disease only (**D**) or capillaritis only (**E**), as assessed by the BVAS/WG. The ratio did not correlate with disease activity as assessed by BVAS/WG (**E**). Time to first remission (BVAS/WG=0, any prednisone dose) (**F**) or time to complete response (BVAS/WG=0, prednisone dose≤10mg/day) (**G**) are represented. When evaluating associations with remission, the subjects that underwent cross over (n=7) or experienced early treatment failure (n=6) during the trial time were excluded from the analysis. P values in the figures are indicated as * $p < 0.05$, ** $p < 0.01$, *** $p < 0.001$

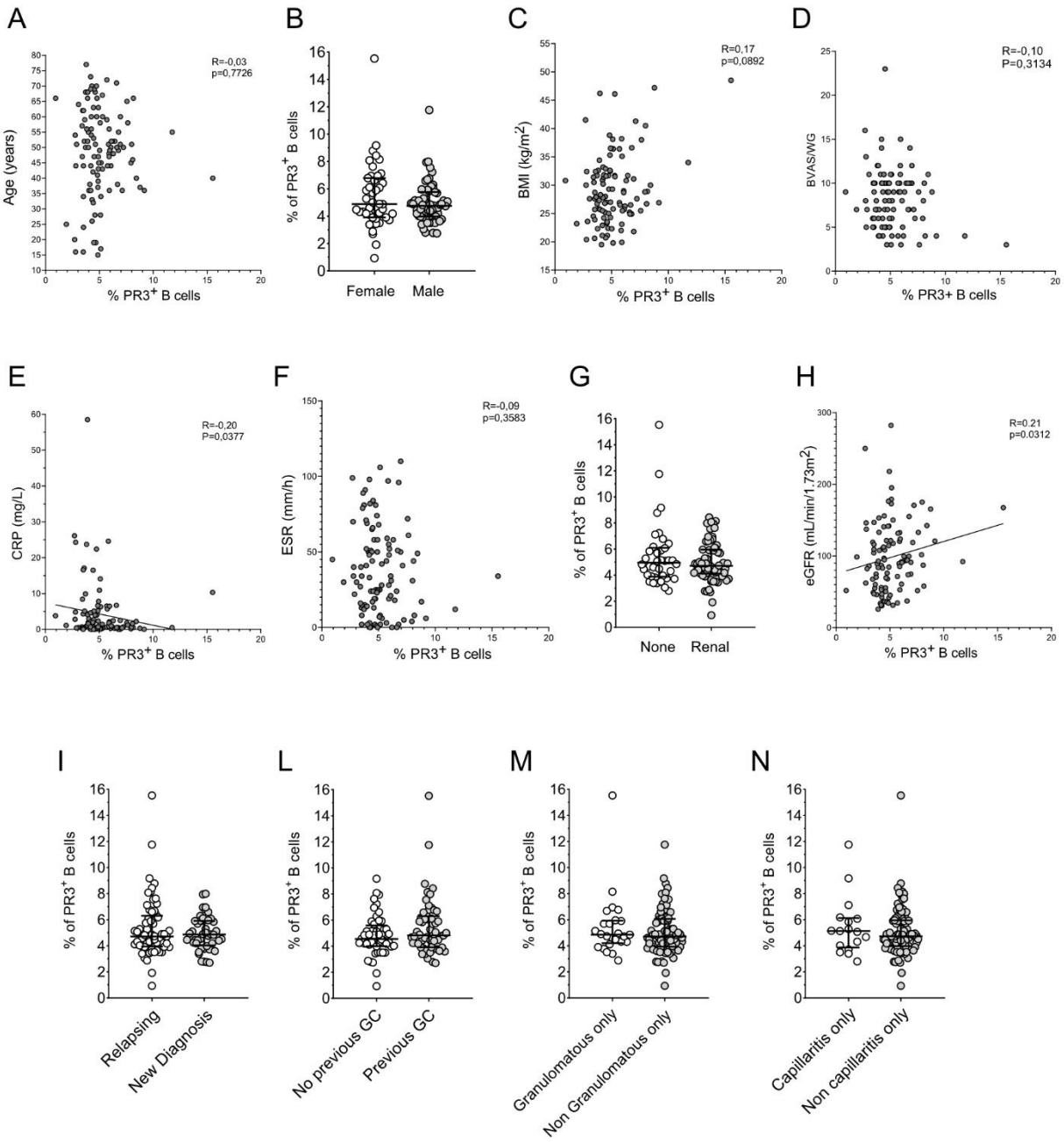

Supplemental Figure 7. Frequency of PR3⁺ B cells and clinical manifestations in PR3-AAV participants. In PR3-AAV patients (n=105), frequency of PR3⁺ B cells did not show any meaningful correlation with age (**A**), sex (**B**), BMI (**C**), BVAS/WG (**D**), CRP (**E**), ESR (**F**), renal involvement (**G**) or creatinine clearance (**H**), relapsing versus new diagnosis (**I**), previous use of glucocorticoids (**L**), the presence manifestations reflecting granulomatous disease only (**M**) or capillaritis only (**N**), as assessed by the BVAS/WG. P values in the figures are indicated as * $p < 0.05$, ** $p < 0.01$, *** $p < 0.001$

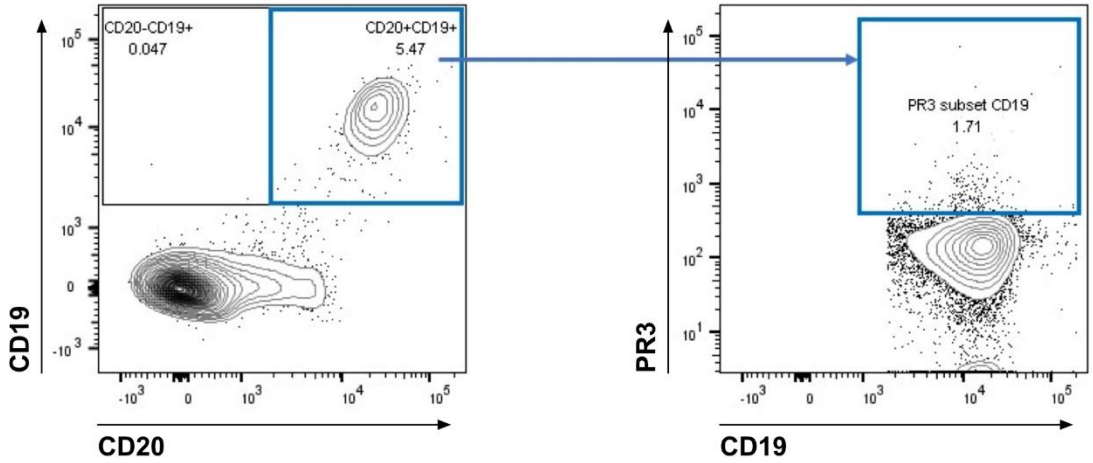

Supplemental Figure 8. The gating strategy for the aim #2 set of experiments. Double positive $CD19^{+}CD20^{+}$ was used to gate immature B cells mounting a BCR on the surface, to avoid inclusion of BM residing plasma cells and pro-B cells.

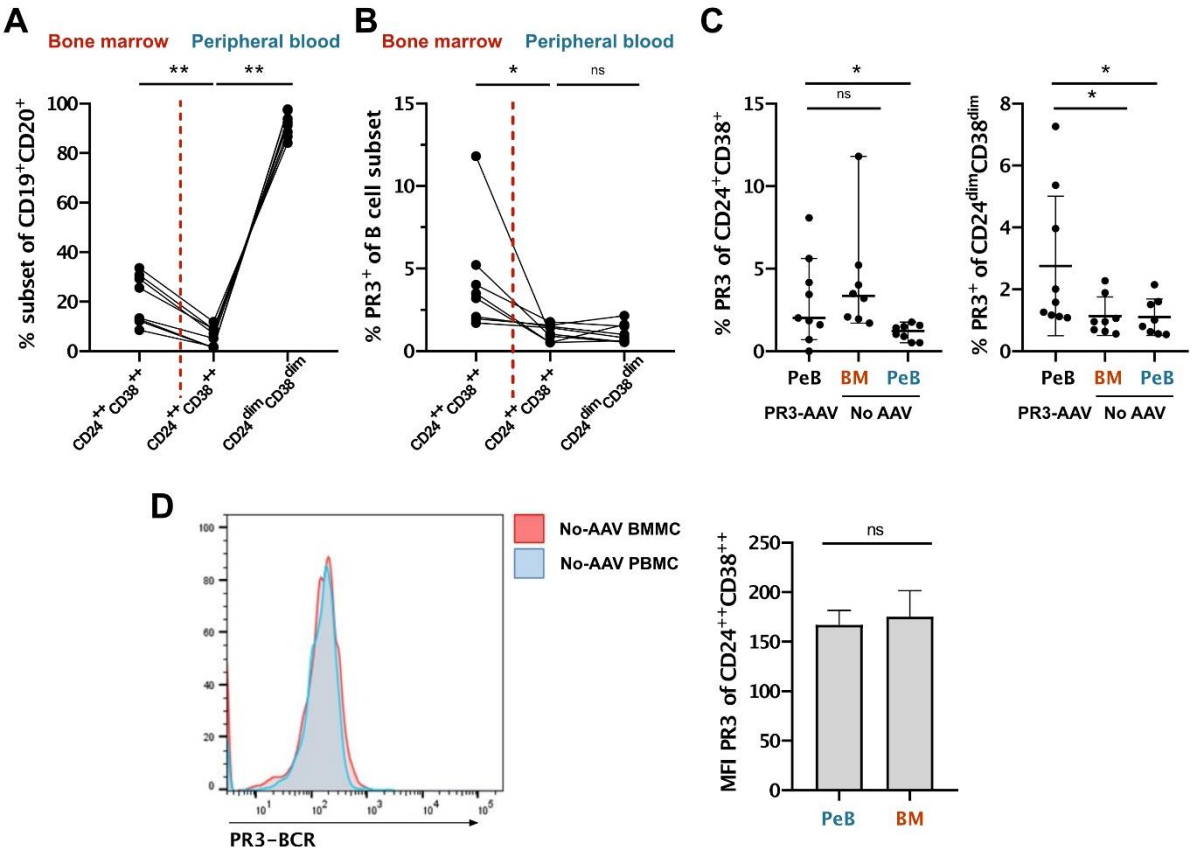

Supplemental Figure 9. PR3⁺ B cells among transitional B cells. Proportion of B cells (**A**) and PR3⁺ B cells among CD24⁺⁺CD38⁺⁺ of BMMC and PBMC and CD24^{dim}CD38^{dim} of PBMC in non-vasculitis (No-AAV) subjects (**B-C**). PR3 membrane expression in CD24⁺⁺CD38⁺⁺ B cells (**D**). Each point represents the frequency in an individual subject; horizontal lines show the median with 25-75% IQR; each histogram represents mean (± SEM). P values were determined by 2-tailed Mann-Whitney test or Student T test, where appropriate. Multiple comparisons between more than 2 groups were performed with Kruskal-Wallis test. P values in the figures are indicated as * $p < 0.05$, ** $p < 0.01$, *** $p < 0.001$ after adjustment for FDR as described by Benjamini and Hochberg. *PeB: Peripheral Blood, BM: bone marrow (blood), BMMC: bone marrow mononuclear cells; PBMC: peripheral blood mononuclear cells.*

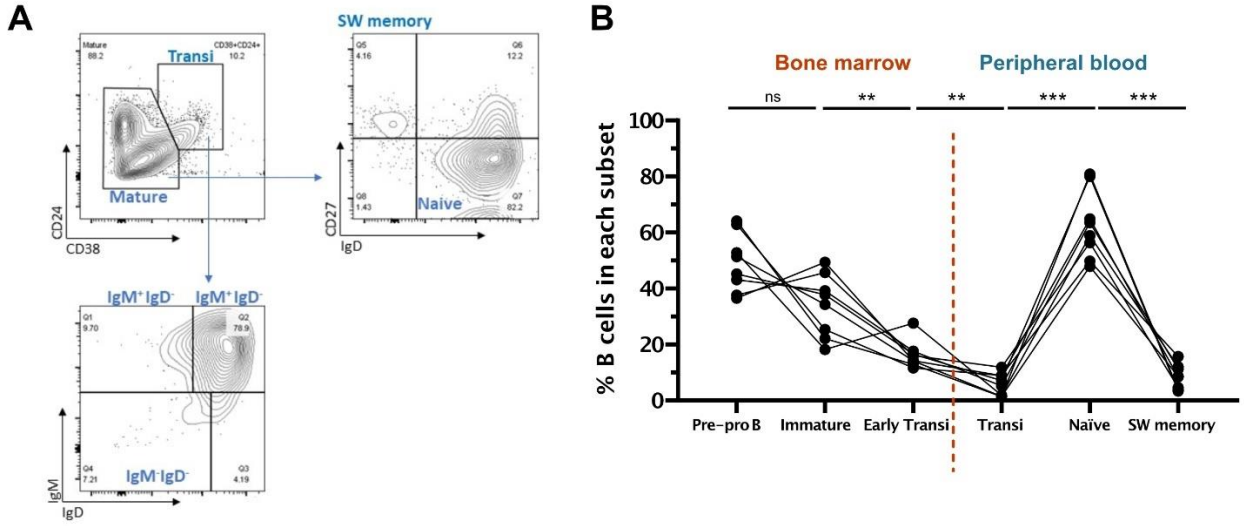

Supplemental Figure 10. Proportions of B cell subsets from bone marrow to peripheral B cells subsets in non-vasculitis patients. The gating strategy for parent gates of bone marrow and peripheral blood subsets (**A**); proportion of B cell subsets among total B cells from bone marrow to peripheral compartment (**B**). Each point represents the frequency in an individual subject. The multiple comparisons on B cell maturation were analyzed by using mixed-effects modelling. P values in the figures are indicated as * $p < 0.05$, ** $p < 0.01$, *** $p < 0.001$ after correction for FDR with Benjamini and Hochberg test.

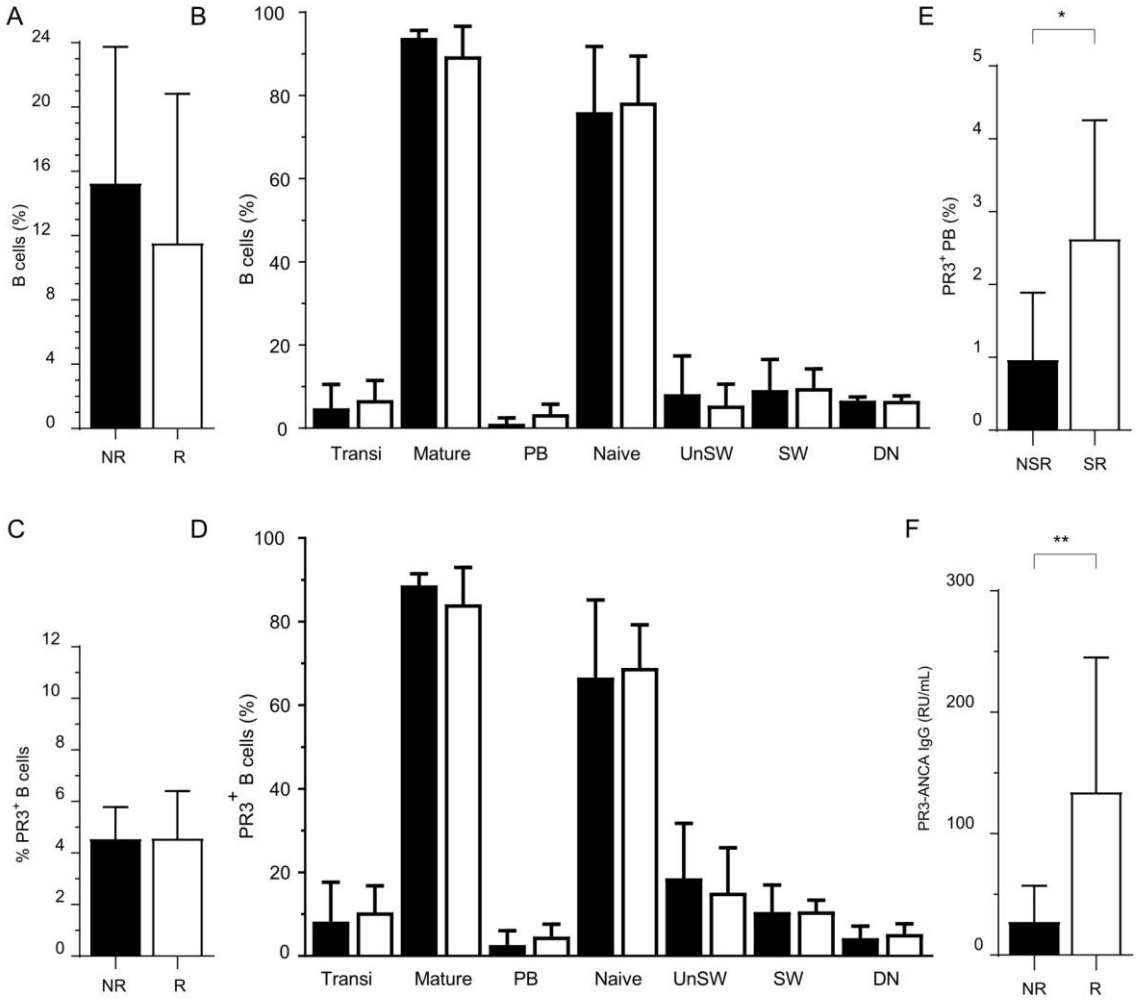

Supplemental Figure 11. Frequency of B cells, PR3⁺ B cell subsets and PR3-ANCA IgG at baseline and at recurrence of B cells. Frequency at baseline of total B cells (among PBMC) (**A**) and subsets within B cells (**B**) in participants that are going to relapse (open bars) or not (black bars). Frequency at baseline of total PR3⁺ B cells (among B cells) (**C**) and subsets within PR3⁺ B cells (**D**) in participants that are going to relapse (open bars) or not (black bars). PR3⁺ PBs by severe relapse (open bars) and non-severe relapses (black bars) at B cell recurrence (**E**). PR3-ANCA IgG titer at B cell recurrence in subjects that are going to severely relapse (open bars) and those that are not going to relapse (black bars) (**F**). P values in the figures are indicated as * $p < 0.05$, ** $p < 0.01$, *** $p < 0.001$.

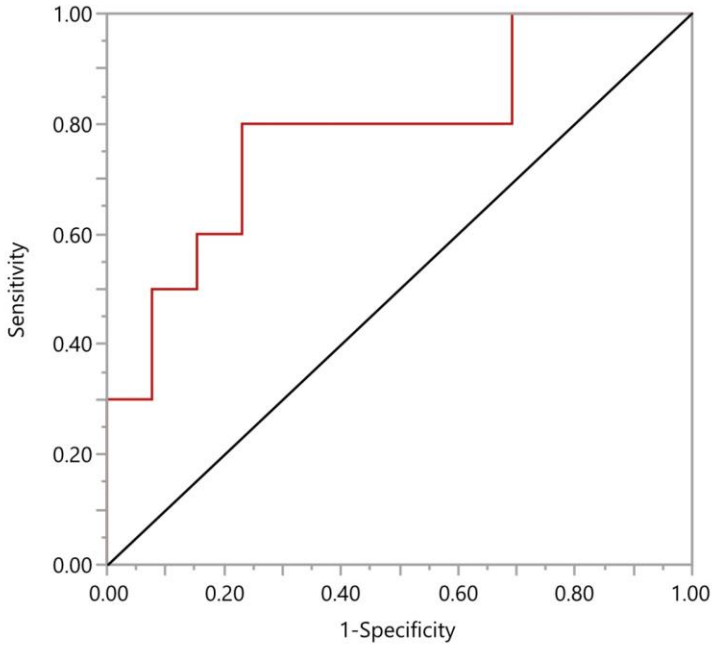

Supplemental Figure 12. Receiver operating characteristic curve (in red), showing the ability of PB within PR3+ pool to distinguish relapsing from non-relapsing patients at B cell recurrence. The Area Under the Curve (AUC) correspond to 0.79, showing that PB-PR3+ equal to 1.6% is the optimal cut-off to separate relapsers from long-term remitters (sensitivity=80%, specificity 77%, p=0.0129).

Supplemental Tables

Supplemental Table 1. Baseline features of patients with AAV and HC included in the aim #1 of the study.

Characteristics	PR3-AAV (N=105)	MPO-AAV (N=49)	HC (N=27)	p value
Age at study entry, media (SD)	48.7 (14.5)	59.0 (13.5)	53.9 (17.9)	**0.0004***
Sex				**0.0202***
Male, % (number)	59% (62)	37% (18)	41% (11)	
Female, % (number)	41% (43)	63% (31)	599% (16)	
Clinical Diagnosis,% (number)				**<0.001**
GPA	97% (102)	33% (16)	-	-
MPA	3% (3)	65% (32)	-	-
New Disease at enrollment (vs relapsing disease), % (number)	42% (44)	78% (38)	-	**<0.001**
Any granulomatous manifestation, % (number)	76% (80)	35% (17)	-	**<0.001**
Any capillaritis' manifestation, % (number)	84% (88)	96% (47)	-	**0.0363**
Any renal involvement, % (number)	64% (67)	82% (40)	-	**0.0259**
Alveolar hemorrhage, % (number)	30% (32)	18% (9)		**0.1133**
Glucocorticoid treatment at screening, % (number)	54% (57)	59% (29)	-	0.6047
Baseline BVAS/WG score, mean (SD)	8.2 (3.3)	8.0 (3.1)	-	0.7351
ESR (SD), mm/1 hr, median [IQR]	33 [14.5; 56.5]	44 [15;77.5]	-	0.1414
CRP (SD), mg/L, median [IQR]	1.2 [0.35; 4.45]	1.2 [0.3; 3.025]	-	0.8521
Baseline eGFR (SD), mL/min/1.73 m^2, median [IQR]	92.0 [57.0; 127.6]	45.9 [30.1; 71.2]	-	**<0.001**
ANCA levels (normal <20 IU)				
MPO-ANCA	0.6 [0.3;1.1]	121 [56.9; 177]	-	**<0.001**
PR3-ANCA	258 [165.5; 346]	2.7 [1.4; 4.65]	-	**<0.001**
Randomized Treatment group				0.8629
Rituximab, % (number)	49% (52)	47% (23)	-	-
Cyclophosphamide/Azathioprine, % (number)	50% (53)	53% (26)	-	-

*One-way ANOVA: cut-off for p value interpretation after Bonferroni correction**: 0,0167**

Abbreviations: ANCA=anti-neutrophil cytoplasmic antibodies; BVAS/WG=Birmingham Vasculitis Activity Score for Wegener's Granulomatosis; CRP= C-reactive protein; ESR=erythrocyte sedimentation rate; eGFR=estimated glomerular filtration rate, by means the Modification of Diet in Renal Disease (MDRD) study equation; GPA=granulomatosis with polyangiitis; MPA-microscopic polyangiitis; MPO=myeloperoxidase; PR3=proteinase-3; SD=standard deviation; IQR=Interquartile range. P values are for the comparison of MPO-AAV and PR3-AAV groups.

Footnotes*: Capillaritis was defined as the presence of one or more of the following BVAS/WG items: cutaneous purpura, scleritis, retinal hemorrhage or exudate, sensorineural deafness, hematuria, red blood cell casts on urinalysis or glomerulonephritis, increase in creatinine level, alveolar hemorrhage, mesenteric ischemia, sensory peripheral neuropathy, or motor mononeuritis multiplex. In contrast, BVAS/WG items reflecting underlying necrotizing granulomatous inflammation included mouth ulcers, retro-orbital mass/proptosis, bloody nasal discharge, sinus involvement, salivary gland enlargement, subglottic inflammation, conductive deafness, other major or minor ear/nose/throat involvement, pulmonary nodule/cavity, endobronchial involvement, meningitis, and cord lesion. Patients were considered to have renal disease if any renal item on the BVAS/WG (hematuria, red blood cell casts or glomerulonephritis, increase in creatinine level, or "other") was scored. A patient was categorized as having alveolar hemorrhage only if that item was scored on the BVAS/WG. All other BVAS/WG items cannot be clearly attributed to either necrotizing granulomatous inflammation or capillaritis and were, therefore, not considered to categorize the patient one way or another.*

Supplemental Table 2. Glucocorticoid treatment at screening (before sample collection). Results are represented as median (25-75% IQR).

Subset of disease	Glucocorticoids	No Glucocorticoids	P values
PR3-AAV patients			
Lymphocytes # (10^9cells/L)	1.12 (0.72,1.69)	1.16 (0.89,1.65)	0.591
Lymphocytes (% of PBMCs)	25.31 (15.66, 34.61)	28.93 (19.66, 40.19)	0.129
B cells (cells/μL)	123.69 (66.63, 182.64)	102.94 (68.98,217.63)	0.940
B cells (% of Lymphocytes)	10.61 (5.43, 16.22)	10.2 (5.32, 15.60)	0.589
$PR3^+$ B cells (cells/μL)	5.85 (3.33, 8.97)	4.69 (2.72, 10.12)	0.445
$PR3^+$ B cells (% of B cells)	4.82 (3.92, 6.30)	4.55 (3.99, 5.59)	0.246
Tfh (cells/mm^3)	20.95 (10.14, 48.62)	20.75 (8.44, 46.62)	0.599
Tfh (% of $CD4^+$ T cells)	3.58 (2.21, 4.88)	3.06 (1.83, 4.63)	0.144
MPO-AAV patients			
Lymphocytes # (10^9cells/L)	1.23 (0.93, 2.12)	1.25 (0.72, 2.33)	0.622
Lymphocytes (% of PBMCs)	25.57 (18.33, 34.64)	26.99 (19.89, 34.68)	0.504
B cells (cells/μL)	112.58 (56.22, 205.39)	118.92 (55.53, 236.65)	0.991
B cells (% of Lymphocytes)	8.43 (5.94, 17.87)	8.90 (6.07, 12.35)	1.000
$PR3^+$ B cells (cells/μL)	2.74 (2.02, 8.34)	3.68 (1.61, 9.66)	0.801
$PR3^+$ B cells (% of B cells)	3.13 (2.39, 5.04)	3.18 (2.72, 5.66)	0.569
Tfh (cells/mm^3)	27.52 (15.18, 48.50)	24.96 (10.21, 33.43)	0.411
Tfh (% of $CD4^+$ T cells)	4.05 (2.23, 5.59)	3.63 (2.69, 5.36)	0.954

ANCA=anti-neutrophil cytoplasmic antibodies; MPO=myeloperoxidase; PR3=proteinase-3; Tfh= T follicular helper cells; IQR=Interquartile range.

P values were determined by 2-tailed Mann-Whitney test.

Supplemental Table 3. Baseline features of subjects included in the aim #2 of the study.

Characteristics	Non vasculitis subjects (n=8)	PR3-AAV patients (n=9)	p value
Demographics			
Age at sampling, year, median [IQR]	65.75 [46.8, 72.85]	66.0 [58.2, 75.95]	0.3840
Male sex, M/F (number)	5/3	7/2	0.4901
Previous Diagnosis	2 HCs/2 MDS/2 AML/1 HES/1 CML*	PR3-AAV	-
Treatment at sampling			-
Oral Glucocorticoid, number	0	4	-
Imatinib, number	2	-	-
Azathioprine, number	-	4	-
Off-therapy, number	7	4	-
Laboratory features			
WBC, x10^9/ul, median [IQR]	4150 [3325, 5250]	6900 [5750, 8250]	0.0164
Ly, x10^9/ul, median [IQR]	1300 [1225, 1775]	1500 [900, 1650]	0.7606
Hb, g/dL, median [IQR]	13.3 [11.2, 13.8]	13.5 [10.8, 14.8]	0.4368
Detectable PR3-ANCA, >20 U/L, number (%)	0 (0%)	9 (100%)	-
Detectable MPO-ANCA >20 U/L, number (%)	0 (0%)	0 (0%)	-

All the subjects were white and Caucasian**.**

* all the non-vasculitis subjects were healthy or had a chronic myeloproliferative disorder (MDS, HES, CML) or were in long-standing remission after treatment for an acute myeloproliferative disorder AML, > 12 months after achieving remission)

Abbreviations: WBC=white blood cells; Ly=Lymphocyte; CRP= C-reactive protein; Hb=Hemoglobin, PR3=proteinase-3; MPO=myeloperoxidase, ANCA=anti-neutrophil cytoplasmic antibodies, SD=standard deviation, IQR= Interquartile range.

Supplemental Table 4. Baseline features of AAV subjects included in the aim #2 of the study.

Characteristics	PR3-AAV patients (n=9)
At diagnosis	
Age at diagnosis, years, median [IQR]	56.6 [46.35, 67.65]
BVAS.v3 at diagnosis, median [IQR]	21 [16, 22.5]
Positive circulating PR3-ANCA,% (number)	100% (9)
GPA diagnosis,% (number)	77.8% (7)
Relapsing disease,% (number)	33.3% (3)
Intravenous glucocorticoid at induction, % (number)	100%
Induction regiment used, CYC / RTX / CYC+ RTX	5 / 2 / 2
At sampling	
Age at sampling, years, median [IQR]	66.0 [58.2, 75.95]
Active/inactive patients at sampling, (number)	3/6
BVAS.v3 at sampling, active/inactive, median [IQR]	20 [13,21] / 0 [0. 0]
CRP, mg/L, median [IQR]	5.50 [1.70, 27.45]
Baseline eGFR mL/min/1.73 m^2, median [IQR]	50.4 [32.5; 87.50]
Active/Inactive Urinary Sediment, (number)	3/6
PR3-ANCA IgG, IU, median [IQR]	266 [86.4;366]
Oral glucocorticoid at sampling, active/inactive, % (number)*	2/2
DMARDs treatment at sampling, active/inactive, % (number)**	0/4

* In active cases daily oral prednisone dose was 1 mg/Kg and sample was withdrawn before intravenous bolus of methylprednisolone, while in patients in remission daily oral prednisone dose ranged between 2.5 and 5 mg.

**In all cases DMARD used was Azathioprine

Abbreviations: BVAS.v3 =Birmingham Vasculitis Activity Score version 3, PR3=proteinase-3; ANCA=anti-neutrophil cytoplasmic antibodies; GPA=granulomatosis with polyangiitis, CYC=cyclophosphamide, RTX=Rituximab, CRP= C-reactive protein; eGFR=estimated glomerular filtration rate, by means the Modification of Diet in Renal Disease (MDRD) study equation, DMARDs= Disease modifying antirheumatic drugs, SD=standard deviation; IQR= Interquartile range.

Supplemental Table 5. Baseline features of subjects with AAV included in the aim #3 of the study, by future relapse.

Characteristics	Relapsers (n=10)	Non-relapsers (n=13)	p value
Age at diagnosis, median [IQR]	45 [27.25;54]	54 [47,70]	0.0761
Male sex, % (number)	80% (8)	54% (7)	0.9624
GPA,% (number)	100% (10)	100% (13)	1.000
New Disease at enrollment (vs relapsing disease), % (number)	40% (4)	61% (8)	0.4136
Any granulomatous manifestation, % (number)	100% (10)	77% (10)	0.2292
Any capillaritis' manifestation, % (number)	80% (8)	92% (12)	0.5596
Any renal involvement, % (number)	50% (5)	77% (10)	0.2213
Glucocorticoid treatment at screening, % (number)	80% (8)	77% (10)	1.000
Baseline BVAS/WG score, median [IQR]	9.5 [7; 11]	9 [6.5; 10]	0.777
Albumin,g/dL,median [IQR]	3.8[3.25;3.9]	3.8 [3.2; 4.05]	0.1414
CRP, mg/L, median [IQR]	0.8 [0.45; 2.25]	2.8 [1.1; 6.3]	0.3094
Baseline eGFR mL/min/1.73 m^2, median [IQR]	113.4 [90.5; 156.3]	62.2 [34.4; 107.7]	0.0369
PR3-ANCA IgG, IU, median [IQR]	243.5 [95.7; 327]	266 [86.4;366]	0.6418

All the subjects were white except a Hispanic subjects in the non-relapsers group**.**

Abbreviations: GPA=granulomatosis with polyangiitis; BVAS/WG=Birmingham Vasculitis Activity Score for Wegener's Granulomatosis; CRP= C-reactive protein; eGFR=estimated glomerular filtration rate, by means the Modification of Diet in Renal Disease (MDRD) study equation; PR3=proteinase-3; ANCA=anti-neutrophil cytoplasmic antibodies; SD=standard deviation; IQR= Interquartile range.

Supplemental Table 6. Relationship between PR3-ANCA IgG titer increase and frequency of plasmablasts within PR3-reactive B cell increase.

Characteristics	All (n=23)	Relapsers (n=10)	Non-relapsers (n=13)
PR3-ANCA IgG titer increase before PB-PR3 increase	0	0	0
PR3-ANCA IgG titer increase with PB-PR3 increase	13 (57%)	7 (70%)	6 (46%)
PR3-ANCA IgG titer increase after PB-PR3 increase	7 (30%)	3 (30%)	4 (31%)
PR3-ANCA IgG remain undetectable	3 (13%)	0 (0%)	3 (23%)

All comparisons between relapsers and non relapsers were nonsignificant (p>0.05).

PR3-ANCA IgG=Proteinase 3 ANCA Immunoglobulin G; ANCA=anti-neutrophil cytoplasmic antibodies; PB=Plasmablasts

References

1. T. W. Lebien, T. F. Tedder, B lymphocytes: How they develop and function, *Blood* **112** (2008), doi:10.1182/blood-2008-02-078071.

2. W. Hoffman, F. G. Lakkis, G. Chalasani, B cells, antibodies, and more, *Clin. J. Am. Soc. Nephrol.* **11** (2016), doi:10.2215/CJN.09430915.

3. K. Pieper, B. Grimbacher, H. Eibel, B-cell biology and development*J. Allergy Clin. Immunol.* **131** (2013), doi:10.1016/j.jaci.2013.01.046.

4. W. A. Figgett, F. B. Vincent, D. Saulep-Easton, F. Mackay, Roles of ligands from the TNF superfamily in B cell development, function, and regulation*Semin. Immunol.* **26** (2014), doi:10.1016/j.smim.2014.06.001.

5. C. Weaver, K. Murphy, *Janeway's Immunobiology* G. Science, Ed. (London, New York, 2012).

6. C. M. Grimaldi, R. Hicks, B. Diamond, B Cell Selection and Susceptibility to Autoimmunity, *J. Immunol.* **174** (2005), doi:10.4049/jimmunol.174.4.1775.

7. I. C. M. MacLennan, Germinal Centers, *Annu. Rev. Immunol.* (1994), doi:10.1146/annurev.iy.12.040194.001001.

8. M. A. Linterman, R. J. Rigby, R. K. Wong, D. Yu, R. Brink, J. L. Cannons, P. L. Schwartzberg, M. C. Cook, G. D. Walters, C. G. Vinuesa, Follicular helper T cells are required for systemic autoimmunity, *J. Exp. Med.* (2009), doi:10.1084/jem.20081886.

9. J.-Y. Wang, *B Cells in Immunity and Tolerance* (2020).

10. D. P. Harris, L. Haynes, P. C. Sayles, D. K. Duso, S. M. Eaton, N. M. Lepak, L. L.

Johnson, S. L. Swain, F. E. Lund, Reciprocal regulation of polarized cytokine production by effector B and T cells, *Nat. Immunol.* **1** (2000), doi:10.1038/82717.

11. A. Mizoguchi, A. K. Bhan, A Case for Regulatory B Cells, *J. Immunol.* **176** (2006), doi:10.4049/jimmunol.176.2.705.

12. K. Yanaba, J. D. Bouaziz, K. M. Haas, J. C. Poe, M. Fujimoto, T. F. Tedder, A Regulatory B Cell Subset with a Unique CD1dhiCD5+ Phenotype Controls T Cell-Dependent Inflammatory Responses, *Immunity* **28** (2008), doi:10.1016/j.immuni.2008.03.017.

13. D. Nemazee, Mechanisms of central tolerance for B cells*Nat. Rev. Immunol.* (2017), doi:10.1038/nri.2017.19.

14. J. J. Sabatino, A. K. Pröbstel, S. S. Zamvil, B cells in autoimmune and neurodegenerative central nervous system diseases*Nat. Rev. Neurosci.* **20** (2019), doi:10.1038/s41583-019-0233-2.

15. M. Ichii, Early B lymphocyte development: Similarities and differences in human and mouse, *World J. Stem Cells* **6** (2014), doi:10.4252/wjsc.v6.i4.421.

16. R. Pelanda, R. M. Torres, Central B-Cell tolerance: Where selection begins, *Cold Spring Harb. Perspect. Biol.* **4** (2012), doi:10.1101/cshperspect.a007146.

17. S. A. Greaves, J. N. Peterson, P. Strauch, R. M. Torres, R. Pelanda, Active PI3K abrogates central tolerance in high-avidity autoreactive B cells, *J. Exp. Med.* **216** (2019), doi:10.1084/jem.20181652.

18. M. Perez-Andres, B. Paiva, W. G. Nieto, A. Caraux, A. Schmitz, J. Almeida, R. F.

Vogt, G. E. Marti, A. C. Rawstron, M. C. Van Zelm, J. J. M. Van Dongen, H. E. Johnsen, B. Klein, A. Orfao, Human peripheral blood B-Cell compartments: A crossroad in B-cell traffic*Cytom. Part B - Clin. Cytom.* **78** (2010), doi:10.1002/cyto.b.20547.

19. S. M. Kerfoot, G. Yaari, J. R. Patel, K. L. Johnson, D. G. Gonzalez, S. H. Kleinstein, A. M. Haberman, Germinal Center B Cell and T Follicular Helper Cell Development Initiates in the Interfollicular Zone, *Immunity* **34** (2011), doi:10.1016/j.immuni.2011.03.024.

20. M. Kitano, S. Moriyama, Y. Ando, M. Hikida, Y. Mori, T. Kurosaki, T. Okada, Bcl6 Protein Expression Shapes Pre-Germinal Center B Cell Dynamics and Follicular Helper T Cell Heterogeneity, *Immunity* **34** (2011), doi:10.1016/j.immuni.2011.03.025.

21. T. Okada, M. J. Miller, I. Parker, M. F. Krummel, M. Neighbors, S. B. Hartley, A. O'Garra, M. D. Cahalan, J. G. Cyster, Antigen-engaged B cells undergo chemotaxis toward the T zone and form motile conjugates with helper T cells, *PLoS Biol.* **3** (2005), doi:10.1371/journal.pbio.0030150.

22. D. Suan, C. Sundling, R. Brink, Plasma cell and memory B cell differentiation from the germinal center*Curr. Opin. Immunol.* **45** (2017), doi:10.1016/j.coi.2017.03.006.

23. S. L. Nutt, P. D. Hodgkin, D. M. Tarlinton, L. M. Corcoran, The generation of antibody-secreting plasma cells, *Nat. Rev. Immunol.* **15** (2015), doi:10.1038/nri3795.

24. T. Inoue, I. Moran, R. Shinnakasu, T. G. Phan, T. Kurosaki, Generation of memory B cells and their reactivation*Immunol. Rev.* **283** (2018), doi:10.1111/imr.12640.

25. T. F. Tedder, CD19: A promising B cell target for rheumatoid arthritis*Nat. Rev.*

Rheumatol. **5** (2009), doi:10.1038/nrrheum.2009.184.

26. S. A. Beers, C. H. T. Chan, R. R. French, M. S. Cragg, M. J. Glennie, CD20 as a target for therapeutic type i and ii monoclonal antibodies, *Semin. Hematol.* **47** (2010), doi:10.1053/j.seminhematol.2010.01.001.

27. G. Clavarino, N. Delouche, C. Vettier, D. Laurin, M. Pernollet, T. Raskovalova, J. Y. Cesbron, C. Dumestre-Pérard, M. C. Jacob, Novel strategy for phenotypic characterization of Human B lymphocytes from precursors to effector cells by flow cytometry, *PLoS One* **11** (2016), doi:10.1371/journal.pone.0162209.

28. Q. Simon, J. O. Pers, D. Cornec, L. Le Pottier, R. A. Mageed, S. Hillion, In-depth characterization of CD24highCD38high transitional human B cells reveals different regulatory profiles, *J. Allergy Clin. Immunol.* (2016), doi:10.1016/j.jaci.2015.09.014.

29. N. Dumoitier, B. Terrier, J. London, S. Lofek, L. Mouthon, Implication of B lymphocytes in the pathogenesis of ANCA-associated vasculitides, *Autoimmun Rev* **14**, 996–1004 (2015).

30. J. Gladitz, Rubin, Donald B.: Multiple Imputation for Nonresponse in Surveys. John Wiley & Sons, Chichester – New York – Brisbane – Toronto – Singapore 1987, xxx, 258 S., 6 Abb., £ 30.25, ISSN 0271-6232, *Biometrical J.* (1989), doi:10.1002/bimj.4710310118.

31. M. Ota, B. H. Duong, A. Torkamani, C. M. Doyle, A. L. Gavin, T. Ota, D. Nemazee, Regulation of the B Cell Receptor Repertoire and Self-Reactivity by BAFF, *J. Immunol.* (2010), doi:10.4049/jimmunol.1002176.

32. S. A. Jenks, K. S. Cashman, E. Zumaquero, U. M. Marigorta, A. V. Patel, X. Wang, D. Tomar, M. C. Woodruff, Z. Simon, R. Bugrovsky, E. L. Blalock, C. D. Scharer, C. M. Tipton, C. Wei, S. S. Lim, M. Petri, T. B. Niewold, J. H. Anolik, G. Gibson, F. E. H. Lee, J. M. Boss, F. E. Lund, I. Sanz, Distinct Effector B Cells Induced by Unregulated Toll-like Receptor 7 Contribute to Pathogenic Responses in Systemic Lupus Erythematosus, *Immunity* (2018), doi:10.1016/j.immuni.2018.08.015.

33. V. J. Sindhava, M. A. Oropallo, K. Moody, M. Naradikian, L. E. Higdon, L. Zhou, A. Myles, N. Green, K. Nündel, W. Stohl, A. M. Schmidt, W. Cao, S. Dorta-Estremera, T. Kambayashi, A. Marshak-Rothstein, M. P. Cancro, A TLR9-dependent checkpoint governs B cell responses to DNA-containing antigens, *J. Clin. Invest.* **127** (2017), doi:10.1172/JCI89931.

34. S. J. S. Rubin, M. S. Bloom, W. H. Robinson, B cell checkpoints in autoimmune rheumatic diseases*Nat. Rev. Rheumatol.* **15** (2019), doi:10.1038/s41584-019-0211-0.

35. M. S. Bynoe, L. Spatz, B. Diamond, Characterization of anti-DNA B cells that escape negative selection, *Eur. J. Immunol.* (1999), doi:10.1002/(sici)1521-4141(199904)29:04<1304::aid-immu1304>3.3.co;2-y.

36. S. Malkiel, V. Jeganathan, S. Wolfson, N. Manjarrez Orduño, E. Marasco, C. Aranow, M. Mackay, P. K. Gregersen, B. Diamond, Checkpoints for Autoreactive B Cells in the Peripheral Blood of Lupus Patients Assessed by Flow Cytometry, *Arthritis Rheumatol.* (2016), doi:10.1002/art.39710.

37. S. Malkiel, A. N. Barlev, Y. Atisha-Fregoso, J. Suurmond, B. Diamond, Plasma cell differentiation pathways in systemic lupus erythematosus*Front. Immunol.* **9** (2018),

doi:10.3389/fimmu.2018.00427.

38. J. F. Scheid, H. Mouquet, J. Kofer, S. Yurasov, M. C. Nussenzweig, H. Wardemann, Differential regulation of self-reactivity discriminates between IgG + human circulating memory B cells and bone marrow plasma cells, *Proc. Natl. Acad. Sci. U. S. A.* **108** (2011), doi:10.1073/pnas.1113395108.

39. J. Suurmond, Y. Atisha-Fregoso, E. Marasco, A. N. Barlev, N. Ahmed, S. A. Calderon, M. Y. Wong, M. C. Mackay, C. Aranow, B. Diamond, Loss of an IgG plasma cell checkpoint in patients with lupus, *J. Allergy Clin. Immunol.* (2019), doi:10.1016/j.jaci.2018.10.041.

40. A. Coutinho, M. D. Kazatchkine, S. Avrameas, Natural autoantibodies, *Curr. Opin. Immunol.* **7** (1995), doi:10.1016/0952-7915(95)80053-0.

41. S. Avrameas, C. Selmi, Natural autoantibodies in the physiology and pathophysiology of the immune system*J. Autoimmun.* **41** (2013), doi:10.1016/j.jaut.2013.01.006.

42. P. I. Lobo, Role of natural autoantibodies and natural IgM anti-leucocyte autoantibodies in health and disease*Front. Immunol.* **7** (2016), doi:10.3389/fimmu.2016.00198.

43. C. Grönwall, J. Vas, G. J. Silverman, Protective roles of natural IgM antibodies*Front. Immunol.* **3** (2012), doi:10.3389/fimmu.2012.00066.

44. N. Baumgarth, The double life of a B-1 cell: Self-reactivity selects for protective effector functions, *Nat. Rev. Immunol.* **11** (2011), doi:10.1038/nri2901.

45. S. Pillai, A. Cariappa, The follicular versus marginal zone B lymphocyte cell fate

decision*Nat. Rev. Immunol.* **9** (2009), doi:10.1038/nri2656.

46. A. Cerutti, M. Cols, I. Puga, Marginal zone B cells: Virtues of innate-like antibody-producing lymphocytes*Nat. Rev. Immunol.* **13** (2013), doi:10.1038/nri3383.

47. T. H. Winkler, R. E. Voll, Introduction: B cell-mediated autoimmune diseases*Semin. Immunopathol.* **36** (2014), doi:10.1007/s00281-014-0432-x.

48. B. Bolon, M. Stolina, C. King, S. Middleton, J. Gasser, D. Zack, U. Feige, Rodent preclinical models for developing novel antiarthritic molecules: Comparative biology and preferred methods for evaluating efficacy*J. Biomed. Biotechnol.* **2011** (2011), doi:10.1155/2011/569068.

49. D. M. Klinman, Polyclonal B cell activation in lupus-prone mice precedes and predicts the development of autoimmune disease, *J. Clin. Invest.* **86** (1990), doi:10.1172/JCI114831.

50. M. Starobinski, M. Lacour, L. Reininger, S. Izui, Autoantibody repertoire analysis in normal and lupus-prone mice, *J. Autoimmun.* **2** (1989), doi:10.1016/S0896-8411(89)80005-8.

51. Z. Liu, A. Davidson, BAFF and selection of autoreactive B cells*Trends Immunol.* (2011), doi:10.1016/j.it.2011.06.004.

52. N. Lepse, J. Land, A. Rutgers, C. G. Kallenberg, C. A. Stegeman, W. H. Abdulahad, P. Heeringa, Toll-like receptor 9 activation enhances B cell activating factor and interleukin-21 induced anti-proteinase 3 autoantibody production in vitro, *Rheumatol.* **55**, 162–172 (2016).

53. N. Nishimoto, T. Kishimoto, Interleukin 6: From bench to bedside*Nat. Clin. Pract. Rheumatol.* (2006), doi:10.1038/ncprheum0338.

54. S. Kuchen, R. Robbins, G. P. Sims, C. Sheng, T. M. Phillips, P. E. Lipsky, R. Ettinger, Essential Role of IL-21 in B Cell Activation, Expansion, and Plasma Cell Generation during CD4 + T Cell-B Cell Collaboration , *J. Immunol.* **179** (2007), doi:10.4049/jimmunol.179.9.5886.

55. T. F. Tedder, J. C. Poe, K. M. Haas, CD22: A multifunctional receptor that regulates B lymphocyte survival and signal transduction*Adv. Immunol.* **88** (2005), doi:10.1016/S0065-2776(05)88001-0.

56. N. R. Pritchard, K. G. C. Smith, B cell inhibitory receptors and autoimmunity*Immunology* **108** (2003), doi:10.1046/j.1365-2567.2003.01592.x.

57. R. de la Varga-Martínez, B. Rodríguez-Bayona, A. Campos-Caro, G. A. Añez, F. Medina-Varo, C. Rodríguez, Autoreactive B-lymphocytes in SLE and RA patients: Isolation and characterisation using extractable nuclear and citrullinated antigens bound to immunobeads, *Eur. J. Immunol.* (2019), doi:10.1002/eji.201848065.

58. K. Germar, C. M. Fehres, H. U. Scherer, N. van Uden, S. Pollastro, N. Yeremenko, M. Hansson, P. F. Kerkman, E. I. H. van der Voort, E. Reed, H. Maassen, M. J. Kwakkenbos, A. Q. Bakker, L. Klareskog, V. Malmström, N. de Vries, R. E. M. Toes, K. Lundberg, H. Spits, D. L. Baeten, Generation and Characterization of Anti–Citrullinated Protein Antibody–Producing B Cell Clones From Rheumatoid Arthritis Patients, *Arthritis Rheumatol.* **71** (2019), doi:10.1002/art.40739.

59. B. Zhang, Y. Wang, Y. Yuan, J. Sun, L. Liu, D. Huang, J. Hu, M. Wang, S. Li, W.

Song, H. Chen, D. Zhou, X. Zhang, In vitro elimination of autoreactive B cells from rheumatoid arthritis patients by universal chimeric antigen receptor T cells, *Ann. Rheum. Dis.* **80** (2021), doi:10.1136/annrheumdis-2020-217844.

60. J. S. Dekkers, M. K. Verheul, J. N. Stoop, B. Liu, A. Ioan-Facsinay, P. A. Van Veelen, A. H. De Ru, G. M. C. Janssen, M. Hegen, S. Rapecki, T. W. J. Huizinga, L. A. Trouw, R. E. M. Toes, Breach of autoreactive B cell tolerance by post-translationally modified proteins, *Ann. Rheum. Dis.* **76** (2017), doi:10.1136/annrheumdis-2016-210772.

61. L. Winger, C. Winger, P. Shastry, A. Russell, M. Longenecker, Efficient generation in vitro, from human peripheral blood cells, of monoclonal Epstein-Barr virus transformants producing specific antibody to a variety of antigens without prior deliberate immunization, *Proc. Natl. Acad. Sci. U. S. A.* **80** (1983), doi:10.1073/pnas.80.14.4484.

62. A. L. Foreman, J. Van de Water, M. L. Gougeon, M. E. Gershwin, B cells in autoimmune diseases: Insights from analyses of immunoglobulin variable (Ig V) gene usage*Autoimmun. Rev.* **6** (2007), doi:10.1016/j.autrev.2006.12.005.

63. D. Corti, F. Sallusto, A. Lanzavecchia, High throughput cellular screens to interrogate the human T and B cell repertoires*Curr. Opin. Immunol.* **23** (2011), doi:10.1016/j.coi.2011.04.006.

64. E. Meffre, The establishment of early B cell tolerance in humans: Lessons from primary immunodeficiency diseases, *Ann. N. Y. Acad. Sci.* **1246** (2011), doi:10.1111/j.1749-6632.2011.06347.x.

65. Y. Atisha-Fregoso, S. Malkiel, K. M. Harris, M. Byron, L. Ding, S. Kanaparthi, W. T. Barry, W. Gao, K. Ryker, P. Tosta, A. D. Askanase, S. A. Boackle, W. W. Chatham, D. L.

Kamen, D. R. Karp, K. A. Kirou, S. Sam Lim, B. Marder, M. McMahon, S. V. Parikh, W. F. Pendergraft, A. S. Podoll, A. Saxena, D. Wofsy, B. Diamond, D. E. Smilek, C. Aranow, M. Dall'Era, Phase II Randomized Trial of Rituximab Plus Cyclophosphamide Followed by Belimumab for the Treatment of Lupus Nephritis, *Arthritis Rheumatol.* (2020), doi:10.1002/art.41466.

66. J. Suurmond, Y. Atisha-Fregoso, A. N. Barlev, S. A. Calderon, M. C. Mackay, C. Aranow, B. Diamond, Patterns of ANA+ B cells for SLE patient stratification, *JCI Insight* **4** (2019), doi:10.1172/jci.insight.127885.

67. P. F. Kerkman, E. Fabre, E. I. H. Van Der Voort, A. Zaldumbide, Y. Rombouts, T. Rispens, G. Wolbink, R. C. Hoeben, H. Spits, D. L. P. Baeten, T. W. J. Huizinga, R. E. M. Toes, H. U. Scherer, Identification and characterisation of citrullinated antigen-specific B cells in peripheral blood of patients with rheumatoid arthritis, *Ann. Rheum. Dis.* **75** (2016), doi:10.1136/annrheumdis-2014-207182.

68. A. Mahendra, X. Yang, S. Abnouf, J. R. T. Adolacion, D. Park, S. Soomro, J. Roszik, C. Coarfa, G. Romain, K. Wanzeck, S. L. Bridges, A. Aggarwal, P. Qiu, S. K. Agarwal, C. Mohan, N. Varadarajan, Beyond Autoantibodies: Biologic Roles of Human Autoreactive B Cells in Rheumatoid Arthritis Revealed by RNA-Sequencing, *Arthritis Rheumatol.* **71** (2019), doi:10.1002/art.40772.

69. H. Kristyanto, N. J. Blomberg, L. M. Slot, E. I. H. van der Voort, P. F. Kerkman, A. Bakker, L. E. Burgers, R. M. ten Brinck, A. H. M. van der Helm-Van Mil, H. Spits, D. L. Baeten, T. W. J. Huizinga, R. E. M. Toes, H. U. Scherer, Persistently activated, proliferative memory autoreactive b cells promote inflammation in rheumatoid arthritis,

Sci. Transl. Med. **12** (2020), doi:10.1126/SCITRANSLMED.AAZ5327.

70. R. Eming, A. Nagel, S. Wolff-Franke, E. Podstawa, D. Debus, M. Hertl, Rituximab exerts a dual effect in pemphigus vulgaris, *J. Invest. Dermatol.* **128** (2008), doi:10.1038/jid.2008.172.

71. N. Colliou, D. Picard, F. Caillot, S. Calbo, S. Le Corre, A. Lim, B. Lemercier, B. Le Mauff, M. Maho-Vaillant, S. Jacquot, C. Bedane, P. Bernard, F. Caux, C. Prost, E. Delaporte, M. S. Doutre, B. Dreno, N. Franck, S. Ingen-Housz-Oro, O. Chosidow, C. Pauwels, C. Picard, J. C. Roujeau, M. Sigal, E. Tancrede-Bohin, I. Templier, R. Eming, M. Hertl, M. D'Incan, P. Joly, P. Musette, Long-term remissions of severe pemphigus after rituximab therapy are associated with prolonged failure of desmoglein B cell response, *Sci. Transl. Med.* (2013), doi:10.1126/scitranslmed.3005166.

72. K. Nishifuji, M. Amagai, M. Kuwana, T. Iwasaki, T. Nishikawa, Detection of antigen-specific B cells in patients with pemphigus vulgaris by enzyme-linked immunospot assay: Requirement of T cell collaboration for autoantibody production, *J. Invest. Dermatol.* **114** (2000), doi:10.1046/j.1523-1747.2000.00840.x.

73. V. Hébert, M. Maho-Vaillant, M. L. Golinski, M. Petit, G. Riou, O. Boyer, P. Musette, S. Calbo, P. Joly, Modifications of the BAFF/BAFF-Receptor Axis in Patients With Pemphigus Treated With Rituximab Versus Standard Corticosteroid Regimen, *Front. Immunol.* **12** (2021), doi:10.3389/fimmu.2021.666022.

74. V. Hébert, M. Petit, M. Maho-Vaillant, M. L. Golinski, G. Riou, C. Derambure, O. Boyer, P. Joly, S. Calbo, Modifications of the Transcriptomic Profile of Autoreactive B Cells From Pemphigus Patients After Treatment With Rituximab or a Standard

Corticosteroid Regimen, *Front. Immunol.* **10** (2019), doi:10.3389/fimmu.2019.01794.

75. D. Cornec, A. Berti, A. Hummel, T. Peikert, J. O. Pers, U. Specks, Identification and phenotyping of circulating autoreactive proteinase 3-specific B cells in patients with PR3-ANCA associated vasculitis and healthy controls, *J Autoimmun* **84**, 122–131 (2017).

76. S. Glauzy, B. Olson, C. K. May, D. Parisi, C. Massad, J. E. Hansen, C. Ryu, E. L. Herzog, E. Meffre, Defective early B cell tolerance checkpoints in patients with systemic sclerosis allow the production of self-antigen-specific clones, *Arthritis Rheumatol.* (2021), doi:10.1002/art.41927.

77. B. A. Joosse, J. H. Jackson, A. Cisneros, A. B. Santhin, S. A. Smith, D. J. Moore, L. J. Crofford, E. M. Wilfong, R. H. Bonami, High-Throughput Detection of Autoantigen-Specific B Cells Among Distinct Functional Subsets in Autoimmune Donors, *Front. Immunol.* **12** (2021), doi:10.3389/fimmu.2021.685718.

78. J. Sun, D. N. Fass, M. A. Viss, A. M. Hummel, H. Tang, H. A. Homburger, U. Specks, A proportion of proteinase 3 (PR3)-specific anti-neutrophil cytoplasmic antibodies (ANCA) only react with PR3 after cleavage of its N-terminal activation dipeptide, *Clin. Exp. Immunol.* (1998), doi:10.1046/j.1365-2249.1998.00730.x.

79. J. Sun, D. N. Fass, J. A. Hudson, M. A. Viss, J. Wieslander, H. A. Homburger, U. Specks, Capture-ELISA based on recombinant PR3 is sensitive for PR3-ANCA testing and allows detection of PR3 and PR3-ANCA/PR3 immunecomplexes, *J. Immunol. Methods* (1998), doi:10.1016/S0022-1759(97)00203-2.

80. F. Silva, A. M. Hummel, D. E. Jenne, U. Specks, Discrimination and variable impact of ANCA binding to different surface epitopes on proteinase 3, the Wegener's

autoantigen, *J. Autoimmun.* **35** (2010), doi:10.1016/j.jaut.2010.06.021.

81. O. Wiesner, R. D. Litwiller, A. M. Hummel, M. A. Viss, C. J. McDonald, D. E. Jenne, D. N. Fass, U. Specks, Differences between human proteinase 3 and neutrophil elastase and their murine homologues are relevant for murine model experiments, *FEBS Lett.* **579** (2005), doi:10.1016/j.febslet.2005.08.056.

82. G. Weppner, O. Ohlei, C. M. Hammers, K. Holl-Ulrich, J. Voswinkel, J. Bischof, K. Hasselbacher, G. Riemekasten, P. Lamprecht, S. Ibrahim, C. Iking-Konert, A. Recke, A. Müller, In situ detection of PR3-ANCA+ B cells and alterations in the variable region of immunoglobulin genes support a role of inflamed tissue in the emergence of auto-reactivity in granulomatosis with polyangiitis, *J. Autoimmun.* (2018), doi:10.1016/j.jaut.2018.07.004.

83. J. Voswinkel, A. Müller, P. Lamprecht, in *Annals of the New York Academy of Sciences*, (2005).

84. A. S. Fauci, B. F. Haynes, P. Katz, S. M. Wolff, Wegener's granulomatosis: prospective clinical and therapeutic experience with 85 patients for 21 years, *Ann Intern Med* **98**, 76–85 (1983).

85. J. H. Stone, P. A. Merkel, R. Spiera, P. Seo, C. A. Langford, G. S. Hoffman, C. G. Kallenberg, E. W. St Clair, A. Turkiewicz, N. K. Tchao, L. Webber, L. Ding, L. P. Sejismundo, K. Mieras, D. Weitzenkamp, D. Ikle, V. Seyfert-Margolis, M. Mueller, P. Brunetta, N. B. Allen, F. C. Fervenza, D. Geetha, K. A. Keogh, E. Y. Kissin, P. A. Monach, T. Peikert, C. Stegeman, S. R. Ytterberg, U. Specks, Rituximab versus cyclophosphamide for ANCA-associated vasculitis, *N Engl J Med* **363**, 221–232 (2010).

86. U. Specks, P. A. Merkel, P. Seo, R. Spiera, C. A. Langford, G. S. Hoffman, C. G. Kallenberg, E. W. St Clair, B. J. Fessler, L. Ding, L. Viviano, N. K. Tchao, D. J. Phippard, A. L. Asare, N. Lim, D. Ikle, B. Jepson, P. Brunetta, N. B. Allen, F. C. Fervenza, D. Geetha, K. Keogh, E. Y. Kissin, P. A. Monach, T. Peikert, C. Stegeman, S. R. Ytterberg, M. Mueller, L. P. Sejismundo, K. Mieras, J. H. Stone, Efficacy of remission-induction regimens for ANCA-associated vasculitis, *N Engl J Med* **369**, 417–427 (2013).

87. L. Guillevin, C. Pagnoux, A. Karras, C. Khouatra, O. Aumaitre, P. Cohen, F. Maurier, O. Decaux, J. Ninet, P. Gobert, T. Quemeneur, C. Blanchard-Delaunay, P. Godmer, X. Puechal, P. L. Carron, P. Y. Hatron, N. Limal, M. Hamidou, M. Ducret, E. Daugas, T. Papo, B. Bonnotte, A. Mahr, P. Ravaud, L. Mouthon, Rituximab versus azathioprine for maintenance in ANCA-associated vasculitis, *N Engl J Med* **371**, 1771–1780 (2014).

88. R. B. Jones, J. W. Tervaert, T. Hauser, R. Luqmani, M. D. Morgan, C. A. Peh, C. O. Savage, M. Segelmark, V. Tesar, P. van Paassen, D. Walsh, M. Walsh, K. Westman, D. R. Jayne, Rituximab versus cyclophosphamide in ANCA-associated renal vasculitis, *N Engl J Med* **363**, 211–220 (2010).

89. R. Cartin-Ceba, J. M. Golbin, K. a Keogh, T. Peikert, M. Sánchez-Menéndez, S. R. Ytterberg, F. C. Fervenza, U. Specks, Rituximab for remission induction and maintenance in refractory granulomatosis with polyangiitis (Wegener's): ten-year experience at a single center., *Arthritis Rheum.* **64**, 3770–8 (2012).

90. M. Y. Md Yusof, E. M. Vital, S. Das, S. Dass, G. Arumugakani, S. Savic, A. C. Rawstron, P. Emery, Repeat cycles of rituximab on clinical relapse in ANCA-associated vasculitis: Identifying B cell biomarkers for relapse to guide retreatment decisions, *Ann.*

Rheum. Dis. (2015), doi:10.1136/annrheumdis-2014-206496.

91. A. R. Kitching, H.-J. Anders, N. Basu, E. Brouwer, J. Gordon, R. D. Jayne, J. Kullman, P. A. Lyons, P. A. Merkel, C. O. S. Savage, U. Specks, R. Kain, ANCA-associated vasculitis, *Nat. Rev. Dis. Prim.* **6** (2020).

92. J. Savige, D. Davies, R. J. Falk, J. C. Jennette, A. Wiik, in *Kidney International*, (2000), vol. 57.

93. R. Kain, M. Exner, R. Brandes, R. Ziebermayr, D. Cunningham, C. A. Alderson, A. Davidovits, I. Raab, R. Jahn, O. Ashour, S. Spitzauer, G. Sunder-Plassmann, M. Fukuda, P. Klemm, A. J. Rees, D. Kerjaschki, Molecular mimicry in pauci-immune focal necrotizing glomerulonephritis, *Nat Med* **14**, 1088–1096 (2008).

94. D. Cornec, E. Cornec-Le Gall, F. C. Fervenza, U. Specks, ANCA-associated vasculitis - clinical utility of using ANCA specificity to classify patients, *Nat Rev Rheumatol* **12**, 570–579 (2016).

95. S. Lionaki, E. R. Blyth, S. L. Hogan, Y. Hu, B. A. Senior, C. E. Jennette, P. H. Nachman, J. C. Jennette, R. J. Falk, Classification of antineutrophil cytoplasmic autoantibody vasculitides: the role of antineutrophil cytoplasmic autoantibody specificity for myeloperoxidase or proteinase 3 in disease recognition and prognosis, *Arthritis Rheum* **64**, 3452–3462 (2012).

96. C. G. M. Kallenberg, P. Heeringa, C. a Stegeman, Mechanisms of Disease: pathogenesis and treatment of ANCA-associated vasculitides., *Nat. Clin. Pract. Rheumatol.* **2**, 661–70 (2006).

97. U. Schonermarck, E. Csernok, W. L. Gross, Pathogenesis of anti-neutrophil cytoplasmic antibody-associated vasculitis: challenges and solutions 2014, *Nephrol Dial Transpl.* **30 Suppl 1**, i46-52 (2015).

98. H. Xiao, A. Schreiber, P. Heeringa, R. J. Falk, J. C. Jennette, Alternative complement pathway in the pathogenesis of disease mediated by anti-neutrophil cytoplasmic autoantibodies, *Am. J. Pathol.* (2007), doi:10.2353/ajpath.2007.060573.

99. A. Schreiber, H. Xiao, J. C. Jennette, W. Schneider, F. C. Luft, R. Kettritz, C5a receptor mediates neutrophil activation and ANCA-induced glomerulonephritis, *J. Am. Soc. Nephrol.* (2009), doi:10.1681/ASN.2008050497.

100. K. Kessenbrock, M. Krumbholz, U. Schönermarck, W. Back, W. L. Gross, Z. Werb, H.-J. Gröne, V. Brinkmann, D. E. Jenne, Netting neutrophils in autoimmune small-vessel vasculitis., *Nat. Med.* **15**, 623–5 (2009).

101. J. C. Jennette, R. J. Falk, Small-vessel vasculitis, *N Engl J Med* **337**, 1512–1523 (1997).

102. A. Berti, D. Cornec, C. S. Crowson, U. Specks, E. L. Matteson, The epidemiology of ANCA associated vasculitis in Olmsted County, Minnesota (USA): a 20 year population-based study, *Arthritis Rheumatol* (2017), doi:10.1002/art.40313.

103. K. K. Berti A, Cornec D, Casal Moura M, Smyth RJ, Dagna L, Specks U, Eosinophilic Granulomatosis With Polyangiitis: Clinical Predictors of Long-term Asthma Severity., *Chest* , pii: S0012-3692(20)30023-4. (2020).

104. A. Berti, G. W. Volcheck, D. Cornec, R. J. Smyth, U. Specks, K. A. Keogh,

Severe/uncontrolled asthma and overall survival in atopic patients with eosinophilic granulomatosis with polyangiitis, *Respir Med* **142**, 66–72 (2018).

105. M. Yates, R. A. Watts, I. M. Bajema, M. C. Cid, B. Crestani, T. Hauser, B. Hellmich, J. U. Holle, M. Laudien, M. A. Little, R. A. Luqmani, A. Mahr, P. A. Merkel, J. Mills, J. Mooney, M. Segelmark, V. Tesar, K. Westman, A. Vaglio, N. Yalcindag, D. R. Jayne, C. Mukhtyar, EULAR/ERA-EDTA recommendations for the management of ANCA-associated vasculitis, *Ann Rheum Dis* **75**, 1583–1594 (2016).

106. M. Hilhorst, P. van Paassen, J. W. Tervaert, Proteinase 3-ANCA Vasculitis versus Myeloperoxidase-ANCA Vasculitis, *J Am Soc Nephrol* **26**, 2314–2327 (2015).

107. P. A. Lyons, T. F. Rayner, S. Trivedi, J. U. Holle, R. A. Watts, D. R. Jayne, B. Baslund, P. Brenchley, A. Bruchfeld, A. N. Chaudhry, J. W. Cohen Tervaert, P. Deloukas, C. Feighery, W. L. Gross, L. Guillevin, I. Gunnarsson, L. Harper, Z. Hruskova, M. A. Little, D. Martorana, T. Neumann, S. Ohlsson, S. Padmanabhan, C. D. Pusey, A. D. Salama, J. S. Sanders, C. O. Savage, M. Segelmark, C. A. Stegeman, V. Tesar, A. Vaglio, S. Wieczorek, B. Wilde, J. Zwerina, A. J. Rees, D. G. Clayton, K. G. Smith, Genetically distinct subsets within ANCA-associated vasculitis, *N Engl J Med* **367**, 214–223 (2012).

108. A. Berti, R. Warner, K. Johnson, D. Cornec, D. Schroeder, B. Kabat, C. A. Langford, G. S. Hoffman, F. C. Fervenza, C. G. M. Kallenberg, P. Seo, R. Spiera, E. W. St Clair, P. Brunetta, J. H. Stone, P. A. Merkel, U. Specks, P. A. Monach, Circulating Cytokine Profiles and Antineutrophil Cytoplasmic Antibody Specificity in Patients With Antineutrophil Cytoplasmic Antibody-Associated Vasculitis, *Arthritis Rheumatol* (2018), doi:10.1002/art.40471.

109. A. Berti, R. Warner, K. Johnson, D. Cornec, D. R. Schroeder, B. F. Kabat, C. A. Langford, C. G. M. Kallenberg, P. Seo, R. F. Spiera, E. W. St Clair, F. C. Fervenza, J. H. Stone, P. A. Monach, U. Specks, P. A. Merkel, The association of serum interleukin-6 levels with clinical outcomes in antineutrophil cytoplasmic antibody-associated vasculitis, *J. Autoimmun.* (2019), doi:10.1016/j.jaut.2019.07.001.

110. S. Unizony, M. Villarreal, E. M. Miloslavsky, N. Lu, P. A. Merkel, R. Spiera, P. Seo, C. A. Langford, G. S. Hoffman, C. M. Kallenberg, E. W. St Clair, D. Ikle, N. K. Tchao, L. Ding, P. Brunetta, H. K. Choi, P. A. Monach, F. Fervenza, J. H. Stone, U. Specks, Clinical outcomes of treatment of anti-neutrophil cytoplasmic antibody (ANCA)-associated vasculitis based on ANCA type, *Ann Rheum Dis* **75**, 1166–1169 (2016).

111. S. L. Hogan, R. J. Falk, H. Chin, J. Cai, C. E. Jennette, J. C. Jennette, P. H. Nachman, Predictors of relapse and treatment resistance in antineutrophil cytoplasmic antibody-associated small-vessel vasculitis, *Ann Intern Med* **143**, 621–631 (2005).

112. L. A. Fussner, A. M. Hummel, D. R. Schroeder, F. Silva, R. Cartin-Ceba, M. R. Snyder, G. S. Hoffman, C. G. Kallenberg, C. A. Langford, P. A. Merkel, P. A. Monach, P. Seo, R. F. Spiera, E. William St Clair, N. K. Tchao, J. H. Stone, U. Specks, Factors Determining the Clinical Utility of Serial Measurements of Antineutrophil Cytoplasmic Antibodies Targeting Proteinase 3, *Arthritis Rheumatol* **68**, 1700–1710 (2016).

113. A. J. Mohammad, M. Segelmark, A population-based study showing better renal prognosis for proteinase 3 antineutrophil cytoplasmic antibody (ANCA)-associated nephritis versus myeloperoxidase ANCA-associated nephritis, *J Rheumatol* **41**, 1366–1373 (2014).

114. S. Sethi, L. Zand, A. S. De Vriese, U. Specks, J. A. Vrana, S. Kanwar, P. Kurtin, J. D. Theis, A. Angioi, L. Cornell, F. C. Fervenza, Complement activation in pauci-immune necrotizing and crescentic glomerulonephritis: results of a proteomic analysis, *Nephrol Dial Transpl.* **32**, i139–i145 (2017).

115. J. C. Jennette, R. J. Falk, P. A. Bacon, N. Basu, M. C. Cid, F. Ferrario, L. F. Flores-Suarez, W. L. Gross, L. Guillevin, E. C. Hagen, G. S. Hoffman, D. R. Jayne, C. G. Kallenberg, P. Lamprecht, C. A. Langford, R. A. Luqmani, A. D. Mahr, E. L. Matteson, P. A. Merkel, S. Ozen, C. D. Pusey, N. Rasmussen, A. J. Rees, D. G. Scott, U. Specks, J. H. Stone, K. Takahashi, R. A. Watts, 2012 revised International Chapel Hill Consensus Conference Nomenclature of Vasculitides, *Arthritis Rheum* **65**, 1–11 (2013).

116. E. M. Miloslavsky, N. Lu, S. Unizony, H. K. Choi, P. A. Merkel, P. Seo, R. Spiera, C. A. Langford, G. S. Hoffman, C. G. Kallenberg, E. W. St Clair, N. K. Tchao, F. Fervenza, P. A. Monach, U. Specks, J. H. Stone, Myeloperoxidase-Antineutrophil Cytoplasmic Antibody (ANCA)-Positive and ANCA-Negative Patients With Granulomatosis With Polyangiitis (Wegener's): Distinct Patient Subsets, *Arthritis Rheumatol* **68**, 2945–2952 (2016).

117. J. H. Schirmer, M. N. Wright, K. Herrmann, M. Laudien, B. Nolle, E. Reinhold-Keller, J. P. Bremer, F. Moosig, J. U. Holle, Myeloperoxidase-Antineutrophil Cytoplasmic Antibody (ANCA)-Positive Granulomatosis With Polyangiitis (Wegener's) Is a Clinically Distinct Subset of ANCA-Associated Vasculitis: A Retrospective Analysis of 315 Patients From a German Vasculitis Referral Cent, *Arthritis Rheumatol* **68**, 2953–2963 (2016).

118. R. Y. Leavitt, A. S. Fauci, D. A. Bloch, B. A. Michel, G. G. Hunder, W. P. Arend, L.

H. Calabrese, J. F. Fries, J. T. Lie, R. W. Lightfoot Jr., et al., The American College of Rheumatology 1990 criteria for the classification of Wegener's granulomatosis, *Arthritis Rheum* **33**, 1101–1107 (1990).

119. A. T. Masi, G. G. Hunder, J. T. Lie, B. A. Michel, D. A. Bloch, W. P. Arend, L. H. Calabrese, S. M. Edworthy, A. S. Fauci, R. Y. Leavitt, et al., The American College of Rheumatology 1990 criteria for the classification of Churg-Strauss syndrome (allergic granulomatosis and angiitis), *Arthritis Rheum* **33**, 1094–1100 (1990).

120. R. Watts, S. Lane, T. Hanslik, T. Hauser, B. Hellmich, W. Koldingsnes, A. Mahr, M. Segelmark, J. W. Cohen-Tervaert, D. Scott, Development and validation of a consensus methodology for the classification of the ANCA-associated vasculitides and polyarteritis nodosa for epidemiological studies, *Ann Rheum Dis* **66**, 222–227 (2007).

121. C. A., R. J., P. C., G. P.C., S. R., J. A., W. R., M. P.A., ACR/EULAR-endorsed study to develop Diagnostic and Classification Criteria for Vasculitis (DCVAS), *Clin. Exp. Nephrol.* (2013), doi:http://dx.doi.org/10.1007/s10157-013-0854-0.

122. R. A. Luqmani, P. A. Bacon, R. J. Moots, B. A. Janssen, A. Pall, P. Emery, C. Savage, D. Adu, Birmingham Vasculitis Activity Score (BVAS) in systemic necrotizing vasculitis, *Qjm* **87**, 671–678 (1994).

123. J. H. Stone, G. S. Hoffman, P. A. Merkel, Y. I. Min, M. L. Uhlfelder, D. B. Hellmann, U. Specks, N. B. Allen, J. C. Davis, R. F. Spiera, L. H. Calabrese, F. M. Wigley, N. Maiden, R. M. Valente, J. L. Niles, K. H. Fye, J. W. McCune, E. W. St Clair, R. A. Luqmani, A disease-specific activity index for Wegener's granulomatosis: modification of the Birmingham Vasculitis Activity Score. International Network for the Study of the Systemic

Vasculitides (INSSYS), *Arthritis Rheum* **44**, 912–920 (2001).

124. C. Mukhtyar, R. Lee, D. Brown, D. Carruthers, B. Dasgupta, S. Dubey, O. Flossmann, C. Hall, J. Hollywood, D. Jayne, R. Jones, P. Lanyon, A. Muir, D. Scott, L. Young, R. A. Luqmani, Modification and validation of the Birmingham Vasculitis Activity Score (version 3), *Ann Rheum Dis* **68**, 1827–1832 (2009).

125. A. Berti, U. Specks, Remission maintenance in ANCA-associated vasculitis: does one size fit all?*Expert Rev. Clin. Immunol.* (2019), doi:10.1080/1744666X.2020.1693260.

126. X. Puechal, C. Pagnoux, E. Perrodeau, M. Hamidou, J. J. Boffa, X. Kyndt, F. Lifermann, T. Papo, D. Merrien, A. Smail, P. Delaval, C. Hanrotel-Saliou, B. Imbert, C. Khouatra, M. Lambert, C. Leske, K. H. Ly, E. Pertuiset, P. Roblot, M. Ruivard, J. F. Subra, J. F. Viallard, B. Terrier, P. Cohen, L. Mouthon, C. Le Jeunne, P. Ravaud, L. Guillevin, Long-Term Outcomes Among Participants in the WEGENT Trial of Remission-Maintenance Therapy for Granulomatosis With Polyangiitis (Wegener's) or Microscopic Polyangiitis, *Arthritis Rheumatol* **68**, 690–701 (2016).

127. R. M. Smith, R. B. Jones, U. Specks, S. Bond, M. Nodale, R. Aljayyousi, J. Andrews, A. Bruchfeld, B. Camilleri, S. Carette, C. K. Cheung, V. Derebail, T. Doulton, L. Forbess, S. Fujimoto, S. Furuta, O. Gewurz-Singer, L. Harper, T. Ito-Ihara, N. Khalidi, R. Klocke, C. Koening, Y. Komagata, C. Langford, P. Lanyon, R. A. Luqmani, H. Makino, C. McAlear, P. Monach, L. W. Moreland, K. Mynard, P. Nachman, C. Pagnoux, F. Pearce, C. A. Peh, C. Pusey, D. Ranganathan, R. L. Rhee, R. Spiera, A. G. Sreih, V. Tesar, G. Walters, M. H. Weisman, C. Wroe, P. Merkel, D. Jayne, Rituximab as therapy to induce remission after relapse in ANCA-associated vasculitis, *Ann. Rheum. Dis.* **79** (2020),

doi:10.1136/annrheumdis-2019-216863.

128. J. G. McGregor, R. Negrete-Lopez, C. J. Poulton, J. M. Kidd, S. L. Katsanos, L. Goetz, Y. Hu, P. H. Nachman, R. J. Falk, S. L. Hogan, Adverse events and infectious burden, microbes and temporal outline from immunosuppressive therapy in antineutrophil cytoplasmic antibody-associated vasculitis with native renal function, *Nephrol Dial Transpl.* **30 Suppl 1**, i171-81 (2015).

129. J. Robson, H. Doll, R. Suppiah, O. Flossmann, L. Harper, P. Hoglund, D. Jayne, A. Mahr, K. Westman, R. Luqmani, Glucocorticoid treatment and damage in the anti-neutrophil cytoplasm antibody-associated vasculitides: long-term data from the European Vasculitis Study Group trials, *Rheumatol.* **54**, 471–481 (2015).

130. J. Robson, H. Doll, R. Suppiah, O. Flossmann, L. Harper, P. Hoglund, D. Jayne, A. Mahr, K. Westman, R. Luqmani, Damage in the anca-associated vasculitides: long-term data from the European vasculitis study group (EUVAS) therapeutic trials, *Ann Rheum Dis* **74**, 177–184 (2015).

131. J. A. Tan, N. Dehghan, W. Chen, H. Xie, J. M. Esdaile, J. A. Avina-Zubieta, Mortality in ANCA-associated vasculitis: ameta-analysis of observational studies, *Ann Rheum Dis* **76**, 1566–1574 (2017).

132. S. Jardel, X. Puéchal, A. Le Quellec, C. Pagnoux, M. Hamidou, F. Maurier, O. Aumaitre, A. Aouba, T. Quemeneur, J.-F. Subra, V. Cottin, J. Sibilia, P. Godmer, P. Cacoub, A. L. Fauchais, E. Hachulla, D. Maucort-Boulch, L. Guillevin, J.-C. Lega, Mortality in systemic necrotizing vasculitides: A retrospective analysis of the French Vasculitis Study Group registry, *Autoimmun Rev* ,

doi:https://doi.org/10.1016/j.autrev.2018.01.022.

133. A. Berti, E. L. Matteson, C. S. Crowson, U. Specks, D. Cornec, Risk of Cardiovascular Disease and Venous Thromboembolism Among Patients With Incident ANCA-Associated Vasculitis: A 20-Year Population-Based Cohort Study, *Mayo Clin Proc* **93**, 597–606 (2018).

134. J. W. Tervaert, F. J. van der Woude, A. S. Fauci, J. L. Ambrus, J. Velosa, W. F. Keane, S. Meijer, M. van der Giessen, G. K. van der Hem, T. H. The, et al., Association between active Wegener's granulomatosis and anticytoplasmic antibodies, *Arch Intern Med* **149**, 2461–2465 (1989).

135. J. D. Finkielman, P. A. Merkel, D. Schroeder, G. S. Hoffman, R. Spiera, E. W. St Clair, J. C. Davis Jr., W. J. McCune, A. K. Lears, S. R. Ytterberg, A. M. Hummel, M. A. Viss, T. Peikert, J. H. Stone, U. Specks, Antiproteinase 3 antineutrophil cytoplasmic antibodies and disease activity in Wegener granulomatosis, *Ann Intern Med* **147**, 611–619 (2007).

136. M. J. Kemna, J. Damoiseaux, J. Austen, B. Winkens, J. Peters, P. van Paassen, J. W. Cohen Tervaert, ANCA as a predictor of relapse: useful in patients with renal involvement but not in patients with nonrenal disease, *J Am Soc Nephrol* **26**, 537–542 (2015).

137. J. W. Tervaert, M. G. Huitema, R. J. Hene, W. J. Sluiter, T. H. The, G. K. van der Hem, C. G. Kallenberg, Prevention of relapses in Wegener's granulomatosis by treatment based on antineutrophil cytoplasmic antibody titre, *Lancet* **336**, 709–711 (1990).

138. B. Terrier, D. Saadoun, D. Sene, P. Ghillani, Z. Amoura, G. Deray, B. Fautrel, J. C.

Piette, P. Cacoub, Antimyeloperoxidase antibodies are a useful marker of disease activity in antineutrophil cytoplasmic antibody-associated vasculitides, *Ann Rheum Dis* **68**, 1564–1571 (2009).

139. G. Tomasson, P. C. Grayson, A. D. Mahr, M. LaValley, P. A. Merkel, Value of ANCA measurements during remission to predict a relapse of ANCA-associated vasculitis-a meta-analysis, *Rheumatology* (2012), doi:10.1093/rheumatology/ker280.

140. U. Specks, Accurate relapse prediction in ANCA-associated vasculitis-the search for the Holy Grail, *J Am Soc Nephrol* **26**, 505–507 (2015).

141. N. Lepse, W. H. Abdulahad, A. Rutgers, C. G. M. Kallenberg, C. A. Stegeman, P. Heeringa, Altered B cell balance, but unaffected B cell capacity to limit monocyte activation in anti-neutrophil cytoplasmic antibody-associated vasculitis in remission, *Rheumatol. (United Kingdom)* (2014), doi:10.1093/rheumatology/keu149.

142. L. T. Aybar, J. G. Mcgregor, S. L. Hogan, Y. Hu, C. E. Mendoza, E. J. Brant, C. J. Poulton, C. D. Henderson, R. J. Falk, D. O. Bunch, Reduced CD5(+) CD24(hi) CD38(hi) and interleukin-10(+) regulatory B cells in active anti-neutrophil cytoplasmic autoantibody-associated vasculitis permit increased circulating autoantibodies, *Clin. Exp. Immunol.* (2015), doi:10.1111/cei.12483.

143. S. Unizony, N. Lim, D. J. Phippard, V. J. Carey, E. M. Miloslavsky, N. K. Tchao, D. Iklé, A. L. Asare, P. A. Merkel, P. A. Monach, P. Seo, E. W. St.clair, C. A. Langford, R. Spiera, G. S. Hoffman, C. G. M. Kallenberg, U. Specks, J. H. Stone, Peripheral CD5+ B cells in antineutrophil cytoplasmic antibody-associated vasculitis, *Arthritis Rheumatol.* (2015), doi:10.1002/art.38916.

144. S. K. Todd, R. J. Pepper, J. Draibe, A. Tanna, C. D. Pusey, C. Mauri, A. D. Salama, Regulatory B cells are numerically but not functionally deficient in anti-neutrophil cytoplasm antibody-associated vasculitis, *Rheumatol. (United Kingdom)* (2014), doi:10.1093/rheumatology/keu136.

145. C. Havenar-Daughton, M. Lindqvist, A. Heit, J. E. Wu, S. M. Reiss, K. Kendric, S. Bélanger, S. P. Kasturi, E. Landais, R. S. Akondy, H. M. McGuire, M. Bothwell, P. A. Vagefi, E. Scully, G. D. Tomaras, M. M. Davis, P. Poignard, R. Ahmed, B. D. Walker, B. Pulendran, M. J. McElrath, D. E. Kaufmann, S. Crotty, CXCL13 is a plasma biomarker of germinal center activity, *Proc. Natl. Acad. Sci. U. S. A.* (2016), doi:10.1073/pnas.1520112113.

146. Y. Zhao, P. M. K. Lutalo, J. E. Thomas, S. Sangle, L. M. Choong, J. R. Tyler, T. Tree, J. Spencer, D. P. D'cruz, Circulating T follicular helper cell and regulatory T cell frequencies are influenced by B cell depletion in patients with granulomatosis with polyangiitis, *Rheumatol. (United Kingdom)* (2014), doi:10.1093/rheumatology/ket406.

147. J. Voswinkle, A. Mueller, J. A. Kraemer, P. Lamprecht, K. Herlyn, K. Holl-Ulrich, A. C. Feller, S. Pitann, A. Gause, W. L. Gross, B lymphocyte maturation in Wegener's qranulomatosis: A comparative analysis of VH genes from endonasal lesions, *Ann. Rheum. Dis.* **65** (2006), doi:10.1136/ard.2005.044909.

148. J. Erikson, M. Z. Radic, S. A. Camper, R. R. Hardy, C. Carmack, M. Weigert, Expression of anti-DNA immunoglobulin transgenes in non-autoimmune mice, *Nature* (1991), doi:10.1038/349331a0.

149. L. Mandik-Nayak, A. Bui, H. Noorchashm, A. Eaton, J. Erikson, Regulation of anti-

double-stranded DNA B cells in nonautoimmune mice: Localization to the T-B interface of the splenic follicle, *J. Exp. Med.* (1997), doi:10.1084/jem.186.8.1257.

150. H. Li, Y. Jiang, E. L. Prak, M. Radic, M. Weigert, Editors and editing of anti-DNA receptors, *Immunity* (2001), doi:10.1016/S1074-7613(01)00251-5.

151. Y. Pewzner-Jung, D. Friedmann, E. Sonoda, S. Jung, K. Rajewsky, D. Eilat, B cell deletion, anergy, and receptor editing in “knock in” mice targeted with a germline-encoded or somatically mutated anti-DNA heavy chain., *J. Immunol.* (1998).

152. S. Ohlsson, J. Wieslander, M. Segelmark, Increased circulating levels of proteinase 3 in patients with anti-neutrophilic cytoplasmic autoantibodies-associated systemic vasculitis in remission, *Clin. Exp. Immunol.* (2003), doi:10.1046/j.1365-2249.2003.02083.x.

153. P. A. Lyons, T. F. Rayner, S. Trivedi, J. U. Holle, R. A. Watts, D. R. Jayne, B. Baslund, P. Brenchley, A. Bruchfeld, A. N. Chaudhry, J. W. Cohen Tervaert, P. Deloukas, C. Feighery, W. L. Gross, L. Guillevin, I. Gunnarsson, L. Harper, Z. Hruskova, M. A. Little, D. Martorana, T. Neumann, S. Ohlsson, S. Padmanabhan, C. D. Pusey, A. D. Salama, J. S. Sanders, C. O. Savage, M. Segelmark, C. A. Stegeman, V. Tesar, A. Vaglio, S. Wieczorek, B. Wilde, J. Zwerina, A. J. Rees, D. G. Clayton, K. G. Smith, Genetically distinct subsets within ANCA-associated vasculitis, *N Engl J Med* **367**, 214–223 (2012).

154. T. D. Chan, K. Wood, J. R. Hermes, D. Butt, C. J. Jolly, A. Basten, R. Brink, Elimination of Germinal-Center-Derived Self-Reactive B Cells Is Governed by the Location and Concentration of Self-Antigen, *Immunity* (2012), doi:10.1016/j.immuni.2012.07.017.

155. J. H. Reed, J. Jackson, D. Christ, C. C. Goodnow, Clonal redemption of autoantibodies by somatic hypermutation away from self-reactivity during human immunization, *J. Exp. Med.* (2016), doi:10.1084/jem.20151978.

156. I. MacLennan, K. M. Toellner, Extrafollicular antibody responses - MacLennan - 2003 - Immunological Reviews - Wiley Online Library, *Immunol. {…}* (2003).

157. P. A. Monach, R. L. Warner, G. Tomasson, U. Specks, J. H. Stone, L. Ding, F. C. Fervenza, B. J. Fessler, G. S. Hoffman, D. Ikle, C. G. Kallenberg, J. Krischer, C. A. Langford, M. Mueller, P. Seo, E. W. St Clair, R. Spiera, N. Tchao, S. R. Ytterberg, K. J. Johnson, P. A. Merkel, Serum proteins reflecting inflammation, injury and repair as biomarkers of disease activity in ANCA-associated vasculitis, *Ann Rheum Dis* **72**, 1342–1350 (2013).

158. W. B. Dyer, S. L. Pett, J. S. Sullivan, S. Emery, D. A. Cooper, A. D. Kelleher, A. Lloyd, S. R. Lewin, Substantial improvements in performance indicators achieved in a peripheral blood mononuclear cell cryopreservation quality assurance program using single donor samples, *Clin. Vaccine Immunol.* **14** (2007), doi:10.1128/CVI.00214-06.

159. L. M. Brown, J. W. Clark, C. Y. Neuland, D. L. Mann, L. K. Pankiw-Trost, W. A. Blattner, D. J. Tollerud, Cryopreservation and long-term liquid nitrogen storage of peripheral blood mononuclear cells for flow cytometry analysis effects on cell subset proportions and fluorescence intensity, *J. Clin. Lab. Anal.* **5** (1991), doi:10.1002/jcla.1860050406.

160. F. T. Lauer, J. L. Denson, S. W. Burchiel, Isolation, Cryopreservation, and Immunophenotyping of Human Peripheral Blood Mononuclear Cells, *Curr. Protoc.*

Toxicol. **74** (2017), doi:10.1002/cptx.31.

161. Y. Dieudonné, V. Gies, A. Guffroy, C. Keime, A. K. Bird, J. Liesveld, J. L. Barnas, V. Poindron, N. Douiri, P. Soulas-Sprauel, T. Martin, E. Meffre, J. H. Anolik, A. S. Korganow, Transitional B cells in quiescent SLE: An early checkpoint imprinted by IFN, *J. Autoimmun.* **102** (2019), doi:10.1016/j.jaut.2019.05.002.

162. A. Palanichamy, J. Barnard, B. Zheng, T. Owen, T. Quach, C. Wei, R. J. Looney, I. Sanz, J. H. Anolik, Novel Human Transitional B Cell Populations Revealed by B Cell Depletion Therapy, *J. Immunol.* (2009), doi:10.4049/jimmunol.0801859.

163. A. Malaspina, S. Moir, J. Ho, W. Wang, M. L. Howell, M. A. O'Shea, G. A. Roby, C. A. Rehm, J. A. M. Mican, T. W. Chun, A. S. Fauci, Appearance of immature/transitional B cells in HIV-infected individuals with advanced disease: Correlation with increased IL-7, *Proc. Natl. Acad. Sci. U. S. A.* **103** (2006), doi:10.1073/pnas.0511094103.

164. M. P. Cancro, J. F. Kearney, B Cell Positive Selection: Road Map to the Primary Repertoire?, *J. Immunol.* **173** (2004), doi:10.4049/jimmunol.173.1.15.

165. S. Suryani, D. A. Fulcher, B. Santner-Nanan, R. Nanan, M. Wong, P. J. Shaw, J. Gibson, A. Williams, S. G. Tangye, Differential expression of CD21 identifies developmentally and functionally distinct subsets of human transitional B cells, *Blood* **115** (2010), doi:10.1182/blood-2009-07-234799.

166. H. Wardemann, M. C. Nussenzweig, B-Cell Self-Tolerance in Humans*Adv. Immunol.* **95** (2007), doi:10.1016/S0065-2776(07)95003-8.

167. I. C. M. MacLennan, Autoimmunity: Deletion of autoreactive B cells, *Curr. Biol.* **5**

(1995), doi:10.1016/S0960-9822(95)00025-X.

168. S. Julien, P. Soulas, J.-C. Garaud, T. Martin, J.-L. Pasquali, B Cell Positive Selection by Soluble Self-Antigen, *J. Immunol.* **169** (2002), doi:10.4049/jimmunol.169.8.4198.

169. J. C. Jennette, R. J. Falk, The rise and fall of horror autotoxicus and forbidden clones*Kidney Int.* **78** (2010), doi:10.1038/ki.2010.237.

170. Y. S. Ng, H. Wardemann, J. Chelnis, C. Cunningham-Rundles, E. Meffre, Bruton's tyrosine kinase is essential for human B cell tolerance, *J. Exp. Med.* **200** (2004), doi:10.1084/jem.20040920.

171. M. De Weers, G. S. Brouns, S. Hinshelwood, C. Kinnon, R. K. B. Schuurman, R. W. Hendriks, J. Borst, B-cell antigen receptor stimulation activates the human Bruton's tyrosine kinase, which is deficient in X-linked agammaglobulinemia, *J. Biol. Chem.* **269** (1994), doi:10.1016/s0021-9258(19)51014-6.

172. R. Cartin-Ceba, J. M. Golbin, K. A. Keogh, T. Peikert, M. Sanchez-Menendez, S. R. Ytterberg, F. C. Fervenza, U. Specks, Rituximab for remission induction and maintenance in refractory granulomatosis with polyangiitis (Wegener's): ten-year experience at a single center, *Arthritis Rheum* **64**, 3770–3778 (2012).

173. E. Besada, W. Koldingsnes, J. C. Nossent, Long-term efficacy and safety of pre-emptive maintenance therapy with rituximab in granulomatosis with polyangiitis: results from a single centre, *Rheumatol.* **52**, 2041–2047 (2013).

174. A. Marie-Cardine, F. Divay, I. Dutot, A. Green, A. Perdrix, O. Boyer, N. Contentin, H. Tilly, F. Tron, J. P. Vannier, S. Jacquot, Transitional B cells in humans:

Characterization and insight from B lymphocyte reconstitution after hematopoietic stem cell transplantation, *Clin. Immunol.* (2008), doi:10.1016/j.clim.2007.11.013.

175. A. von Borstel, J. Land, W. H. Abdulahad, A. Rutgers, C. A. Stegeman, A. Diepstra, P. Heeringa, J. S. Sanders, CD27+CD38hi B Cell Frequency During Remission Predicts Relapsing Disease in Granulomatosis With Polyangiitis Patients, *Front. Immunol.* (2019), doi:10.3389/fimmu.2019.02221.

176. A. S. Fauci, D. C. Dale, The effect of in vivo hydrocortisone on subpopulations of human lymphocytes., *J. Clin. Invest.* (1974), doi:10.1172/JCI107544.

177. A. Saxon, R. H. Stevens, S. J. Ramer, P. J. Clements, D. T. Yu, Glucocorticoids administered in vivo inhibit human suppressor T lymphocyte function and diminish B lymphocyte responsiveness in in vitro immunoglobulin synthesis, *J. Clin. Invest.* (1978), doi:10.1172/JCI109017.

178. J. H. Stone, P. a Merkel, R. Spiera, P. Seo, C. a Langford, G. S. Hoffman, C. G. M. Kallenberg, E. W. St Clair, A. Turkiewicz, N. K. Tchao, L. Webber, L. Ding, L. P. Sejismundo, K. Mieras, D. Weitzenkamp, D. Ikle, V. Seyfert-Margolis, M. Mueller, P. Brunetta, N. B. Allen, F. C. Fervenza, D. Geetha, K. a Keogh, E. Y. Kissin, P. a Monach, T. Peikert, C. Stegeman, S. R. Ytterberg, U. Specks, Rituximab versus cyclophosphamide for ANCA-associated vasculitis., *N. Engl. J. Med.* **363**, 221–32 (2010).

179. J. H. Stone, P. A. Merkel, R. Spiera, P. Seo, C. A. Langford, G. S. Hoffman, C. G. Kallenberg, E. W. St Clair, A. Turkiewicz, N. K. Tchao, L. Webber, L. Ding, L. P. Sejismundo, K. Mieras, D. Weitzenkamp, D. Ikle, V. Seyfert-Margolis, M. Mueller, P. Brunetta, N. B. Allen, F. C. Fervenza, D. Geetha, K. A. Keogh, E. Y. Kissin, P. A. Monach,

T. Peikert, C. Stegeman, S. R. Ytterberg, U. Specks, Rituximab versus cyclophosphamide for ANCA-associated vasculitis, *N Engl J Med* **363**, 221–232 (2010).

180. S. A. Capizzi, M. A. Viss, A. M. Hummel, D. N. Fass, U. Specks, Effects of carboxy-terminal modifications of proteinase 3 (PR3) on the recognition by PR3-ANCA, *Kidney Int.* (2003), doi:10.1046/j.1523-1755.2003.00765.x.

181. S. M. Rasmussen, A. E. Bilgrau, A. Schmitz, S. Falgreen, K. S. Bergkvist, A. M. Tramm, J. Bæch, C. L. Jacobsen, M. Gaihede, M. K. Kjeldsen, J. S. Bødker, K. Dybkær, M. Bøgsted, H. E. Johnsen, Stable phenotype of B-cell subsets following cryopreservation and thawing of normal human lymphocytes stored in a tissue biobank, *Cytom. Part B - Clin. Cytom.* (2015), doi:10.1002/cyto.b.21192.

182. A. K. Kimball, L. M. Oko, B. L. Bullock, R. A. Nemenoff, L. F. van Dyk, E. T. Clambey, A Beginner's Guide to Analyzing and Visualizing Mass Cytometry Data, *J. Immunol.* (2018), doi:10.4049/jimmunol.1701494.

183. R. Itoua Maïga, G. Bonnaure, J. Tremblay Rochette, S. Néron, Human CD38hiCD138+ plasma cells can be generated in vitro from CD40-activated switched-memory B lymphocytes, *J. Immunol. Res.* **2014** (2014), doi:10.1155/2014/635108.

184. M. Jourdan, A. Caraux, J. De Vos, G. Fiol, M. Larroque, C. Cognot, C. Bret, C. Duperray, D. Hose, B. Klein, An in vitro model of differentiation of memory B cells into plasmablasts and plasma cells including detailed phenotypic and molecular characterization, *Blood* **114** (2009), doi:10.1182/blood-2009-07-235960.

185. K. Tarte, J. De Vos, T. Thykjaer, F. Zhan, G. Fiol, V. Costes, T. Rème, E. Legouffe, J. F. Rossi, J. Shaughnessy, T. F. Ørntoft, B. Klein, Generation of polyclonal plasmablasts

from peripheral blood B cells: A normal counterpart of malignant plasmablasts, *Blood* **100** (2002), doi:10.1182/blood.v100.4.1113.h81602001113_1113_1122.

186. M. Cocco, S. Stephenson, M. A. Care, D. Newton, N. A. Barnes, A. Davison, A. Rawstron, D. R. Westhead, G. M. Doody, R. M. Tooze, In Vitro Generation of Long-lived Human Plasma Cells, *J. Immunol.* **189** (2012), doi:10.4049/jimmunol.1103720.

187. A. Li, R. F. Barber, Multiple testing with the structure-adaptive Benjamini–Hochberg algorithm, *J. R. Stat. Soc. Ser. B Stat. Methodol.* **81** (2019), doi:10.1111/rssb.12298.

Publications During the PhD Course

Experimental work related to the PhD project

Circulating Autoreactive Proteinase 3$^+$ B Cells and Tolerance Checkpoints in ANCA-Associated Vasculitis.

Alvise Berti, Sophie Hillion, Amber M. Hummel, Young Min Son, Nedra Chriti, Tobias Peikert, Eva Carmona, Wayel Abdulahad, Peter Heeringa, Kristina M. Harris, E. William St. Clair, Paul Brunetta, Fernando C. Fervenza, Carol A. Langford, Cees G.M. Kallenberg, Peter A. Merkel, Paul A. Monach, Philip Seo, Robert F. Spiera, John H. Stone, Guido Grandi, Jie Sun, Jacques-Olivier Pers, Ulrich Specks, and Divi Cornec for the RAVE-ITN Research Group.

Under revision in JCI Insight. 2021.

I perform the flow cytometry analyses and personally contributed to do the PBMC cultures. I analyzed all the data, performed the statistical analysis, critically interpreted the findings, and drafted the manuscript. I conceived the experiment on cell sorting to functionally validate PR3$^+$ PR3$^-$ B cells, and set up ultra-sensitive biotin-streptavidin direct ELISA that we used for the PR3-ANCA IgG detection in the culture supernatants. I set up the culture stimulation of this experiment in order to optimize memory B cells differentiation into plasmablasts/antigen secreting cells. I performed cytospin smears, stained and read them.

Autoreactive plasmablasts after B cell depletion with RTX and relapses in ANCA-associated vasculitis.

Alvise Berti, Sophie Hillion, Marta Casal Moura, Amber M. Hummel, Eva Carmona, Tobias Peikert, Fernando C. Fervenza, Cees G.M. Kallenberg, Carol A. Langford, Peter A. Merkel, Paul A. Monach, Philip Seo, Robert F. Spiera, Paul Brunetta, E. William St. Clair, Kristina M. Harris, John H. Stone, Guido Grandi, Jacques-Olivier Pers, Ulrich Specks, and Divi Cornec for the RAVE-ITN Research Group.

Under revision in Arthritis and Rheumatology, 2021.

I perform the flow cytometry analyses. I analyzed all the data, performed the statistical analysis, critically interpreted the findings, and drafted the manuscript.

Identification of the central tolerance checkpoint for autoreactive proteinase 3$^+$ B cells in human bone marrow.

Alvise Berti, Michele Tomasi, Isabella Pesce, Anna Guella, Enrico Lista, Roberto Bortolotti, Giuseppe Paolazzi, Sophie Hillion, Ulrich Specks, Guido Grandi, Divi Cornec.

In preparation, 2021.

I conceived the original idea, collected the samples, and set up the extensive panel that we used for the flow cytometry analysis. I designed and performed the experiments, analyzed the data, critically interpreted the findings, performed the statistical analysis, and drafted the manuscript.

Publications on AAV

The association of serum interleukin-6 levels with clinical outcomes in antineutrophil cytoplasmic antibody-associated vasculitis.

Berti A, Warner R, Johnson K, Cornec D, Schroeder DR, Kabat BF, Langford CA, Kallenberg CGM, Seo P, Spiera RF, St Clair EW, Fervenza FC, Stone JH, Monach PA, Specks U, Merkel PA; RAVE-ITN Research Group.

J Autoimmun. 2019 Jul 15:102302. doi: 10.1016/j.jaut.2019.07.001

The severe long-term outcomes of 'non-severe' eosinophilic granulomatosis with polyangiitis.

Berti A.

Rheumatology (Oxford).2019 Jun 29.pii: kez250. doi: 10.1093/rheumatology/kez250

Orbital masses in ANCA-associated vasculitis: an unsolved challenge?

Berti A, Kronbichler A.

Rheumatology (Oxford). 2019 Sep 1;58(9):1520-1522. doi: 10.1093/rheumatology/kez136.

Remission maintenance in ANCA-associated vasculitis: does one size fit all?

Berti A, Specks U.

Expert Rev Clin Immunol. 2019 Nov 24. DOI: 10.1080/1744666X.2020.1693260

The Incidence of Arterial and Venous Thrombosis in Antineutrophil Cytoplasmic Antibody-associated Vasculitis.

Berti A, Matteson EL, Crowson CS, Specks U, Cornec D.

J Rheumatol. 2019 Sep;46(9):1243. doi: 10.3899/jrheum.181351

Chronic rhinosinusitis in eosinophilic granulomatosis with polyangiitis: clinical presentation and antineutrophil cytoplasmic antibodies.

Low CM, Keogh KA, Saba ES, Gruszczynski NR, Berti A, Specks U, Baqir M, Smith BM, Choby G, Stokken JK, O'Brien EK.

Int Forum Allergy Rhinol. 2019 Dec 2. DOI: 10.1002/alr.22503

Eosinophilic granulomatosis with polyangiitis: the multifaceted spectrum of clinical manifestations at different stages of the disease.

Berti A, Boukhlal S, Groh M, Cornec D.

Expert Rev Clin Immunol. 2020 Jan. DOI: 10.1080/1744666X.2019.1697678

Aging in Primary Systemic Vasculitis: Implications for Diagnosis, Clinical Manifestations, and Management.

Berti A, Caporali R, Montecucco C, Paolazzi G, Monti S.

Drugs Aging. 2019 DOI: 10.1007/s40266-018-0617-4

Incidence, prevalence, mortality and chronic renal damage of anti-neutrophil cytoplasmic antibody-associated glomerulonephritis in a 20-year population-based cohort.

Berti A, Cornec-Le Gall E, Cornec D, Casal Moura M, Matteson EL, Crowson CS, Ravindran A, Sethi S, Fervenza FC, Specks U.

Nephrol Dial Transplant. 2019 Sep 1;3 DOI: 10.1093/ndt/gfy250

Eosinophilic Granulomatosis with Polyangiitis: clinical predictors of long-term asthma severity.

Berti A, Cornec D, Moura MC, Smyth RJ, Dagna L, Specks U, Keogh KA.

Chest. 2020 Jan 17. DOI: 10.1016/j.chest.2019.11.045

Asthma control in eosinophilic granulomatosis with polyangiitis treated with rituximab.

Casal Moura M, Berti A, Keogh KA, Volcheck GW, Specks U, Baqir M.

Clin Rheumatol. 2020 Jan 2. DOI: 10.1007/s10067-019-04891-w

Disease and treatment-related morbidity in young and elderly patients with granulomatosis with polyangiitis and microscopic polyangiitis.

Berti A, Felicetti M, Monti S, Ortolan A, Padoan R, Brunori G, Bortolotti R, Caporali R, Montecucco C, Schiavon F, Paolazzi G.

Semin Arthritis Rheum. 2020 Dec;50(6):1441-1448. doi: 10.1016/j.semarthrit.2020.02.008.

Efficacy of Rituximab and Plasma Exchange in Antineutrophil Cytoplasmic Antibody-Associated Vasculitis with Severe Kidney Disease.

Casal Moura M, Irazabal MV, Eirin A, Zand L, Sethi S, Borah BJ, Winters JL, Moriarty JP, Cartin-Ceba R, Berti A, Baqir M, Thompson GE, Makol A, Warrington KJ, Thao V, Specks U, Fervenza FC.

J Am Soc Nephrol. 2020 Nov;31(11):2688-2704.

The Survival of Patients With Alveolar Hemorrhage Secondary to Antineutrophil Cytoplasmic Antibody-associated Vasculitis.

Berti A, Specks U.

J Rheumatol. 2021 Mar;48(3):314-317. doi: 10.3899/jrheum.201297.

Mepolizumab for Eosinophilic Granulomatosis with Polyangiitis (EGPA): a European multicenter observational study.

Bettiol A, Urban ML, Dagna L, Cottin V, Franceschini F, Del Giacco S, Schiavon F, Neumann T, Lopalco G, Novikov P, Baldini C, Lombardi C, Berti A, et el. European EGPA Study Group.

Arthritis Rheumatol. 2021 Aug 4. doi: 10.1002/art.41943.

Other publications

Clinical Characterization and Predictors of IOS-Defined Small-Airway Dysfunction in Asthma.

Cottini M, Licini A, Lombardi C, Berti A.

J Allergy Clin Immunol Pract. 2019 Nov 11. DOI: 10.1016/j.jaip.2019.10.040

Association of Smoking and Obesity on the Risk of Developing Primary Sjögren Syndrome: A Population-based Cohort Study.

Servioli L, Maciel G, Nannini C, Crowson CS, Matteson EL, Cornec D, Berti A.

J Rheumatol. 2019 Jul; DOI: 10.3899/jrheum.180481

Predicting Disease Activity in Systemic Vasculitides: On the Hunt for Potential Candidates.

Kronbichler A, Shin JI, Berti A.

J Rheumatol. 2020 Jul 1;47(7):947-950. doi: 10.3899/jrheum.190885

Prevalence and features of IOS-defined small airway disease across asthma severities.

Cottini M, Licini A, Lombardi C, Berti A.

Respir Med. 2021 Jan;176:106243. doi: 10.1016/j.rmed.2020.106243. Epub 2020 Nov 19

Obesity is a Major Risk Factor for Hospitalization in Community-Managed COVID-19 Pneumonia.

Cottini M, Lombardi C, Berti A.

Mayo Clin Proc. 2021 Apr;96(4):921-931. doi: 10.1016/j.mayocp.2021.01.021. Epub 2021 Feb 4.

Meta-analysis of immune-related adverse events in phase 3 clinical trials assessing immune checkpoint inhibitors for lung cancer.

Berti A, Bortolotti R, Dipasquale M, Kinspergher S, Prokop L, Grandi G, Inchiostro S, Paolazzi G, Caffo O, Veccia A.

Crit Rev Oncol Hematol . 2021 Jun;162:103351. doi: 10.1016/j.critrevonc.2021.103351. Epub 2021May 12.

Asthma and COVID-19: a dangerous liaison?

Lombardi C, Gani F, Berti A, Comberiati P, Peroni D, Cottini M.

Asthma Res Pract. 2021 Jul 15;7(1):9. doi: 10.1186/s40733-021-00075-z.

Immune and cellular damage biomarkers to predict COVID-19 mortality in hospitalized patients.

Lombardi C, Roca E, Bigni B, Bertozzi B, Ferrandina C, Franzin A, Vivaldi O, Cottini M, D'Alessio A, Del Poggio P, Conte GM, Berti A.

Curr Res Immunol. 2021 Sep 16. doi: 10.1016/j.crimmu.2021.09.001.

Acknowledgments

I would like to thank my PhD tutor, Prof. Guido Grandi for giving me the opportunity to do my PhD in his laboratory, and for the support and guidance during these years. Thanks to him my PhD in immunology was possible in Trento, this means a lot to me. Likewise, I would like to express my sincere gratitude to my advisors Prof. Ulrich Specks and Prof. Divi Cornec. Both were columns for my scientific growth, in different and complementary ways: thanks to Prof. Specks for his continuous guidance, I have learned so much throughout this experience and have grown as a scientist and a person, and to Prof. Cornec that took me under his wing from the start, helping me to get to grips with how things work, while spreading positive energy and enthusiasm.

Thank you to all the past and present members of the Laboratory of Synthetic and Structural Vaccinology, good friends before than amazing colleagues, Mirel, Ilaria, Enrico, Mattia B., Mattia D., Lorenzo, Sebastiano, Samine, Carmela, and Luca. A super special thanks to Amber Hummel and Marta Casal Moura from the TDRU Laboratory of Mayo Clinic. Thanks to Sophie Hillion from the B Cells and Autoimmunity Laboratory of Brest for the precious advice.

I need to also give my appreciation to Dr. Giuseppe Paolazzi and Dr. Roberto Bortolotti, from the Rheumatology clinic of Trento, never would have made it without their support.

Words aren’t able to express my gratitude to Francesca, for support, words of encouragement and endless affection. And the huge amount of patience. You’re the best, ever. My son Zeno, who made my day so many times, unconsciously. Thank you. And thanks to my family, my parents, brothers and sister, and all my friends near and far.